Canonical Correlations of Energy-Momentum Tensor and Transport Coefficients from Lattice Gauge Simulation

Yasuhiro Kohno

Department of Physics, Graduate School of Science, Osaka University
1-1 Machikaneyama-cho, Toyonaka, Osaka, 560-0043, Japan

A Dissertation in candidacy for
the degree of Doctor of Philosophy

Canonical Correlations of Energy-Momentum Tensor and Transport Coefficients from Lattice Gauge Simulation

(格子ゲージシミュレーションによるエネルギー運動量テンソルのカノニカル相関と輸送係数の測定)

Abstract

Quark-Gluon Plasma (QGP) is a matter expected to exist in the early universe. Relativistic heavy ion collision is only experimental approach to create the QGP on the earth. Recent heavy ion experimental data are known to be reproduced by relativistic hydrodynamic models with low viscosity. This fact provided a new aspect of matter, i.e. strongly coupled or correlated QGP for us. However the hydrodynamic models depend on several inputs, such as equation of state and transport coefficients. It is highly desirable to determine these inputs by microscopic theory. In this thesis, we focus on Israel-Stewart (IS) theory and the ratios of viscosity to corresponding relaxation time. IS theory is a causal dissipative hydrodynamics which is frequently used by the hydrodynamic models. The ratios are related to canonical correlations of energy-momentum tensor by an application of relaxation-time approximation to Kubo formulas. We measure the canonical correlations with SU(3) lattice gauge simulation for the temperature range reached by RHIC and LHC. We show that two kinds of subtraction (vacuum and contact terms subtractions) are required for the correlations on the lattice to obtain the ratios. From the analyses, the transport coefficients are constrained by the first principle. Then we also analyze characteristic speed of transverse and sound modes with the ratios. We find that the sound mode can be superluminal from our lattice measurements. This means that an application of the IS theory to the hot QCD matter requires some modification to keep the causality.

Contents

Chapter 1

Introduction

Standard Model

Standard model is a theoretical framework to describe elementary particles and three fundamental interactions among them, i.e. *strong, electromagnetic*, and *weak interactions*. *Quarks* and *leptons* are the smallest elements constructing our world in the standard model (Fig. 1.1). The quarks are divided into three generations and carry internal degrees of freedom called *flavor* and *color*. There are six flavors (*up* (u), *down* (d), *charm* (c), *strange* (s), *top* (t), and *bottom* (b)) and three colors (*red* (R), *green* (G), and *blue* (B)), and the anti-quarks carry anti-colors ($\bar{\text{R}}$, $\bar{\text{G}}$, and $\bar{\text{B}}$). The quarks are affected by the *strong interaction* because of the color charge. The leptons are also classified into three generations i.e. *electron* (e), *muon* (μ), *tau* (τ), and *neutrinos* (ν_e, ν_μ, and ν_τ). The leptons do not feel the strong interaction because they are colorless. The strong interaction is described by an exchange of elementary particle called *gluon* (g). Particles which mediate interactions are called *gauge particles*. The gluon is one of the gauge particles. In the standard model, *photons* (γ) and *weak bosons* (W, Z) are also known as the gauge particles which mediate the electromagnetic and weak interactions, respectively. Since the gluons also carry the color charge, they interact not only with quarks but also themselves (self-interaction). This is an inherent property of the gluons. Because of the self-interaction, quark-gluon systems show various non-trivial aspects as discussed in the following.

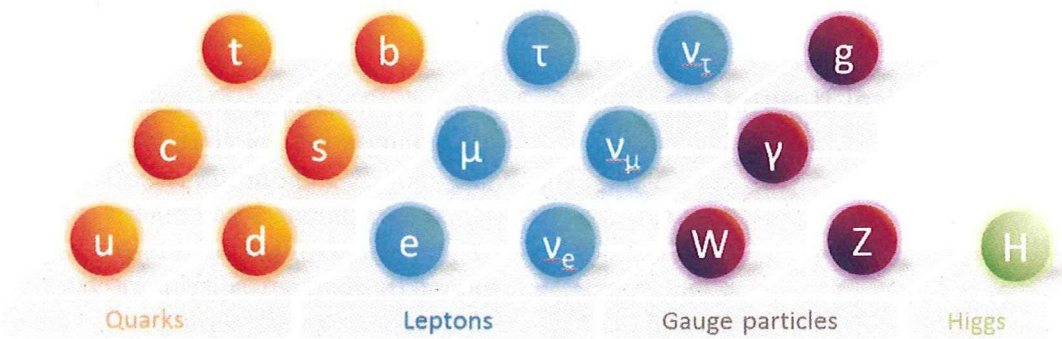

Figure 1.1: Standard model.

Asymptotic Freedom

The first principle that governs the strong interaction is *Quantum Chromodynamics* (QCD). QCD is described by SU(3) gauge field theory. One of the most important features of QCD is *asymptotic freedom* [1, 2]. According to a perturbative calculation of renormalization group equation

$$\kappa \frac{\partial g}{\partial \kappa} = \beta(g), \tag{1.1}$$

QCD coupling α_s in the leading order behaves as

$$\alpha_s(\kappa) = \frac{g^2}{4\pi} = \frac{1}{4\pi b_0 \ln(\kappa^2/\Lambda^2_{QCD})}, \tag{1.2}$$

$$b_0 = \frac{1}{(4\pi)^2}\left(11 - \frac{2}{3}N_f\right), \tag{1.3}$$

where g, κ, and N_f are the running coupling constant, the renormalization scale, and the number of flavors, respectively. $\beta(g)$ is called the beta function. Λ_{QCD} is called QCD scale parameter which is determined by experiments, $\Lambda_{QCD} \sim 200$ MeV. In the case of $N_f \leq 16$, the running coupling constant becomes small as increasing the renormalization scale κ. Since the high (low) energy scale corresponds to the short (long) distance scale, the running coupling constant g between two color charges becomes small (large) in the short (long) distance,

$$\text{high } \kappa \Leftrightarrow \text{short distance scale} \Leftrightarrow \text{small } g, \tag{1.4}$$

$$\text{low } \kappa \Leftrightarrow \text{long distance scale} \Leftrightarrow \text{large } g. \tag{1.5}$$

This property is called the asymptotic freedom. Note that the above argument is based on perturbation theory. The behavior of the running coupling constant in the low energy scale has to be investigated by non-perturbative approaches because of the large coupling.

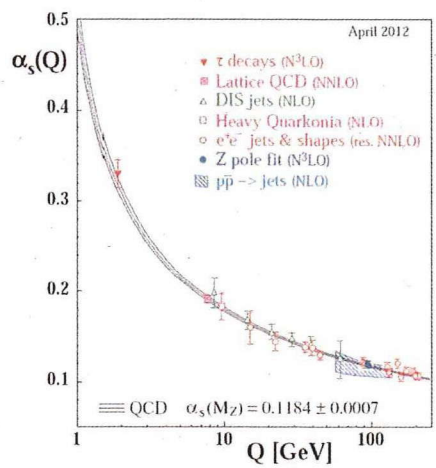

Figure 1.2: Asymptotic freedom of QCD coupling α_s from Ref. [3].

Confinement of Color

Although the quarks and the gluons are regarded as elementary particles in the standard model, no one has ever observed single quark or gluon as an isolated state. There are only several indirect evidences for their existences in experiments. Because of the asymptotic freedom, they are always confined inside particles called *hadrons*. The hadrons are classified into two kinds, *baryons* and *mesons*. In *constituent quark model*, the baryons are composed of three quarks with different colors among them. On the other hand, the mesons consist of a quark and an anti-quark having opposite colors. Thus the baryons and mesons are always *white*, i.e. color singlet states (Fig. 1.3). Only white particles can be observed in experiments. If one attempts to isolate single quark or gluon from hadrons, infinite energy is required. This is a phenomenological interpretation of *confinement of color*.

Figure 1.3: Baryons and mesons in the constituent quark model.

Deconfinement Phase Transition

The quarks and the gluons are expected to be released from hadrons in extremely high temperature and/or baryon density conditions. In such situations, a large number of hadrons overlap each other and the hadronic matter makes a transition to the quark-gluon one (Fig. 1.4). The quarks and the gluons can exist as isolated state in the matter. This phenomenon is called *deconfinement phase transition*. There are two natural and one artificial candidates where such a deconfined matter is realized. The candidates in nature are *early universe* and *compact stars*. The artificial situation is *heavy ion collisions*. In the early universe and the relativistic heavy ion collision, high temperature

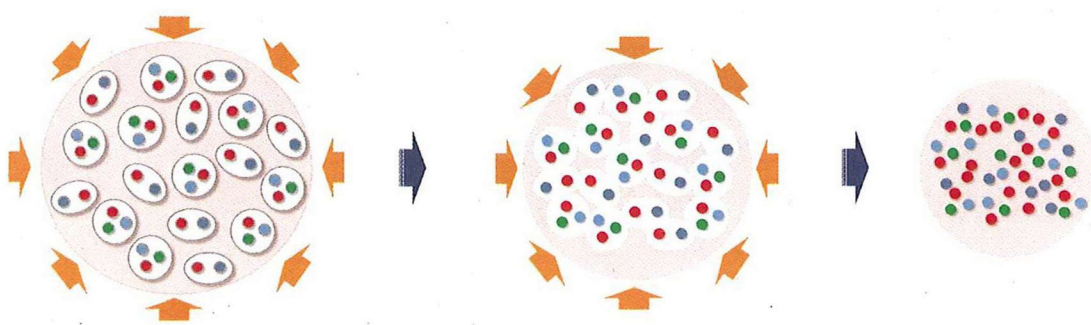

Figure 1.4: An example of deconfinement phase transition.

and low baryon density state is realized. The deconfined matter under such a condition is called *Quark-Gluon Plasma* (QGP) because of an analogy with the ionized plasma. The electrons and nuclei that form the atoms are ionized in the plasma. Similarly the quarks and the gluons that constitute hadrons are separated in the QGP. On the other hand, the deconfined matter at low temperature and high baryon density is expected to be realized inside the compact stars. Another deconfined matter called *color superconductor* is expected to exist there [4, 5]. This matter is an analogy with the electric superconductor. In the case of the electric superconductor, the electrons near the Fermi surface form *Cooper pairs* and show macroscopic collective mode. Since the dense quark matter has the Fermi surface, the quarks also form the Cooper pairs near the Fermi surface at sufficiently low temperature.

QCD Phase Diagram

The matters described by QCD show various aspects depending on temperature and baryon density as discussed above. They are drawn in a T-μ_B plane called *QCD phase diagram* as in Fig. 1.5a. In Fig. 1.5a, the vertical axis denotes the temperature T and the horizontal one is the baryon chemical potential μ_B. The solid phase transition line represents the first order transition. There are expected to exist two critical end points at both ends of the transition line [6, 7]. The deconfined phase transition at high T and low μ_B is expected to be crossover. The transition temperature T_c on high temperature side is about $T_c \simeq 160$ MeV, according to the first principle calculation, i.e. *lattice QCD simulation*. The relativistic heavy ion collisions at RHIC (LHC) reach about $T \simeq 2T_c$ ($5T_c$). The transition baryon chemical potential on the low temperature side is expected to take place at $\mu_{Bc} = 1 - 1.2$ GeV, which is almost the same value that realized at the core of neutron stars. Fig. 1.5b shows another sketch of QCD phase diagram with three light flavors, i.e. up, down, and strange quarks. The bare masses of up and down quarks are treated as the same value $m_u = m_d$ and strange quark is little heavier than them $m_s > m_{u,d}$. As shown in the figure, the deconfined phase transition is believed to be crossover for the case of two light and one heavy flavors $N_f = 2 + 1$.

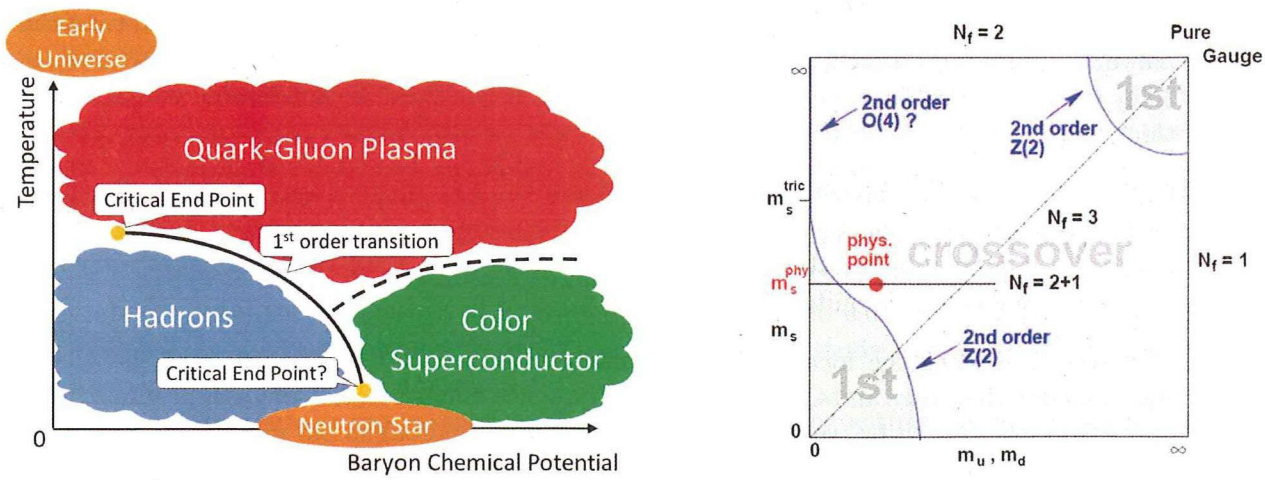

Figure 1.5: a): An illustration of QCD phase diagram in T-μ_B plane. There are expected to exist three main phases that are hadrons, quark-gluon plasma, and color superconductor ones. b): QCD phase diagram with three light quarks [8]. The deconfinement phase transition is believed to be crossover.

Relativistic Heavy Ion Collision

The relativistic heavy ion collision is only practical approach to create QGP on the earth. The basic concept is to collide two heavy nuclei accelerated to almost light speed and produce high temperature and density situation called a fireball. The quarks and the gluons are then deconfined inside the fireball in which QGP is realized. The critical energy density is about $\epsilon_c \simeq 0.5$ Gev/fm^3 which is corresponding to $T_c \simeq 160$ MeV. In the relativistic heavy ion collisions at RHIC (LHC), the energy density reaches $\epsilon \simeq 5$ GeV/fm^3 (15 GeV/fm^3). It is thus expected that QGP can be created in the present heavy ion experiments. Space-time evolution of the relativistic heavy ion collisions based on Bjorken picture [9] is shown below:

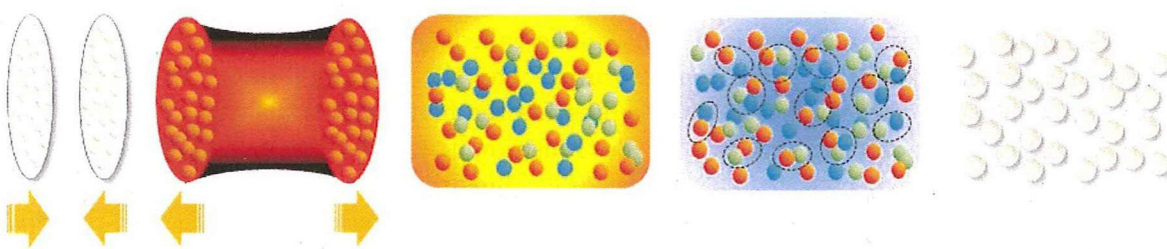

Figure 1.6: Cartoon of a relativistic heavy ion collisions.

1. Accelerate heavy nuclei such as ^{197}Au (^{208}Pb) up to $\sqrt{s} = 200$ (5600) $\times A$ GeV at RHIC, Relativistic Heavy Ion Collider (LHC, Large Hadron Collider), where $\sqrt{s}$ represents the colliding energy at the center of mass frame of two nuclei. Each nucleus is compressed because of Lorentz contraction. The nuclei are composed of valence quarks with high momentum which carry the net baryon number, and gluons and sea quarks (quark and anti-quark pairs) with low momentum. They are also called fast and slow partons, respectively. Thus the accelerated nuclei have some thickness.

2. Collide the heavy nuclei with each other. While the fast partons pass through the other nucleus, the slow ones form the fireball with high temperature and low baryon density. Since this stage is in non-equilibrium state and the farthest away from observation in heavy ion collisions, theoretical prediction is quite difficult.

3. The system reaches the local thermodynamical equilibrium. The quarks and the gluons are deconfined in this stage and QGP is created. The space-time evolution of QGP produced at RHIC and LHC is known to be well described by *relativistic hydrodynamic models*. The temperature decreases with the expansion of the system.

4. The quarks and the gluons are confined inside the hadrons again with decreasing temperature and the number of each species is frozen (*chemical freeze-out*). The hadrons repeat the inelastic collisions among of them and exchange their momenta with each other. The system then reaches the kinetic equilibrium and the hadrons no longer interact (*kinetic freeze-out*). At last, the hadrons are observed by detectors.

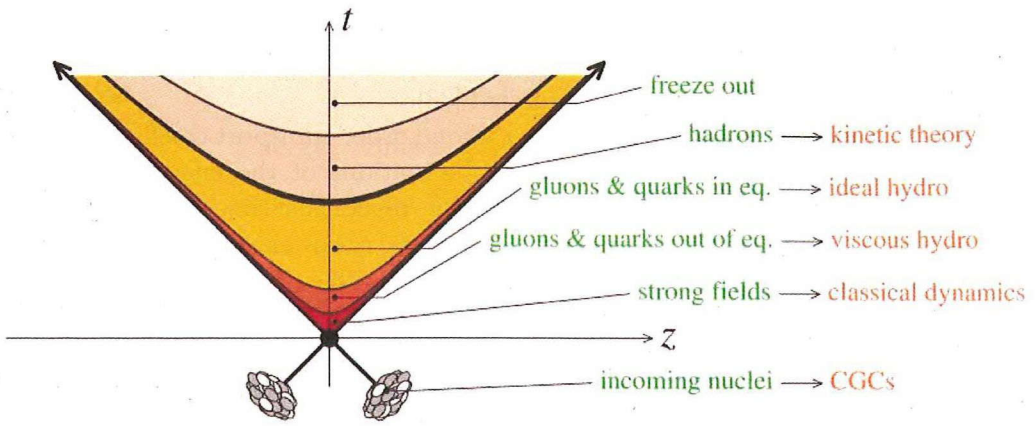

Figure 1.7: Space-time evolution of relativistic heavy ion collisions from Ref. [10].

This is a brief current of the relativistic heavy ion collisions. One of the highlights at RHIC is a success of ideal hydrodynamic descriptions for the space-time evolution of QGP created by heavy ion collisions [11, 12, 13, 14, 15]. Furthermore LHC also supports the hydrodynamic picture of QGP [16, 17]. This novel feature revealed that the QGP is a strongly coupled and/or correlated system, which is one of the most significant subjects over broad areas in physics.

Purpose

Although the success of relativistic hydrodynamic models at RHIC provided a new aspect of hot QCD matter for us, the hydrodynamic simulation depends on various input parameters, such as the equation of state and the transport coefficients, and contains ambiguity. Recently, for more quantitative argument the importance of dissipative effects in the hydrodynamic models has been recognized [18, 19, 20, 21]. Thus theoretical comprehension of the transport coefficients is desirable.

The simplest relativistic dissipative hydrodynamics is the first order theory, which in the non-relativistic limit reduces to Navier-Stokes theory [22, 23]. The first order theory is, however, accompanied with the acausal problem and instability in numerical simulations [24, 25]. One of the strategies to evade these problems is to extend the theory up to second order with respect to dissipative currents [26, 27]. In the second order theory, however, there appear new phenomenological parameters as second order transport coefficients in addition to the first order ones. These transport coefficients cannot be determined within the framework of hydrodynamics. Ab initio calculation based on microscopic theory, i.e. QCD in the case of heavy ion collisions, is required to study and constrain the parameters in the dissipative hydrodynamic models.

Since the temperature range realized at RHIC and LHC is not within the reach of perturbation theory due to the asymptotic freedom of QCD, we need to employ some non-perturbative approach to investigate the transport coefficients of the hot QCD matter. At present, lattice QCD simulation is the only systematic way to calculate physical quantities in such a non-perturbative situation. There are several pioneering works which analyzed the transport coefficients by lattice QCD simulations [28, 29, 30, 31, 32]. These works have used Kubo formulas, which relate the first order transport coefficients to a low energy behavior of corresponding spectral functions. In this approach, one needs to extract the spectral functions from Euclidean correlators measured on the lattice. This step is,

however, non-trivial because of an ill-posed problem [33].

In this thesis, we focus on the ratios of first and second order transport coefficients. In Refs. [34, 35], it is argued that the ratios are related to static fluctuations of the energy-momentum tensor by rewriting the classical limit of Kubo formulas with the relaxation time approximation. We modify their arguments to treat quantum systems and show that the ratios are related to canonical correlations of the energy-momentum tensor. It enables us to evade the difficulty in analysis of spectral functions and obtain the ratios directly from lattice QCD simulations. Whereas the ratios themselves are not the transport coefficients, analysis of them can constrain free phenomenological parameters of the dissipative hydrodynamic models. We note that a similar argument has been also given in Ref. [36, 37].

We need to regularize the canonical correlations to extract physical quantities because they are ultraviolet divergent. We perform the regularization by vacuum subtraction. In addition to this prescription, we argue a contribution from contact terms. This contribution is usually removed solely by the vacuum subtraction, because the coefficients of contact terms are not dependent on the temperature. However, the coefficients of contact terms in the canonical correlation of energy-momentum tensor are proportional to the energy-momentum tensor. Therefore the contact terms are dependent on the temperature and cannot be removed by the vacuum subtraction. Thus we must deal with the contact terms separately besides the vacuum subtraction.

The structure of this thesis is as follows. In Chapter 2, we review the basics of QCD and the lattice gauge theory at finite temperature. The lattice gauge theory is that the field theory defined on the discretized space-time. We introduce the fermion and gauge actions on the lattice, and then discuss the confinement of quarks and the deconfinement phase transition for pure gauge theory. We also argue thermodynamics on the lattice in this chapter. In Chapter 3, we discuss the Monte Carlo method for lattice QCD simulations. What we obtain from the simulations are equilibrium expectation values of various physical quantities with statistical errors. We see how to obtain the statistical expectation values from lattice QCD simulations. The relativistic hydrodynamics is argued in Chapter 4. We present the first and second order dissipative hydrodynamics with a phenomenological derivation by Israel and Stewart [27]. We show how to introduce the relaxation times of each dissipative current to hydrodynamics. Also the causality conditions for pure gauge theory are introduced in this chapter. In Chapter 5, we derive formulas that relate the ratios of transport coefficients to the canonical correlation of energy-momentum tensor. First we see the classical formulations in Refs. [34, 35] and then derive the quantum ones. We also discuss how to remove the unphysical divergence and to extract the ratios with physical meaning from the canonical correlations. We formulate a method to observe the ratios on the lattice and show numerical results in SU(3) lattice gauge theory in Chapter 6. The ratios of transport coefficients are related to characteristic speeds of plane wave propagating in medium. From the analyses, we also argue the causality in the second order dissipative hydrodynamics. The last chapter is devoted to conclusions and outlooks.

Notation

In the present paper, we use the natural unit $\hbar = c = k_B = 1$,

$$\hbar = \frac{h}{2\pi} = 6.5821 \times 10^{-25}\,\mathrm{GeV}\cdot\mathrm{s} = 1, \tag{1.6}$$

$$c = 2.9979 \times 10^{8}\,\mathrm{m}\cdot\mathrm{s}^{-1} = 1, \tag{1.7}$$

$$k_B = 8.6173 \times 10^{-14}\,\mathrm{GeV}\cdot\mathrm{K}^{-1} = 1, \tag{1.8}$$

where h, c, and k_B are Planck constant, the speed of light, and Boltzmann constant, respectively. In

this unit, one obtains

$$[\text{energy}] = [\text{mass}] = [\text{time}]^{-1} = [\text{length}]^{-1}. \tag{1.9}$$

A useful relation is obtained from these conventions,

$$\hbar c = 197.33\,\text{MeV} \cdot \text{fm} \simeq 200\,\text{MeV} \cdot \text{fm} = 1. \tag{1.10}$$

We adopt the metric tensor in Minkowski space-time as follows

$$g_{\mu\nu} = g^{\mu\nu} = \begin{pmatrix} 1 & 0 & 0 & 0 \\ 0 & -1 & 0 & 0 \\ 0 & 0 & -1 & 0 \\ 0 & 0 & 0 & -1 \end{pmatrix}. \tag{1.11}$$

The Greek indices denote four-dimensional space-time ; $\mu, \nu, \rho, ... = 0, 1, 2, 3 = t, x, y, z$. The Roman indices denote three spatial components ; $i, j, k, ... = 1, 2, 3$ or x, y, z. Arbitrary four-vectors are represented as

$$x^\mu = (x^0, x^1, x^2, x^3), \qquad x_\mu = g_{\mu\nu} x^\nu = (x^0, -x^1, -x^2, -x^3). \tag{1.12}$$

The same indices are summed,

$$x_\mu y^\mu = \sum_{\mu=0}^{3} x_\mu y^\mu, \qquad x_i y^i = \sum_{i=1}^{3} x_i y^i. \tag{1.13}$$

The inner product in Minkowski space-time is defined by

$$x \cdot y = g_{\mu\nu} x^\mu y^\nu = x^0 y^0 - x^1 y^1 - x^2 y^2 - x^3 y^3 = x^0 y^0 - \vec{x} \cdot \vec{y}. \tag{1.14}$$

The metric tensor in Euclidean space is given by

$$\delta_{\mu\nu} = \begin{pmatrix} 1 & 0 & 0 & 0 \\ 0 & 1 & 0 & 0 \\ 0 & 0 & 1 & 0 \\ 0 & 0 & 0 & 1 \end{pmatrix}. \tag{1.15}$$

In this case, the Greek indices denote four-dimensional space ; $\mu, \nu, \rho, ... = 1, 2, 3, 4$ or x, y, z, τ. The inner product in Euclidean space is defined by

$$x \cdot y = \delta_{\mu\nu} x_\mu y_\nu = x_0 y_0 + x_1 y_1 + x_2 y_2 + x_3 y_3 = x_0 y_0 + \vec{x} \cdot \vec{y}. \tag{1.16}$$

In the standard representation, the Dirac matrices in Minkowski space are given by

$$\gamma^0 = \begin{pmatrix} 1 & 0 \\ 0 & -1 \end{pmatrix}, \qquad \gamma^i = \begin{pmatrix} 0 & \sigma_i \\ -\sigma_i & 0 \end{pmatrix}, \qquad \gamma^5 = i\gamma^0\gamma^1\gamma^2\gamma^3 = \begin{pmatrix} 0 & 1 \\ 1 & 0 \end{pmatrix}, \tag{1.17}$$

where σ_i are the Pauli matrices,

$$\sigma_1 = \begin{pmatrix} 0 & 1 \\ 1 & 0 \end{pmatrix}, \qquad \sigma_2 = \begin{pmatrix} 0 & -i \\ i & 0 \end{pmatrix}, \qquad \sigma_3 = \begin{pmatrix} 1 & 0 \\ 0 & -1 \end{pmatrix}. \tag{1.18}$$

The Dirac matrices satisfy the anti-commutation relation

$$\{\gamma^\mu, \gamma^\nu\} = 2g^{\mu\nu}. \tag{1.19}$$

In the Euclidean space, the Dirac matrices are defined as follows,

$$\gamma_\mu = (\gamma_i, \gamma_4) = (\gamma^i, i\gamma^0), \qquad \{\gamma_\mu, \gamma_\nu\} = -2\delta_{\mu\nu}. \tag{1.20}$$

Chapter 2

Lattice QCD

In 1974, K. G. Wilson showed the confinement of quarks with the lattice gauge theory in the strong coupling limit [38]. After that the first numerical simulations of lattice gauge theory were performed by M. Creutz [39, 40, 41], and the lattice gauge theory has achieved success in many studies, e.g. critical temperature, static quark potential, hadronic mass spectrum, and equation of state, and so on [42, 43, 44, 45, 46, 47, 48, 49, 50]. The lattice gauge theory is the only non-perturbative approach based on the first principle in QCD physics and is applied not only to QCD but also to Quantum Electodynamics (QED) [51, 52] or supersymmetric theory [53, 54]. The field theory defined on the lattice has some advantages. Since the space-time is discretized and a momentum cut-off is introduced to the lattice gauge theory, the divergence that troubles the continuum field theory is naturally removed on the lattice. Moreover a gauge fixing procedure is not required on the lattice because the number of degrees of freedom of gauge field is finite. In this chapter, we overview the lattice gauge theory, especially its application to QCD at finite temperature. We also refer to the phase transition and thermodynamics in lattice QCD.

2.1 QCD action in the continuum

Quantum Chromodynamics (QCD) is the first principle to describe dynamics of *quarks* $\psi^f_{\alpha,a}(x)$ and *gluons* $A_\mu(x) = \sum_{i=1}^{8} A^i_\mu(x) T^i$, where the index f runs from 1 to N_f, which is the number of flavors. The spinor index is denoted by $\alpha = 1, 2, 3, 4$, the color indices for quarks and gluons by $a = 1, 2, 3$ and $i = 1, 2, ..., 8$, respectively, and Lorentz index $\mu = 1, 2, 3, 4$. T^i are adjoint representations of the SU(3) Lie algebra, which are traceless hermitian 3×3 matrices. The QCD action in Minkowski space-time is given by

$$S_{\rm QCD} = S_{\rm quark} + S_{\rm gluon} \tag{2.1}$$

$$S_{\rm quark} = \sum_{f=1}^{N_f} \int d^4x \, \bar{\psi}^f_{\alpha,a}(x) \left(i(\gamma^\mu)_{\alpha\beta} (D_\mu(x))_{ab} - m^f \delta_{\alpha\beta}\delta_{ab} \right) \psi^f_{\beta,b}(x), \tag{2.2}$$

$$S_{\rm gluon} = -\frac{1}{4} \int d^4x F^i_{\mu\nu}(x) F^{\mu\nu,i}(x). \tag{2.3}$$

Here the covariant derivative D_μ and the field strength tensor $F_{\mu\nu}$ are defined by

$$(D_\mu(x))_{ab} \equiv \delta_{ab}\partial_\mu + ig(A_\mu(x))_{ab}, \tag{2.4}$$

$$F^i_{\mu\nu}(x) \equiv \partial_\mu A^i_\nu(x) - \partial_\nu A^i_\mu(x) - g f_{ijk} [A^j_\mu(x), A^k_\nu(x)], \tag{2.5}$$

where g and f_{ijk} are the coupling constant of strong interaction and the structure constant of SU(3) Lie algebra, respectively. The commutation relation in Eq. (2.5) causes the self-interaction of gluons, which is one of the most important features of QCD. Due to the self-interaction of gluons, QCD shows various non-trivial properties.

The QCD action Eq. (2.1) has local invariance under the SU(3) gauge transformation,

$$\psi(x) \to \psi'(x) = V(x)\psi(x), \quad \bar{\psi}(x) \to \bar{\psi}'(x) = \bar{\psi}(x)V^\dagger(x), \tag{2.6}$$

$$gA_\mu(x) \to gA'_\mu(x) = V(x)(gA_\mu(x) - i\partial_\mu)V^\dagger(x). \tag{2.7}$$

An element of SU(3) group $V(x)$ is defined as $V(x) \equiv e^{-i\theta^a(x)t^a}$, where $\theta^a(x)$ is a transformation parameter and t^a is the fundamental representation of SU(3) Lie algebra. Under the gauge transformation Eqs. (2.6) and (2.7), $D_\mu(x)$ and $F_{\mu\nu}(x)$ transform covariantly,

$$D_\mu(x) \to D'_\mu(x) = V(x)D_\mu(x)V^\dagger(x), \tag{2.8}$$

$$F_{\mu\nu}(x) \to F'_{\mu\nu}(x) = V(x)F_{\mu\nu}(x)V^\dagger(x). \tag{2.9}$$

In the following, we describe the QCD action simply,

$$S_{QCD} = \int d^4x\, \bar{\psi}(x)(i\gamma_\mu D^\mu - m)\psi(x) - \frac{1}{4}\int d^4x\, F^i_{\mu\nu}(x)F^{\mu\nu,i}(x). \tag{2.10}$$

2.2 QCD action on the lattice

2.2.1 Fermion action

The basic idea of lattice gauge theory is to define the theory on the discretized space-time. In order to formulate the lattice QCD, we start from the single flavor free fermion action in the continuum four-dimensional Euclidean space,

$$S_F^{\text{cont}}[\psi, \bar{\psi}] = \int d^4x\, \bar{\psi}(x)(\gamma_\mu\partial_\mu + m)\psi(x). \tag{2.11}$$

The partial derivative is replaced by the finite difference on the lattice,

$$\partial_\mu\psi(x) \to \frac{1}{2a}(\psi(n+\hat{\mu}) - \psi(n-\hat{\mu})). \tag{2.12}$$

where a and n are the lattice spacing and the lattice site, $x = na$, respectively. $n \pm \hat{\mu}$ denote the nearest neighbor sites of n along μ-direction. Thus the free fermion action on the lattice is given by

$$S_F^{\text{lat}}[\psi, \bar{\psi}] = a^4 \sum_n \bar{\psi}(n)\left(\sum_{\mu=1}^{4}\gamma_\mu \frac{\psi(n+\hat{\mu}) - \psi(n-\hat{\mu})}{2a} + m\psi(n)\right). \tag{2.13}$$

We impose the same gauge transformation as Eq. (2.6) on the lattice fermion field,

$$\psi(n) \to \psi'(n) = V(n)\psi(n), \quad \bar{\psi}(n) \to \bar{\psi}'(n) = \bar{\psi}(n)V^\dagger(n). \tag{2.14}$$

Since $\bar{\psi}(n)\psi(n \pm \hat{\mu})$ in Eq.(2.13) are not gauge invariant,

$$\bar{\psi}(n)\psi(n \pm \hat{\mu}) \to \bar{\psi}'(n)\psi'(n \pm \hat{\mu}) = \bar{\psi}(n)V^\dagger(n)V(n \pm \hat{\mu})\psi(n \pm \hat{\mu}), \tag{2.15}$$

we introduce *link variables* $U_\mu(n)$ (Fig. 2.1), which play a role of the gauge fields on the lattice and transform under the gauge transformation as

$$U_\mu(n) \to U'_\mu(n) = V(n)U_\mu(n)V^\dagger(n+\hat{\mu}). \tag{2.16}$$

Then the gauge invariant quantity is obtained

$$\bar{\psi}'(n)U'_\mu(n)\psi'(n+\hat{\mu}) = \bar{\psi}(n)V^\dagger(n)V(n)U_\mu(n)V^\dagger(n+\hat{\mu})V(n+\hat{\mu})\psi(n+\hat{\mu}) \tag{2.17}$$

$$= \bar{\psi}(n)U_\mu(n)\psi(n). \tag{2.18}$$

Thus the gauge invariant fermion action is given by

$$S_F^{\rm lat}[\psi,\bar{\psi},U] = a^4\sum_n \bar{\psi}(n)\left(\sum_{\mu=1}^{4}\gamma_\mu\frac{U_\mu(n)\psi(n+\hat{\mu}) - U_\mu^\dagger(n-\hat{\mu})\psi(n-\hat{\mu})}{2a} + m\psi(n)\right). \tag{2.19}$$

Note that a fermion propagator derived from Eq. (2.19) includes a problem called *doubling problem* [55, 56]. The fermion propagator has one physical and 15 unphysical poles. The unphysical poles are called *doublers* [1]. To avoid the doubling problem, several lattice fermions are proposed [57, 58, 59, 60, 61, 62, 63].

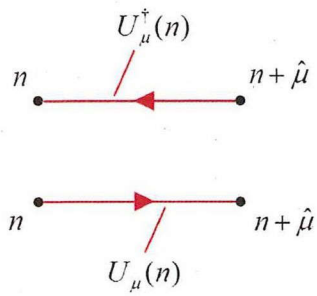

Figure 2.1: Link variables.

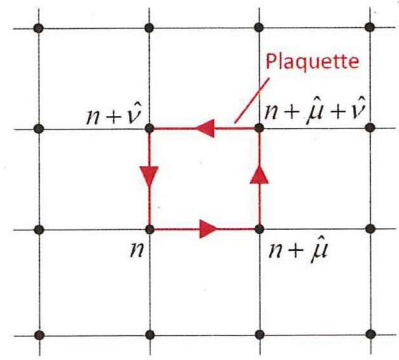

Figure 2.2: Plaquette.

2.2.2 Gauge action

SU(N_c) gauge action [2] in the continuum Euclidean space is given by

$$S_G^{\rm cont}[A] = \frac{1}{4}\int d^4x F^i_{\mu\nu}F^i_{\mu\nu}. \tag{2.20}$$

The corresponding gauge action on the lattice proposed by Wilson [38] is written as

$$S_G^{\rm lat}[U] = \frac{2N_c}{g^2}\sum_n\sum_{\mu<\nu}\left(1 - \frac{1}{N_c}{\rm Re\ Tr}\, U_{\mu\nu}(n)\right), \tag{2.21}$$

[1] In D-dimensional space, $2^D - 1$ doublers exist.

[2] Here we argue general case for the number of colors N_c. If one sets $N_c = 3$, the gauge theory corresponds to QCD.

where g is the bare coupling constant. The trace Tr is taken over the color charge indices. *Plaquette*, $U_{\mu\nu}(n)$, is defined by the product of the link variables along the smallest square on the lattice in μ-ν plane (Fig. 2.2),

$$U_{\mu\nu}(n) = U_\mu(n)U_\nu(n+\hat{\mu})U_\mu^\dagger(n+\hat{\nu})U_\nu^\dagger(n). \tag{2.22}$$

Trace of the plaquette is a gauge invariant quantity and one of the fundamental observables in lattice simulations. Link variables and gauge fields are related to each other by the following relation,

$$U_\mu(n) = \exp[igaA_\mu(n)], \qquad U_\mu^\dagger(n) = \exp[-igaA_\mu(n)]. \tag{2.23}$$

Using this relation, one can easily confirm that the Wilson gauge action Eq. (2.21) reproduces Eq. (2.20) in the continuum limit $a \to 0$. In the following argument, we exclusively consider the gauge theory on the lattice and abbreviate the indices "cont" and "lat".

2.3 Lattice QCD without quarks

2.3.1 Wilson loop and strong coupling expansion

Wilson loop is one of the basic observables in lattice simulations. The Wilson loop on the lattice is composed of the products of link variables along a closed path C,

$$W(C) \equiv \mathrm{Tr}\left[\prod_{i\in C} U_i\right] \quad \text{(path ordered)}. \tag{2.24}$$

It is obvious that $W(C)$ is gauge invariant from Eq. (2.16). The smallest Wilson loop corresponds to the trace of the plaquette. In the following, we consider a rectangular path $n_\sigma \times n_\tau$ in μ-ν plane as a closed path C (for example, Fig. 2.3).

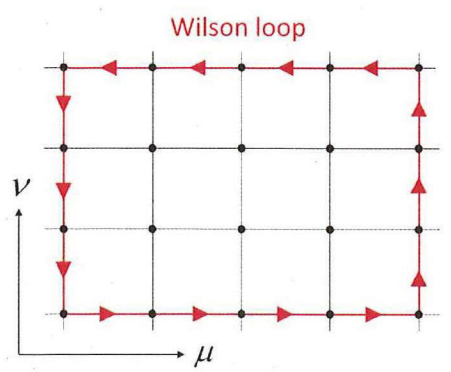

Figure 2.3: Rectangular path.

The vacuum expectation value of some observable O in pure SU(3) gauge theory can be written with path integral formalism as

$$\langle O\rangle = \frac{1}{Z}\int \mathcal{D}U\, O\, e^{-S_G[U]} = \frac{1}{Z}\int \prod_n \prod_{\mu=1}^{4} dU_\mu(n)\, O\, e^{-S_G[U]} \tag{2.25}$$

$$Z = \int \mathcal{D}U\, e^{-S_G[U]}. \tag{2.26}$$

Using the Wilson gauge action Eq. (2.21) and Eq. (2.25), the vacuum expectation value of the Wilson loop becomes

$$\langle W(C)\rangle = \frac{1}{Z}\int \mathcal{D}U\, W(C) \left[\exp[-\frac{2}{g^2}\sum_n\sum_{\mu<\nu}(1-\mathrm{Re\,Tr}\, U_{\mu\nu}(n))]\right] \tag{2.27}$$

$$= \frac{1}{Z'}\int \mathcal{D}U\, W(C) \left[\exp[\frac{1}{g^2}\sum_n\sum_{\mu\neq\nu}(\mathrm{Tr}\, U_{\mu\nu}(n)+\mathrm{Tr}\, U^\dagger_{\mu\nu}(n))]\right]. \tag{2.28}$$

Here Z' means that the constant terms in Eq. (2.27) are canceled out between numerator and denominator. In the second equality, the following relation has been also used,

$$\sum_{\mu<\nu}\mathrm{Re\,Tr}\, U_{\mu\nu}(n) = \sum_{\mu\neq\nu}\frac{1}{2}(\mathrm{Tr}\, U_{\mu\nu}(n)+\mathrm{Tr}\, U^\dagger_{\mu\nu}(n)). \tag{2.29}$$

Now let us consider how to calculate the Wilson loop in Fig. 2.3 for the strong coupling case $g \gg 1$. In this case, the exponential can be expanded in terms of g^{-2}. First we focus on the link variables on the bottom-left corner. The expectation value of the Wilson loop then reduces to

$$\langle W(C)\rangle = \frac{1}{Z'}\int \mathcal{D}U\, W(C) \prod_n\prod_{\mu\neq\nu}(1+\frac{1}{g^2}\mathrm{Tr}\, U_{\mu\nu}(n)+\frac{1}{g^2}\mathrm{Tr}\, U^\dagger_{\mu\nu}(n)+O(\frac{1}{g^4})). \tag{2.30}$$

The first and second terms vanish by performing the group integration. If one describes $W(C)$ as

$$W(C) = \mathrm{Tr}[U_\mu(n)\hat{V}U^\dagger_\nu(n)], \tag{2.31}$$

a contribution from the third term in Eq. (2.30) is calculated as

$$\begin{aligned}
&\frac{1}{g^2}\int dU_\mu(n)dU_\nu(n)\, W(C)\, \mathrm{Tr}[U^\dagger_{\mu\nu}(n)] \\
=&\frac{1}{g^2}\int dU_\mu(n)dU_\nu(n)\, \mathrm{Tr}[U_\mu(n)\hat{V}U^\dagger_\nu(n)]\, \mathrm{Tr}[U_\nu(n)U_\mu(n+\hat{\nu})U^\dagger_\nu(n+\hat{\mu})U^\dagger_\mu(n)] \\
=&\frac{1}{g^2}\int dU_\mu(n)\, [U_\mu(n)\hat{V}]_{ab}\int dU_\nu(n)\, [U^\dagger_\nu(n)]_{ba}[U_\nu(n)]_{cd}[U_\mu(n+\hat{\nu})U^\dagger_\nu(n+\hat{\mu})U^\dagger_\mu(n)]_{dc} \\
=&\frac{1}{g^2N_c}\mathrm{Tr}\,[\hat{V}U_\mu(n+\hat{\nu})U^\dagger_\nu(n+\hat{\mu})].
\end{aligned} \tag{2.32}$$

Thus the factor $1/(g^2N_c)$ appears from the third term in Eq. (2.30) for each plaquette in the Wilson loop. $\langle W(C)\rangle$ becomes

$$\langle W(C)\rangle \propto (g^2N_c)^{-n_\sigma n_\tau}\mathrm{Tr}[1] = N_c\exp[-n_\sigma n_\tau \ln(g^2N_c)]. \tag{2.33}$$

We show this procedure in Fig. 2.4 schematically.

$\langle W(C)\rangle$ with large n_τ is expected to behave as

$$\langle W(C)\rangle \propto \exp[-n_\tau V(n_\sigma)] \quad \text{for} \quad n_\tau \gg 1, \tag{2.34}$$

where $V(n_\sigma)$ is a potential energy between infinitely heavy quark and anti-quark separated by the distance n_σ on the lattice. Wilson loop can be interpreted as the energy required for the process that

a massive quark and an anti-quark pair is generated at $t = 0$ with the distance n_σ and then annihilates each other at $t = n_\tau$. Comparing Eq. (2.33) with Eq. (2.34), $V(n_\sigma)$ reads

$$V(n_\sigma) = n_\sigma \ln(g^2 N_c). \tag{2.35}$$

Using dimensional distance $r = an_\sigma$, the static quark potential is rewritten as

$$V(r) = \frac{1}{a^2} r \ln(g^2 N_c) \equiv \sigma r, \tag{2.36}$$

$$\sigma = \frac{1}{a^2} \ln(g^2 N_c), \tag{2.37}$$

where σ denotes the string tension of the massive quark and anti-quark pair.

The behavior that $\langle W(C) \rangle$ is proportional to the area of a rectangular path in Eq. (2.33) is called *area law*. When $\langle W(C) \rangle$ shows the area law, the static potential between quarks becomes linear potential as in Eq. (2.36). If one attempts to separate the quark and anti-quark, the potential energy is proportional to their distance and increases infinitely. One thus needs infinite energy to obtain free quarks. This phenomenon is called *confinement of quarks*. In the actual case, the separated quark and anti-quark are divided into new pairs when the potential energy becomes large enough to generate a quark and an anti-quark.

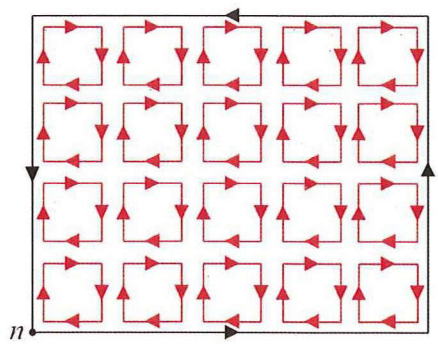

Figure 2.4: Leading contribution to $\langle W_c \rangle$ in the strong coupling expansion.

2.3.2 Polyakov loop and phase transition

Polyakov loop is a useful observable to describe the deconfinement phase transition [64] in the lattice simulation [65, 66, 67, 68, 69, 70]. It is defined by

$$P(\vec{n}) \equiv \frac{1}{N_c} \mathrm{Tr} \left[\prod_{n_4=1}^{N_\tau - 1} U_4(\vec{n}, n_4) \right]. \tag{2.38}$$

N_τ is the number of lattice sites in the temporal direction. The reason why $P(\vec{n})$ is called the Polyakov *loop* is that this quantity is constructed by the product of all temporal link variables and forms a closed loop along the temporal direction with the periodic boundary condition as shown in Fig. 2.5. The periodic boundary condition is generally imposed on a finite temperature system as will be discussed in the next section. The expectation value of the Polyakov loop is related to the free energy of an isolated quark F_q

$$\langle P(\vec{n}) \rangle \propto e^{-F_q/T}, \tag{2.39}$$

where T denotes the temperature. Since the value of the Polyakov loop is independent of its spatial position, one can rewrite $\langle P(\vec{n})\rangle$ by the spatial average

$$P \equiv \frac{1}{N_\sigma^3}\sum_{\vec{n}} P(\vec{n}), \tag{2.40}$$

where N_σ is the number of spatial lattice sites. Eq. (2.39) indicates that the expectation value of the Polyakov loop can be regarded as an order parameter of a deconfinement phase transition, i.e.

$$\langle P\rangle = 0 \Leftrightarrow F_q = \infty \Leftrightarrow \text{Confinement}, \tag{2.41}$$

$$\langle P\rangle \neq 0 \Leftrightarrow F_q = \text{finite} \Leftrightarrow \text{Deconfinement}. \tag{2.42}$$

Moreover the spatial correlation function of the Polyakov loops is expected to behave as

$$\langle P(\vec{m})P^\dagger(\vec{n})\rangle \propto e^{-V(r)/T}, \qquad r \equiv a|\vec{m}-\vec{n}|, \tag{2.43}$$

where $V(r)$ denotes the static quark potential as seen in the last subsection. Therefore the correlation function Eq. (2.43) in the long distance limit vanishes

$$\lim_{r\to\infty}\langle P(\vec{m})P^\dagger(\vec{n})\rangle = \langle P(\vec{m})\rangle\langle P^\dagger(\vec{n})\rangle = |\langle P\rangle|^2 = 0. \tag{2.44}$$

In this way, the non-abelian SU(N_c) gauge theory is expected to show the phase transition at some critical temperature T_c (see also appendix A).

Let us assume the case of $N_c = 3$. The action of SU(3) gauge theory has a Z(3) global symmetry. Under this symmetry transformation, the Polyakov loop transforms as

$$P \to zP, \qquad z = 1, e^{2\pi i/3}, e^{4\pi i/3}, \tag{2.45}$$

where z are the group elements of Z(3). Then $\langle P\rangle$ is regarded as an order parameter for the Z(3) global transformation

$$\langle P\rangle = 0 \ (\text{low } T) \Leftrightarrow \text{Z(3) symmetry unbroken}, \tag{2.46}$$

$$\langle P\rangle \neq 0 \ (\text{high } T) \Leftrightarrow \text{Z(3) symmetry broken}. \tag{2.47}$$

The order of the phase transition can be analyzed by three-dimensional effective theory. With an appropriate gauge transformation, all link variables $U_4(\vec{n}, n_4)$ can be set to the unit SU(3) matrix except $n_4 = 1$ in Eq. (2.38). The Polyakov loop then becomes

$$P(\vec{n}) = \frac{1}{3}\mathrm{Tr}[U_4(\vec{n}, 1)]. \tag{2.48}$$

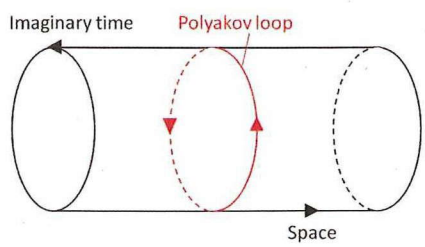

Figure 2.5: Polyakov loop.

Integrating out the spatial link variables, an effective SU(3) spin theory in three dimensions which describes the interactions of U_4 on the time slice $n_4 = 1$ is derived. If one considers the nearest neighbor interactions for the effective theory, its universality class is the same as that of the three state Potts model in three dimensions having a first order phase transition. Therefore the phase transition of SU(3) gauge theory is expected to be the first order.

2.4 Thermodynamics in Lattice QCD

2.4.1 Thermal expectation value in the continuum

According to quantum statistical mechanics, the expectation value of some physical operator O in thermal equilibrium is given by

$$\langle O \rangle = \frac{1}{Z} \mathrm{Tr}\,[O e^{-\frac{H}{T}}] = \frac{1}{Z} \int dn\, \langle n | O e^{-\frac{H}{T}} | n \rangle, \tag{2.49}$$

$$Z = \int dn\, \langle n | e^{-\frac{H}{T}} | n \rangle, \tag{2.50}$$

where H is Hamiltonian in Euclidean space. Using path integral formalism, the partition function Z is rewritten as follows :

$$Z = \int \mathcal{D}q\, e^{-\int_0^{1/T} dt L[q,\dot{q}]} = \int \mathcal{D}q\, e^{-S[q,\dot{q}]}, \tag{2.51}$$

$$\int \mathcal{D}q \equiv \int \prod_{i=1}^{n} dq_i, \tag{2.52}$$

where L and S are the Lagrangian and the action, respectively. Applying this formulation to QCD naively, the partition function reads

$$Z = \int \mathcal{D}A_\mu \mathcal{D}\psi \mathcal{D}\bar{\psi}\, e^{-S_{QCD}[A_\mu,\psi,\bar{\psi}]}, \tag{2.53}$$

$$S_{QCD}[A_\mu,\psi,\bar{\psi}] = S_F[A_\mu,\psi,\bar{\psi}] + S_G[A_\mu], \tag{2.54}$$

where the fermion and the gauge actions in Euclidean space are given by

$$S_F = \int_0^{1/T} dt \int d^3x \bar{\psi}(\gamma_\mu D_\mu + m)\psi, \tag{2.55}$$

$$S_G = \int_0^{1/T} dt \int d^3x \frac{1}{4} F^i_{\mu\nu} F^i_{\mu\nu}. \tag{2.56}$$

Anti-periodic and periodic boundary conditions are imposed on the fermion and the gauge fields, respectively :

$$\psi(\vec{x},0) = -\psi(\vec{x},T^{-1}), \qquad \bar{\psi}(\vec{x},0) = -\bar{\psi}(\vec{x},T^{-1}), \qquad A_\mu(\vec{x},0) = A_\mu(\vec{x},T^{-1}). \tag{2.57}$$

Thus the thermal expectation values in QCD can be written as

$$\langle O \rangle = \frac{\int \mathcal{D}A_\mu \mathcal{D}\psi \mathcal{D}\bar{\psi}\, O\, e^{-S_{QCD}[A_\mu,\psi,\bar{\psi}]}}{\int \mathcal{D}A_\mu \mathcal{D}\psi \mathcal{D}\bar{\psi}\, e^{-S_{QCD}[A_\mu,\psi,\bar{\psi}]}}. \tag{2.58}$$

Note that the quantization of QCD accompanies a divergence in the partition function Eq. (2.53) which arises from the infinite number of degrees of freedom of the gauge fields which are equivalent to each other. To avoid the divergence, *gauge fixing* is performed in the continuum theory. On the other hand, the lattice gauge theory does not require the prescription because of the finite degrees of freedom of the gauge fields on the lattice.

2.4.2 Thermal expectation value on the lattice

From Eq. (2.58), the thermal expectation value of some physical quantity O on the lattice is given by

$$\langle O \rangle = \frac{\int \mathcal{D}U\mathcal{D}\psi\mathcal{D}\bar{\psi}\, O\, e^{-S_F[U,\psi,\bar{\psi}]-S_G[U]}}{\int \mathcal{D}U\mathcal{D}\psi\mathcal{D}\bar{\psi}\, e^{-S_F[U,\psi,\bar{\psi}]-S_G[U]}} = \frac{\int \mathcal{D}U\, O\, \mathrm{Det}F[U]\, e^{-S_G[U]}}{\int \mathcal{D}U\, \mathrm{Det}F[U]\, e^{-S_G[U]}}. \tag{2.59}$$

where we have performed the Grassmann integral for multiple variables

$$\int \mathcal{D}\psi\mathcal{D}\bar{\psi}\, e^{-\bar{\psi}(m)F[U]\psi(n)} = \mathrm{Det}F[U]. \tag{2.60}$$

The fermion determinant $\mathrm{Det}F[U]$ is taken for all indices of F, which are space-time coordinates, spinor, color, and flavor. The relations similar to Eqs. (2.57) hold on the lattice :

$$\psi(\vec{n},0) = -\psi(\vec{n},N_\tau), \qquad \bar{\psi}(\vec{n},0) = -\bar{\psi}(\vec{n},N_\tau), \qquad U_\mu(\vec{n},0) = U_\mu(\vec{n},N_\tau). \tag{2.61}$$

In *quench approximation*, the fermion determinant is replaced by unity, $\mathrm{Det}F[U] = 1$. This corresponds to an approximation that dynamical quark loops, i.e. vacuum polarizations are neglected. In the case of pure SU(3) gauge theory, there are no quarks intrinsically and the thermal expectation value Eq. (2.59) is given by

$$\langle O \rangle = \frac{\int \mathcal{D}U\, O\, e^{-S_G[U]}}{\int \mathcal{D}U\, e^{-S_G[U]}}. \tag{2.62}$$

The numbers of lattice sites in spatial and temporal directions are related to the spatial volume V and temperature T as follows :

$$V = (a_\sigma N_\sigma)^3, \qquad T = \frac{1}{a_\tau N_\tau}. \tag{2.63}$$

Here a_σ and a_τ are the lattice spacings of spatial and temporal directions, respectively. As seen in Eq. (2.63), we must prepare the large number of N_σ to simulate the thermodynamical limit and N_τ for the vacuum, respectively.

2.4.3 QCD thermodynamics on the lattice

Before discussing the thermodynamics on the lattice, let us recall several thermodynamic relations in the continuum space-time. The fundamental quantity in equilibrium thermodynamics is the partition function or the free energy density

$$f = -\frac{T}{V} \ln Z(T,V). \tag{2.64}$$

Basic thermodynamic quantities can be derived from the partition function. In the thermodynamic limit, the pressure can be directly obtained from the free energy density, $P = -f$. Using this relation, one obtains other quantities such as the energy density ϵ or the entropy density s

$$\frac{\epsilon - 3P}{T^4} = T\frac{\partial}{\partial T}\frac{P}{T^4}, \tag{2.65}$$

$$\frac{s}{T^3} = \frac{1}{T^3}\frac{\partial P}{\partial T}. \tag{2.66}$$

In the high temperature limit (Stefan-Boltzmann (SB) limit), the thermodynamic quantities approach those of the ideal gas of free quarks and gluons due to the asymptotic freedom, $\epsilon = 3P$ (see appendix A). The deviations of thermodynamic quantities from the SB limit have been studied by perturbative method in the high temperature region. On the other hand, lattice QCD simulations have been used as one of the non-perturbative methods in the low temperature region, where temperature is less than several times Λ_{QCD}.

The direct calculation of the partition function is, however, impossible on the lattice. Instead, the expectation value of the action is measured in the lattice simulations [3]. The free energy density is related to this expectation value as follows,

$$\left[\frac{f}{T^4}\right]_{\beta_0}^{\beta_T} = N_\tau^4 \int_{\beta_0}^{\beta_T} d\beta' \, S_0, \tag{2.67}$$

where β_T and β_0 denote the inverse couplings, $\beta \equiv 2N_c/g^2$, at finite and zero temperatures, respectively. S_0 means a difference between the actions at finite and zero temperatures, $S_0 \equiv S_T - S_{T=0}$. The lattice simulation at zero temperature is approximated by a symmetric lattice with $N_\tau = N_\sigma$. If one adopts the action given by Eq. (2.21), S_T can be written as

$$S_T = \frac{1}{N_\sigma^3 N_\tau} \sum_n \frac{1}{N_c} \mathrm{ReTr} \left[\frac{1}{3} \sum_{i<j} U_{ij}(n) + \frac{1}{3} \sum_i U_{i4}(n) \right], \quad \text{for} \quad i,j = 1,2,3. \tag{2.68}$$

We have shown the contributions of the space-space and space-time plaquettes separately because the extents of lattice along spatial and temporal directions are different at finite temperature.

From Eq. (2.67), $\epsilon - 3P$ on the lattice is obtained from

$$\frac{\epsilon - 3P}{T^4} = -3N_\tau^4 \, T \frac{d\beta}{dT} \, S_0. \tag{2.69}$$

As is clear from Eq.(2.63), the inverse coupling, i.e. the lattice spacing varies with the temperature for fixed N_τ,

$$B(g) \equiv T\frac{d\beta}{dT} = -2N_c a \frac{dg^{-2}}{da}, \tag{2.70}$$

where we have introduced the beta function $B(g)$. Using this beta function, Eq. (2.69) is rewritten as

$$\frac{\epsilon - 3P}{T^4} = -3N_\tau^4 B(g) S_0. \tag{2.71}$$

The energy density ϵ/T^4 is then obtained by adding the pressure $3p/T^4 = -3f/T^4$ to this equation.

2.4.4 Determination of scale

In order to express the thermodynamic quantities measured on the lattice in physical units, one must know the relation between the lattice spacing a and the inverse coupling β by comparing a quantity measured on the lattice and the corresponding quantity which is measured experimentally at $T = 0$. The string tension σ is often used as such a quantity. The string tension is evaluated by measuring the static quark potential between infinitely heavy quarks (see subsection 2.3.1).

[3] The approach introduced here is called standard integral method.

To set the lattice spacing, we adopt the string tension on the lattice $a\sqrt{\sigma}$ parametrized for the interval of inverse coupling $5.6 \leq \beta \leq 6.5$ as follows [71]

$$a\sqrt{\sigma} = f(g^2)(1 + 0.2731\hat{a}^2 - 0.01545\hat{a}^4 + 0.01975\hat{a}^6)/0.01364, \tag{2.72}$$

$$\hat{a}(g) \equiv \frac{f(g^2)}{f(g^2(\beta = 6.0))}, \tag{2.73}$$

where $f(g^2)$ is the two-loop order scaling function of SU(3) gauge theory

$$f(g^2) = (b_0 g^2)^{-\frac{b_1}{2b_0^2}} \exp\left(-\frac{1}{2b_0 g^2}\right), \tag{2.74}$$

with renormalization-scheme-independent factors b_0 and b_1

$$b_0 = \frac{11}{(4\pi)^2}, \qquad b_1 = \frac{102}{(4\pi)^4}. \tag{2.75}$$

Thus the lattice spacing can be set for a given inverse coupling from Eq. (2.72) with $\sqrt{\sigma}$ at $T = 0$, which is known experimentally.

In addition, let us determine the temperature scale T/T_c for a given temporal extent N_τ. Using the string tension, T/T_c is written as

$$\frac{T}{T_c} = \frac{T}{\sqrt{\sigma}} \frac{\sqrt{\sigma}}{T_c} = \frac{1}{a\sqrt{\sigma} N_\tau} \frac{\sqrt{\sigma}}{T_c}, \tag{2.76}$$

where we have used Eq. (2.63) in the second equality. Once the critical coupling β_c for the deconfinement phase transition is known, the string tension at β_c is determined from Eq. (2.72) for fixed N_τ. Then the ratio $T_c/\sqrt{\sigma}$ and the temperature scale T/T_c can be determined. The critical coupling is, for instance, obtained from the analysis of the location of peak in the Polyakov loop susceptibility

$$\chi_P = N_\sigma^3(\langle P^2 \rangle - \langle P \rangle^2). \tag{2.77}$$

Furthermore, the critical couplings which are measured on several temporal extents is extrapolated to infinite volume limit using the following ansatz

$$\beta_c(N_\tau, N_\sigma) = \beta_c(N_\tau, \infty) - h\left(\frac{N_\tau}{N_\sigma}\right)^3, \tag{2.78}$$

where h is a parameter, $h \lesssim 0.1$. This ansatz is appropriate for the first order phase transition of SU(3) gauge theory.

summary

- We outlined the lattice formulation of quantum chromodynamics (QCD), the confinement of quarks, the phase transition, and the thermodynamics in SU(3) gauge theory.
- In lattice QCD, the quarks and the gluons correspond to the lattice sites and the link variables, respectively.
- The confinement of quarks is explained by using the strong coupling expansion and the Wilson loop, which is one of the basic lattice observables and shows the area law leading the linear potential between quarks.

- The SU(3) gauge theory shows the first order deconfinement phase transition and the Polyakov loop is used as an order parameter of it.
- The thermodynamic quantities are obtained by the integration of gauge action.

Chapter 3

Lattice Simulation

While QCD is admitted to be a fundamental theory of strong interaction, an analysis of QCD at the energy scale $\sim \Lambda_{QCD}$ with analytic or perturbative methods is quite difficult because of the large coupling constant. There are many subjects which need non-perturbative comprehension based on QCD such as hadron structure, nuclear force, QCD phase diagram, and hot/dense QCD matter. Numerical simulation is the most powerful approach for such a non-perturbative QCD physics. Due to the improvement of computer performance, recently lattice simulations have been performing more realistic situations compared to those of the early days. In lattice simulations, one first prepares a set of gauge configurations generated by Monte Carlo methods. Then some observable (for example, correlation function, plaquette, Polyakov loop, etc.) is repeatedly measured on each gauge configuration and enormous amount of data are collected. At last one obtains an expectation value of an observable with statistical error from the lattice data. In this sense, lattice simulation may be regarded as an experiment. In this chapter, we introduce basic concept of Monte Carlo method and several algorithms used in our lattice simulations.

3.1 Monte Carlo method

An expectation value computed on a set of gauge configurations is in principle given by Eqs. (2.59) or (2.62). However the analysis requires a large number of integrations and vast amounts of computer time, so that to perform the multiple integrations naively is not practical. Some efficient method is required for sampling data. In this section, we introduce how to generate the gauge configurations that is first step in lattice QCD simulations and overview some useful algorithms that are used in this thesis.

3.1.1 Importance sampling

An expectation value of some function $f(x)$ with a density function $\rho(x)$ is given by

$$\langle f \rangle = \frac{\int_a^b dx f(x)\rho(x)}{\int_a^b dx \rho(x)}. \tag{3.1}$$

In the Monte Carlo simulation, this expectation value is approximated as

$$\langle f \rangle = \lim_{N\to\infty} \frac{1}{N} \sum_{i=1}^{N} f(x_i), \quad a < x_i < b. \tag{3.2}$$

Here N denotes the number of sample data. x_i is chosen randomly with the normalized distribution density

$$dP(x) = \frac{\rho(x)dx}{\int_a^b dx\rho(x)}. \tag{3.3}$$

Eq. (2.62) takes the same form as Eq. (3.1) and an expectation value of some observable O in the lattice simulation may be obtained from

$$\langle O \rangle = \lim_{N\to\infty} \frac{1}{N} \sum_{i=1}^{N} O[U_i], \tag{3.4}$$

where U_i are the gauge configurations generated randomly with the probability distribution density called Gibbs-measure

$$dP[U] = \frac{e^{-S_G[U]}\mathcal{D}U}{\int \mathcal{D}U e^{-S_G[U]}}. \tag{3.5}$$

Following the weight $e^{-S_G[U]}$, the gauge configurations having a large contribution to the integral in Eq. (2.62) are mainly taken into the summation in Eq. (3.4). This is called *the importance sampling.* The number of gauge configurations is finite in the actual numerical simulations and the statistical error is proportional to $1/\sqrt{N}$. The error estimates will be discussed in section 3.2.

3.1.2 Markov process

What we do first in lattice simulations is to generate gauge configurations following the probability distribution Eq. (3.5). The gauge configurations are generated stochastically starting from an initial gauge configuration U_0,

$$U_0 \to U_1 \to U_2 \to \cdots. \tag{3.6}$$

The new configuration $U' = U_n$ depends only on the last configuration $U = U_{n-1}$ in *Markov process.* Thus the probability $P[U']$ that a gauge configuration U' is realized is written as

$$P[U'] = \sum_U P[U]T(U \to U'), \tag{3.7}$$

$$P[U] = \frac{e^{-S_G[U]}}{\int \mathcal{D}U e^{-S_G[U]}}, \tag{3.8}$$

where $T(U \to U')$ represents a transition probability that U' is adopted after U. $T(U \to U')$ satisfies the following conditions :

$$\sum_{U'} T(U \to U') = 1, \tag{3.9}$$

$$0 \le T(U \to U') \le 1. \tag{3.10}$$

An operation to obtain a new configuration is called *update.* When the configurations in Eq. (3.6) are updated under the Markov process, the sequence of the configurations is called *Markov chain.* If one performs enough number of updates, the gauge configurations are expected to reach an equilibrium state. The probability distribution in the equilibrium state satisfies the balance equation

$$\sum_U P_{\rm eq}[U]T(U \to U') = \sum_U P_{\rm eq}[U']T(U' \to U). \tag{3.11}$$

Thus $P_{\rm eq}$ is a fixed point of the Markov process. A sufficient condition about $T(U \to U')$ for the equilibrium state is *the detailed balance condition* :

$$P_{\rm eq}[U]T(U \to U') = P_{\rm eq}[U']T(U' \to U). \tag{3.12}$$

3.1.3 Heat bath algorithm

In conventional algorithms of lattice QCD simulations, a single link variable $U_\mu(n)$ is renewed by new one $U'_\mu(n)$ in each update. To update all link variables on lattice once is called *sweep*. *Heat bath algorithm* is one of the algorithms for the update of gauge configuration and satisfies the detailed balance condition Eq. (3.12). In the following, we outline the algorithm with the case of SU(2) gauge theory with Wilson gauge action [39, 40]. The case of SU(3) gauge theory can be constructed from the SU(2) case as will be seen later.

In the heat bath algorithm, the candidate link variable $U = U'_\mu(n)$ is updated to satisfy the probability distribution

$$dP(U) \propto e^{-S_G[U]} dU. \tag{3.13}$$

Using the Wilson gauge action given by Eq. (2.21), the probability distribution is written as

$$dP(U) \propto \exp\left(\frac{2}{g^2}\mathrm{Re\ Tr}[UV]\right) dU. \tag{3.14}$$

In the case of four dimensional space, V denotes the sum of *staples* V_i (Fig. 3.1),

$$V \equiv \sum_{i=1}^{6} V_i = \sum_{\mu\neq\nu} (U_\nu(n+\hat{\mu})U^\dagger_\mu(n+\hat{\nu})U^\dagger_\nu(n) + U^\dagger_\nu(n+\hat{\mu}-\hat{\nu})U^\dagger_\mu(n-\hat{\nu})U_\nu(n-\hat{\nu})). \tag{3.15}$$

There are six staples for single link variables which is updated. dU is the Haar measure of the gauge group. We introduce the representation

$$U \equiv u_0 I + i\vec{u}\cdot\vec{\sigma}, \qquad V \equiv v_0 I + i\vec{u}\cdot\vec{\sigma}, \tag{3.16}$$

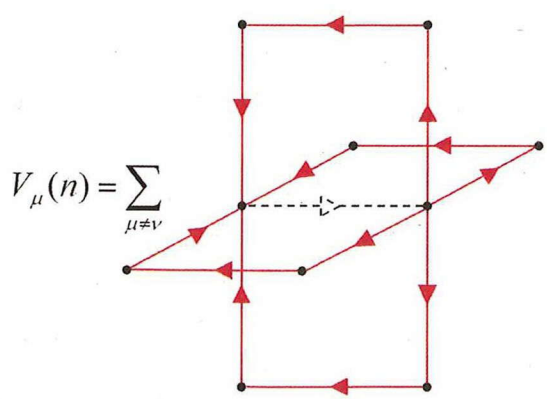

Figure 3.1: Staple.

where I and $\vec{\sigma}$ are 2×2 unit matrix and Pauli matrices, respectively. The exponential in Eq. (3.14) is then rewritten as

$$\begin{aligned} \mathrm{Re\,Tr}\,[UV] &= \mathrm{Re\,Tr}\,[(u_0 I + i\vec{u}\cdot\vec{\sigma})(v_0 I + i\vec{u}\cdot\vec{\sigma})] \\ &= \mathrm{Tr.}[u_0 v_0 - \vec{u}\cdot\vec{v}] \\ &= k\mathrm{Tr}\,[UW]. \end{aligned} \tag{3.17}$$

Here we introduced an SU(2) matrix W defined as follows

$$V = kW, \qquad k = \sqrt{\det[V]}. \tag{3.18}$$

One thus obtains the probability distribution

$$dP(U) \propto \exp\left(\frac{2}{g^2} k\mathrm{Tr}\,[UW]\right) dU. \tag{3.19}$$

If we define a SU(2) matrix $X \equiv UW$, we may rewrite the probability distribution as

$$dP(X) \propto \exp\left(\frac{2}{g^2} k\mathrm{Tr}\,[X]\right) dX. \tag{3.20}$$

Generating X with this probability distribution, one obtains a candidate link variable $U'_\mu(n)$

$$U'_\mu(n) = U = XW^\dagger. \tag{3.21}$$

Introducing the representation of X

$$X = x_0 I + i\vec{x}\cdot\vec{\sigma}, \qquad \det[X] = x_0^2 + |\vec{x}|^2 = 1, \qquad x = (x_0, \vec{x}) \in R^4, \tag{3.22}$$

the problem is replaced by a question of how to choose a point on the four dimensional spherical surface. Then the Haar measure can be written as

$$\begin{aligned} dX &= \frac{1}{\pi^2} d^4x \delta(x_0^2 + |\vec{x}|^2 - 1) \\ &= \frac{1}{\pi^2}\, d|\vec{x}||\vec{x}|^2\, d\cos\theta\, d\phi\, dx_0\, \frac{\theta(1-x_0^2)}{2\sqrt{1-x_0^2}} \left(\delta\left(|\vec{x}| - \sqrt{1-x_0^2}\right) + \delta\left(|\vec{x}| - \sqrt{1-x_0^2}\right)\right) \\ &= \frac{1}{\pi^2}\, d\cos\theta\, d\phi\, dx_0\, \frac{(1-x_0^2)\theta(1-x_0^2)}{2\sqrt{1-x_0^2}} \\ &= \frac{1}{2\pi^2} d\cos\theta\, d\phi\, dx_0\, \sqrt{1-x_0^2}. \end{aligned} \tag{3.23}$$

In the last line, we omitted the step function because of $|x_0| \leq 1$. The probability distribution $dP(X)$ then reduces to

$$dP(X) = \frac{1}{2\pi^2} d\cos\theta\, d\phi\, dx_0\, \sqrt{1-x_0^2}\, e^{k\beta x_0}, \tag{3.24}$$

where we used $\mathrm{Tr}[X] = 2x_0$.

We summarize the procedure to obtain $x = (x_0, \vec{x})$ below :

1. Generate a uniform random number $y \in [0,1]$.

2. Compute x_0 from

$$x_0 = \frac{g^2}{4k}\ln(Ay+B), \qquad A = 2\sinh\left(\frac{4k}{g^2}\right), \qquad B = \exp\left(-\frac{4k}{g^2}\right). \tag{3.25}$$

3. Generate a uniform random number $z \in [0,1]$. Accept x_0 by the following condition :

$$z \leq \sqrt{1-x_0^2} \quad \rightarrow \quad \text{accept} \tag{3.26}$$

$$z > \sqrt{1-x_0^2} \quad \rightarrow \quad \text{reject} \quad \rightarrow \quad \text{Return to step. 1.} \tag{3.27}$$

4. Generate uniform random numbers $\phi \in [0, 2\pi]$ and $\cos\theta \in [-1,1]$.

5. Compute $\vec{x}$.

$$x_1 = \sqrt{1-x_0^2}\cos\theta, \qquad x_2 = \sqrt{1-x_0^2}\sin\theta\cos\phi, \qquad x_3 = \sqrt{1-x_0^2}\sin\theta\sin\phi. \tag{3.28}$$

6. Obtain $X^{\rm new} = x_0 I + i\vec{x}\cdot\vec{\sigma}$.

Once $X^{\rm new}$ is determined, the new link variable is obtained from the relation $U_\mu^{\rm new}(n) = U^{\rm new} = X^{\rm new}W^\dagger$. Thus an update of a link variable is performed in the heat bath algorithm. Repeating this procedure for each link variable, a sweep is completed one time and a new gauge configuration is obtained.

The naive application of the above algorithm to SU(N) gauge theory seems to be difficult. In actual lattice QCD simulations, a method proposed in Ref. [72] called *pseudo heat bath algorithm* is usually used. Here we focus on the SU(3) gauge theory in which a link variable is represented by 3×3 unitary matrix. First, some SU(3) matrix is divided into three SU(2) subgroups, for example

$$U_1 = \begin{pmatrix} a & b & 0 \\ c & d & 0 \\ 0 & 0 & 1 \end{pmatrix}, \qquad U_2 = \begin{pmatrix} 1 & 0 & 0 \\ 0 & a & b \\ 0 & c & d \end{pmatrix}, \qquad U_3 = \begin{pmatrix} a & 0 & b \\ 0 & 1 & 0 \\ c & 0 & d \end{pmatrix}. \tag{3.29}$$

A subgroup U_i is then randomly chosen and the same procedure for SU(2) gauge theory is applied to that. Performing the same way to the other two SU(2) subgroups, an update for SU(3) gauge theory is accomplished. This method is applied to general SU(N) gauge theory.

3.1.4 Overrelaxation

Overrelaxation method [73, 74, 75] is often used in combination with (pseudo) heat bath algorithm in lattice QCD simulation. The basic idea of this method is to pick out a new link variable which locates as far as possible from old value in a configuration space. To obtain more accurate expectation value based on Eq. (3.4) from a finite number of data, one needs to collect samples from a wide region in the configuration space. In other words, the *ergodicity* must be satisfied. However it can happen in lattice simulation with an updating algorithm that many samples are chosen from narrow range in the configuration space. In this case, one cannot expect to get reliable result. The overrelaxation method is valid for this problem.

In the overrelaxation method, an update for a link variable is performed by following transformation

$$U^{\rm new} = VU^{\rm old}V^\dagger, \tag{3.30}$$

where V is a sum of staples given by Eq. (3.15). Then the action is invariant under this update $S^{\rm new} = S^{\rm old}$. Assuming the case of SU(2) gauge theory, the gauge action (2.21) reads

$$S_G^{\rm new} = -\beta {\rm ReTr}[U^{\rm new} V] = -\beta {\rm ReTr}[V U^{\rm old} V^\dagger V] = -\beta {\rm ReTr}[U^{\rm old} V] = S_G^{\rm old}, \tag{3.31}$$

and the detailed balance is satisfied. Here we used a fact that V is unitary, i.e. $V^{-1} = V^\dagger$ in the third equality. The cyclicity of trace is used in forth equality. Thus the new link variable is always adopted and changes the location dramatically in the configuration space.

We note that the overrelaxation method itself is not ergodic because the update procedure is held on specific regions in the configuration space where the gauge action is constant. Thus the gauge configurations generated by this method become the micro canonical ensemble. In order to realize a set of the gauge configurations corresponding to canonical ensemble which is distributed with the weight e^{-S_G}, one needs the other updating algorithm such as the heat bath one.

3.2 Error estimate

After generating gauge configurations and sampling data, one evaluates an expectation value of some physical quantity with statistical error. Error analyses must be performed carefully when the data have correlation. In the following, we see how to estimate the statistical error for uncorrelated and correlated sample data, respectively.

3.2.1 Autocorrelation

In the lattice QCD simulation, sample data are desirable to be uncorrelated for an accurate analysis. A correlation between the sample data measured in the different gauge configurations is called *autocorrelation*. The autocorrelation for sample data in i-th and $(i+t)$-th gauge configurations is given by

$$A(t) = \frac{1}{N-t} \sum_i^{N-t} O_i O_{i+t} - \langle O \rangle^2. \tag{3.32}$$

Autocorrelation time τ is evaluated from the autocorrelation function normalized by $A(0)$,

$$\frac{A(t)}{A(0)} \sim e^{-t/\tau}. \tag{3.33}$$

If one estimates the sample data at every τ sweep, the data are almost uncorrelated. The autocorrelation provides an indication of the number of sweeps to obtain uncorrelated data.

3.2.2 Jackknife method

An average and a statistical error of some observable O approximated by N uncorrelated sample data are respectively given by

$$\langle O \rangle = \frac{1}{N} \sum_{i=1}^{N} O_i, \tag{3.34}$$

$$\delta O = \sqrt{\frac{\langle (O - \langle O \rangle)^2 \rangle}{N-1}} = \sqrt{\frac{\langle O^2 \rangle - \langle O \rangle^2}{N-1}}, \tag{3.35}$$

where in the second equality in Eq. (3.35) we have used the fact that the data are uncorrelated, i.e. $\langle O_i O_j \rangle = \langle O_i \rangle \langle O_j \rangle = \langle O \rangle^2$. If the sample data have correlation, the statistical error cannot be correctly estimated by Eq. (3.35). In such a case, we should use other methods which can evaluate the statistical error for correlated data.

Jackknife method is one of such methods. This method is valid even if the sample data are correlated. The procedure is as follows. First, N data are divided into $N_n = N/n$ groups where n is called bin-size. Then the average for $(N-n)$ sample data where i-th group is removed is computed,

$$\langle O \rangle_i = \frac{1}{N-n} \sum_k O_k. \tag{3.36}$$

This average is regarded as a new sample. Using the new sample data, the average of some physical quantity $f(O)$ and its statistical error are evaluated by

$$\langle f(O) \rangle = \frac{1}{N_n} \sum_{i=1}^{N_n} f(\langle O \rangle_i), \tag{3.37}$$

$$\delta \langle f(O) \rangle = \sqrt{(N_n - 1)(\langle f^2(O) \rangle - \langle f(O) \rangle^2)}. \tag{3.38}$$

The bin-size should be sufficiently large compared with the autocorrelation time.

summary

- Lattice QCD simulation can be divided into three main steps : a generation of gauge configurations, a measurement of lattice observables, and a data analysis.
- The first step is carried out with the Monte Carlo method which provides the gauge configurations based on some stochastic distribution.
- In the heat bath algorithm a link variable is updated with the weight e^{-S_G}.
- Overrelaxation method is often combined with the heat bath algorithm to collect sample data from wider range in the configuration space.
- In the last step one has to estimate the statistical error and pay attention to the correlation between the data observed on different configurations.
- Autocorrelation gives a guide of the number of sweeps which cuts off the correlation of gauge configurations.

Chapter 4

Relativistic Hydrodynamics

In this chapter, we give a brief review of the relativistic hydrodynamics from a phenomenological view point. The quark-gluon plasma is expected to be almost ideal fluid because of the success of ideal hydrodynamic simulations for the space-time evolution of a hot quark-gluon matter produced in relativistic heavy ion collisions [12]. For more realistic and quantitative simulations of the matter, the hydrodynamic model on the basis of the relativistic dissipative hydrodynamics is required. First order theory (relativistic Navier-Stokes theory) is the simplest dissipative hydrodynamics which includes dissipative terms up to the first order. The first order theory, however, is known to violate causality and dissipations can propagate with an infinite speed. This is an undesirable feature for a description of relativistic fluids. This acausal problem can be avoided by taking into account higher order dissipative effects into the hydrodynamics. In the following, we introduce one of the second order theories, proposed by Israel and Stewart, on the basis of Refs. [27, 76, 77]. In the second order theory, new transport coefficients, i.e. relaxation times for dissipations are naturally introduced. We see the second order hydrodynamic equations can be causal due to the relaxation times.

4.1 Basics of relativistic hydrodynamics

4.1.1 Conservation laws

Hydrodynamics is a theory which describes time evolution of a macroscopic fluid element without knowledge of the microscopic components of the fluid. The basic equations of relativistic hydrodynamics are two local conservation laws of the energy-momentum tensor $T^{\mu\nu}$ and the net charge currents N_i^μ such as electric charge, baryon number, and strangeness,

$$\partial_\mu T^{\mu\nu} = 0, \tag{4.1}$$

$$\partial_\mu N_i^\mu = 0, \quad (i = 1, ..., r). \tag{4.2}$$

Here the type of the net charge density is denoted by an index i. $T^{\mu\nu}$ and N_i^μ can be decomposed by using an arbitrary, time-like, normalized four vector u^μ, $u_\mu u^\mu = 1$, as follows,

$$T^{\mu\nu} = \epsilon_{\rm eq} u^\mu u^\nu - (P_{\rm eq} + \Pi)\Delta^{\mu\nu} + W^\mu u^\nu + W^\nu u^\mu + \pi^{\mu\nu}, \tag{4.3}$$

$$N^\mu = n_i u^\mu + V_i^\mu. \tag{4.4}$$

$\Delta^{\mu\nu}$ is the projector onto the three-dimensional space orthogonal to u^μ defined by

$$\Delta^{\mu\nu} \equiv g^{\mu\nu} - u^\mu u^\nu, \qquad u_\mu \Delta^{\mu\nu} = 0, \qquad \Delta^{\mu\alpha}\Delta^\nu_\alpha = \Delta^{\mu\nu}, \qquad \Delta^\mu_\mu = 3, \tag{4.5}$$

where the metric tensor is defined by $g^{\mu\nu} = \mathrm{diag}(+,-,-,-)$.

In the local rest frame (LRF) of a fluid defined by $u^\mu = (1,0,0,0)$, each quantity is given by

$$\epsilon_{\mathrm{eq}} = u_\mu T^{\mu\nu} u_\nu, \quad \text{(the energy density)} \tag{4.6}$$

$$n = u_\mu N^\mu, \quad \text{(the net charge density)} \tag{4.7}$$

$$P_{\mathrm{eq}} + \Pi = -\frac{1}{3}\Delta_{\mu\nu} T^{\mu\nu}, \quad \text{(the pressure)} \tag{4.8}$$

$$W^\mu = u_\nu T^{\nu\rho} \Delta^\mu_\rho, \quad \text{(the energy flow)} \tag{4.9}$$

$$V^\mu = \Delta^\mu_\nu N^\nu, \quad \text{(the net charge flow)} \tag{4.10}$$

$$q^\mu = W^\mu - \frac{\epsilon_{\mathrm{eq}} + P_{\mathrm{eq}}}{n} V^\mu, \quad \text{(the heat flow)} \tag{4.11}$$

$$\pi^{\mu\nu} = T^{\langle\mu\nu\rangle}, \quad \text{(the stress tensor)} \tag{4.12}$$

where the angular bracket means the symmetrized spatial and traceless part of the tensor,

$$A^{\langle\mu\nu\rangle} \equiv \left[\frac{1}{2}(\Delta^\mu_\rho \Delta^\nu_\sigma + \Delta^\nu_\rho \Delta^\mu_\sigma) - \frac{1}{3}\Delta^{\mu\nu}\Delta_{\rho\sigma}\right] A^{\rho\sigma}. \tag{4.13}$$

The dissipative currents are constrained by the orthogonality relations

$$u_\mu V^\mu = 0, \qquad u_\mu W^\mu = 0, \qquad u_\mu q^\mu = 0, \qquad u_\mu \pi^{\mu\nu} = 0. \tag{4.14}$$

Although the conservation laws Eqs. (4.1) and (4.2) include $10 + 4r$ unknown variables ($T^{\mu\nu}$ is a symmetric tensor of rank 2 and then has 10 independent components, and N^μ_i have 4 components for each type of the charge i), there are only $4 + r$ equations. Thus, the hydrodynamic equation system does not close and some additional conditions are required to solve hydrodynamic problems.

One of the prescriptions is an ideal fluid approximation in which the dissipative terms in Eqs. (4.3) and (4.4) are neglected and the number of unknown variables reduces to $5+r$. Therefore one can solve the hydrodynamic equations with an equation of state $\epsilon = \epsilon(p, n)$, which includes information about the microscopic properties of the fluid. Another approach is to derive $5 + 3r$ equations for dissipative terms in addition to the conservation laws from the second law of thermodynamics

$$\partial_\mu s^\mu \geq 0, \qquad s^\mu = s_{\mathrm{eq}} u^\mu + \delta s^\mu, \tag{4.15}$$

where s^μ, s_{eq} and δs^μ are the generalized entropy current, the entropy density in equilibrium, and the entropy flux, respectively. The equations for dissipative terms are obtained from the expansion of s^μ with respect to small deviations from the local thermodynamic equilibrium. Then the dissipative hydrodynamics can be classified by an order of the expansion of the entropy flux δs^μ as will be discussed in Sec. 4.2. In the following, we consider a single type of the net charge density i.e. $i = 1$ for simplicity.

4.1.2 Eckart and Landau frames

Although the four velocity u^μ is arbitrary in general cases, two choices called *Eckart* and *Landau frames* are often used. In Eckart frame, u^μ is defined by

$$u^\mu_E \equiv \frac{N^\mu}{\sqrt{N_\mu N^\mu}}. \tag{4.16}$$

In this frame, u^μ is regarded as the LRF of the net charge flow, i.e. $V^\mu = 0$. Eckart frame is also called *particle frame*. On the other hand, u^μ is identified to be the energy flow in Landau frame,

$$u_L^\mu \equiv \frac{T^\mu_\nu u^\nu}{\sqrt{u_L^\alpha T^\beta_\alpha T_{\beta\gamma} u_L^\gamma}}. \tag{4.17}$$

Landau frame is called *energy frame*. There u^μ is the LRF of the energy flow W^μ, i.e. $W^\mu = 0$ and $q^\mu = -(\epsilon_{\rm eq} + P_{\rm eq})V^\mu/n$.

4.1.3 Ideal fluid approximation

The ideal fluid approximation is one of the prescriptions to close the hydrodynamic equation system. Since the dissipative currents are neglected in this approximation, the energy-momentum tensor and the net charge current can be written as

$$T^{\mu\nu} = \epsilon_{\rm eq} u^\mu u^\nu - P_{\rm eq}\Delta^{\mu\nu}, \qquad N^\mu = n u^\mu. \tag{4.18}$$

In the ideal fluid approximation, the Eckart and Landau frames are equivalent to each other, $u_E^\mu = u_L^\mu$, because $V_\mu = 0$, $W_\mu = 0$, $\Pi = 0$, and $\pi^{\mu\nu} = 0$. The number of the unknown variables then reduce from fourteen to six (i.e. ϵ, P, n, and u^μ with $u^2 = 1$), and the hydrodynamic equation system with an equation of state is closed. The ideal hydrodynamic equations thus can be solved uniquely under a given initial condition.

Let us see that the entropy production rate vanishes for an ideal fluid. From Eq. (4.1) and (4.18), one obtains a relation

$$u_\nu \partial_\mu T^{\mu\nu} = D\epsilon_{\rm eq} + (\epsilon_{\rm eq} + P_{\rm eq})\nabla_\mu u^\mu = 0, \tag{4.19}$$

where $D \equiv u_\mu \partial^\mu$ and $\nabla^\mu \equiv \Delta^{\mu\nu}\partial_\nu$ are the convective time derivative and the gradient operator, respectively. Using the first law of thermodynamics

$$T ds_{\rm eq} = d\epsilon_{\rm eq} - \mu dn, \tag{4.20}$$

and a thermodynamical relation,

$$\epsilon_{\rm eq} + P_{\rm eq} = T s_{\rm eq} + \mu n, \tag{4.21}$$

Eq. (4.19) reduces to

$$T(D s_{\rm eq} + s_{\rm eq}\nabla_\mu u^\mu) + \mu(Dn + n\nabla_\mu u^\mu) = T\partial_\mu s_{\rm eq}^\mu = 0, \tag{4.22}$$

where we used Eq. (4.2) in the first equality. Thus the entropy current does not increase in an ideal fluid,

$$\partial_\mu s_{\rm eq}^\mu = 0. \tag{4.23}$$

In the above argument, we assume that the system has no discontinuity like a shock wave. If the system has such discontinuities, the entropy production rate has a positive value even in an ideal fluid.

4.2 Relativistic dissipative hydrodynamics

Although the ideal fluid approximation is a convenient approach, one cannot apply it to systems where the dissipative effects are significant. The dissipative hydrodynamics should be used for such a case. As noted already, the dissipative hydrodynamics is closed by equations for the dissipative currents in addition to Eqs. (4.1) and (4.2). We derive these equations with a phenomenological way on the basis of the second law of thermodynamics. Before discussing the dissipative hydrodynamics, we summarize the phenomenological procedure in the following :

1. Determine the form of δs^μ as a function of the dissipative currents :

$$\delta s^\mu = \delta s^\mu(V^\mu, q^\mu, \pi_{\mu\nu}, \Pi). \tag{4.24}$$

   For the definition of the entropy current, the dissipative currents are sufficiently small.

2. Substitute the entropy current to the second law of thermodynamics : $\partial_\mu s^\mu \geq 0$.

3. Divide the divergence of the entropy current into the dissipative currents and the conjugate thermodynamic forces :

$$\partial_\mu s^\mu = (\text{Dissipative currents}) \times (\text{Thermodynamic forces}). \tag{4.25}$$

4. Impose linearity between the dissipative currents and the thermodynamic forces :

$$(\text{Dissipative currents}) = (\text{Transport coefficients}) \times (\text{Thermodynamic forces}). \tag{4.26}$$

   Then the equations for dissipative currents Eq. (4.26) are obtained.

In what follows, we discuss the relativistic dissipative hydrodynamics following this procedure. We see that the form of δs^μ determines whether the dissipative hydrodynamics can be causal theory or not in this procedure. In this and next sections, the components of vector and tensor are denoted by $\mu = 0, 1, 2, 3$ and that of partial derivative by $\mu = t, x, y, z$.

4.2.1 First order theory

First order theory, which is the relativistic Navier-Stokes theory, was proposed independently by Eckart and Landau-Lifshitz [22, 23]. We adopt the Eckart frame here. In the first order theory, the entropy current in the Eckart frame is determined by the tensors u^μ, q^μ, Π, and $\pi^{\mu\nu}$ and the orthogonality relations Eq. (4.14),

$$s^\mu = s_{\text{eq}} u^\mu + \frac{q^\mu}{T}. \tag{4.27}$$

Substituting this form to the second law of thermodynamics Eq. (4.15), one obtains the following expression,

$$T\partial_\mu s^\mu = -\Pi \nabla_\mu u^\mu + q^\mu(\nabla_\mu T^{-1} + Du_\mu) + \pi^{\mu\nu}\nabla_\mu u_\nu \geq 0. \tag{4.28}$$

Imposing linearity between the dissipative currents and the thermodynamic forces, one obtains the relations for dissipative currents,

$$\Pi = -\zeta \nabla_\mu u^\mu, \tag{4.29}$$

$$q^\mu = \kappa T \left(\frac{\nabla^\mu T}{T} - D u^\mu \right), \tag{4.30}$$

$$\pi^{\mu\nu} = 2\eta \nabla^{\langle \mu} u^{\nu \rangle}. \tag{4.31}$$

Here the proportional coefficients ζ, κ, and η correspond to the bulk viscosity, the heat conductivity, and the shear viscosity, respectively. We call them the first order transport coefficients. From Eqs. (4.29)-(4.31), the second law of thermodynamics is given by

$$\partial_\mu s^\mu = \frac{\Pi^2}{\zeta T} - \frac{q_\mu q^\mu}{\kappa T^2} + \frac{\pi_{\mu\nu}\pi^{\mu\nu}}{2\eta T} \geq 0. \tag{4.32}$$

We note here that $q_\mu q^\mu < 0$ because of the orthogonality relation $u_\mu q^\mu = 0$ in the LRF. Therefore the first order transport coefficients must be non-negative to satisfy Eq. (4.32). The transport coefficients are free parameters in hydrodynamic simulations. They cannot be determined within the framework of hydrodynamics but by a microscopic theory.

The first order theory is known to violate causality due to the parabolic equation of motion for dissipations [24, 25]. Therefore its application for the relativistic phenomena (for instance, high energy heavy ion collisions or baryonic fluid inside compact stars) contains a principle problem.

- An example : Heat conduction in the first order theory
  Let us consider a heat conduction described by the first order theory. From Eq. (4.1), the energy conservation law in Eckart frame is given by

$$\partial_t T^{00} = \partial_t T^{00}_{\rm eq} + \partial_t \delta T^{00} = \partial_t \epsilon_{\rm eq} + 2\partial_t q^0 = \partial_t \epsilon_{\rm eq} - 2\partial_i q^i = 0. \tag{4.33}$$

  Here we used the orthogonality relation $\partial_\mu q^\mu = 0$ in the third equality. The heat current is given by Eq. (4.30), i.e.

$$q^i = \kappa \nabla^i T = \kappa \partial^i T, \quad \text{(Fourier's law)}. \tag{4.34}$$

  Therefore Eq. (4.33) reduces to

$$\partial_t T = K \partial_i \partial^i T, \qquad K \equiv \frac{2\kappa}{c_V}, \qquad c_V \equiv \frac{\partial \epsilon_{\rm eq}}{\partial T}, \tag{4.35}$$

  where we introduced the thermal diffusion coefficient K and the specific heat c_V. Eq. (4.35) is exactly the diffusion equation which is known to have an acausal propagation of heat conduction.

4.2.2 Second order theory

To evade the acausal problem of the first order theory, Israel and Stewart proposed to use the entropy current extended up to second order in dissipative currents [27]. Due to this prescription, the equations of motion for dissipations become hyperbolic and the propagation of the dissipations can be causal with appropriate choices of parameters.

Here we adopt the following entropy current

$$s^\mu = s_{\rm eq}u^\mu + \frac{q^\mu}{T} - (\beta_\Pi \Pi^2 - \beta_q q_\nu q^\nu + \beta_\pi \pi_{\nu\lambda}\pi^{\nu\lambda})\frac{u^\mu}{2T}, \tag{4.36}$$

where β_A ($A = \Pi, q, \pi$) are thermodynamic coefficients. β_A take nonnegative values because the non-equilibrium entropy density $s = u_\mu s^\mu$ is smaller than the equilibrium one, i.e. $s < s_{\rm eq}$. Performing the phenomenological procedure described in the previous subsection, the second law of thermodynamics becomes

$$\begin{aligned} T\partial_\mu s^\mu = &- \Pi\left[\partial_\mu u^\mu + \beta_\Pi \dot{\Pi} + \frac{1}{2}\Pi T\partial_\mu\left(\frac{\beta_\Pi}{T}u^\mu\right)\right] \\ &- q^\mu\left[\nabla_\mu \ln T - \dot{u}_\mu - \beta_q\dot{q}_\mu - \frac{1}{2}q_\mu T\partial_\nu\left(\frac{\beta_q}{T}u^\nu\right)\right] \\ &+ \pi^{\mu\nu}\left[\sigma_{\mu\nu} - \beta_\pi\dot{\pi}_{\mu\nu} + \frac{1}{2}\pi_{\mu\nu}T\partial_\rho\left(\frac{\beta_\pi}{T}u^\rho\right)\right]. \end{aligned} \tag{4.37}$$

where $\dot{A} \equiv dA/dt$ and the shear tensor $\sigma_{\mu\nu}$ is defined by

$$\sigma_{\mu\nu} \equiv \frac{1}{2}\Delta^\rho_\mu\Delta^\sigma_\nu(\partial_\rho u_\sigma + \partial_\sigma u_\rho) - \frac{1}{3}\Delta_{\mu\nu}\partial_\rho u^\rho. \tag{4.38}$$

Then the evolution equations for the dissipative currents or Israel-Stewart (IS) equations are obtained from the linearity between the dissipative currents and the thermodynamic forces,

$$\dot{\Pi} = -\frac{1}{\tau_\Pi}\left[\Pi + \zeta\partial_\mu u^\mu + \frac{1}{2}\Pi\zeta T\partial_\mu\left(\frac{\beta_\Pi u^\mu}{T}\right)\right], \tag{4.39}$$

$$\dot{q}^\mu = -\frac{1}{\tau_q}\left[q^\mu - \kappa(\nabla^\mu T - T\dot{u}^\mu) + \frac{1}{2}q^\mu\kappa T^2\partial_\nu\left(\frac{\beta_q u^\nu}{T}\right)\right], \tag{4.40}$$

$$\dot{\pi}^{\mu\nu} = -\frac{1}{\tau_\pi}\left[\pi^{\mu\nu} - 2\eta\sigma^{\mu\nu} + \pi^{\mu\nu}\eta T\partial_\rho\left(\frac{\beta_\pi u^\rho}{T}\right)\right]. \tag{4.41}$$

The relaxation times τ_A are the second order transport coefficients and related with the thermodynamic coefficients β_A as follows,

$$\beta_\Pi = \frac{\tau_\Pi}{\zeta}, \qquad \beta_q = \frac{\tau_q}{\kappa T}, \qquad \beta_\pi = \frac{\tau_\pi}{2\eta}. \tag{4.42}$$

The second order theory can be causal due to τ_A. If one takes the limit $\tau_A \to 0$, one can easily confirm that IS equations (4.39)-(4.41) reduce to the first order relations Eqs. (4.29)-(4.31), respectively.

IS equations become simple form in the case of a uniform medium,

$$\dot{A} = -\frac{1}{\tau_A}A. \tag{4.43}$$

From this equation, the dissipative currents are shown to decay exponentially with time,

$$A(t) = A(0)e^{-t/\tau_A}. \tag{4.44}$$

We use this equation in the next chapter.

We close this subsection with three remarks : First, the entropy current Eq. (4.36) is not the most general form in the second order theory. One can add the mixed terms such as Πq^μ and $q_\nu\pi^{\nu\mu}$ or other second order terms to Eq. (4.36) [27, 78]. In such a case, the number of phenomenological coefficients

increases and the hydrodynamic equations become more complicated. Second the relaxation times τ_A are different from the collision time or the mean free time. The relaxation times represent the time scale that the corresponding dissipative current relaxes to its steady state value. While τ_A are the macroscopic time, the mean free time represents the time scale of the microscopic reactions in a fluid. Finally the second order theory can be acausal one if τ_A take too small values. In this case, more higher order theories may be required for describing relativistic phenomena. A strategy to obtain such theories is to expand the entropy current to higher order in dissipative currents and repeat the same procedure as argued in this section. Since τ_A are quantities proper to each matter, one must investigate the validity of the second order hydrodynamics for each case.

- An example : Heat conduction in the second order theory
  We revisit the heat conduction problem discussed in the last subsection. The energy conservation law is given by the same form as Eq. (4.33),

$$\partial_t \epsilon_{\rm eq} = 2\partial_i q^i. \tag{4.45}$$

  In the second order theory, Fourier's law (4.34) is substituted by Eq. (4.40)

$$\tau_q \partial_t q^i = -q^i + \kappa \partial^i T. \quad (\text{Maxwell} - \text{Cattaneo law}) \tag{4.46}$$

  From Eqs. (4.45) and (4.46), one obtains the heat conduction equation in the second order theory

$$\tau_q \partial_t^2 T = K \partial_i \partial^i - \partial_t T. \tag{4.47}$$

  In this way, the heat conduction in the second order theory is governed by the hyperbolic equation and its propagation speed has some finite value.

4.3 Characteristic speed

In this section, we introduce characteristic speeds (group velocities) of transverse and sound modes in pure gauge theory for later discussion. Let us assume that the propagation of dissipations when adding small perturbations to a hydrodynamic system in equilibrium. Since there are no conserved currents in pure gauge theory, the local rest frame is equivalent to the Landau (energy) frame. To linear approximation in the perturbations, deviations from equilibrium state in the energy-momentum tensor are given by

$$\delta T^{00} = \delta\epsilon, \qquad \delta T^{0i} = (\epsilon_{\rm eq} + P_{\rm eq})\delta u^i, \qquad \delta T^{ij} = \begin{cases} c_s^2 \delta\epsilon + \delta\pi^{ii} + \delta\Pi, & (i = j) \\ \delta\pi^{ij}, & (i \neq j) \end{cases} \tag{4.48}$$

where c_s^2 is the square of sound speed defined by $c_s^2 = \partial P/\partial\epsilon$.

4.3.1 Transverse mode

We first derive the characteristic speed of transverse mode under the linear perturbations. For the shear current that travels in y direction with velocity gradient along the x direction, δu^2 and $\delta\pi^{12}$ are nonzero components in δu^i and δT^{ij}, respectively. They depend only on t and x, i.e. $\delta u^2 = \delta u^2(t, x)$ and $\delta T^{12} = \delta T^{12}(t, x)$. The deviations of energy-momentum tensor are then given by

$$\delta T^{00} = \delta\epsilon, \qquad \delta T^{02} = (\epsilon_{\rm eq} + P_{\rm eq})\delta u^2, \qquad \delta T^{12} = \delta\pi^{12}. \tag{4.49}$$

The energy-momentum conservation law $\partial_\mu(\delta T^{\mu\nu}) = 0$ thus provides

$$(\epsilon_{\rm eq} + P_{\rm eq})\partial_t(\delta u^2) + \partial_x(\delta\pi^{12}) = 0. \tag{4.50}$$

From Eq. (4.41) the evolution equation of shear current within the linear perturbations can be written as

$$\tau_\pi \partial_t(\delta\pi^{12}) + \delta\pi^{12} + \eta\partial_x(\delta u^2) = 0. \tag{4.51}$$

Applying plane wave solutions

$$\delta u^2 \sim \exp(-i\omega t + ikx), \qquad \delta\pi^{12} \sim \exp(-i\omega t + ikx), \tag{4.52}$$

to Eqs. (4.50) and (4.51), a following dispersion relation is derived,

$$\omega^2 + \frac{i}{\tau_\pi}\omega - \frac{k^2}{\tau_\pi}\frac{\eta}{\epsilon_{\rm eq} + P_{\rm eq}} = 0. \tag{4.53}$$

From this dispersion relation, one obtains two propagating modes

$$\omega = \frac{1}{2}\left[-\frac{i}{\tau_\pi} \pm \sqrt{\frac{4k^2\eta}{\tau_\pi(\epsilon_{\rm eq} + P_{\rm eq})} - \frac{1}{\tau_\pi^2}}\right]. \tag{4.54}$$

Since we are interested in the maximum value of the propagation speed of current, let us evaluate the large k limit. In this limit, we have

$$\mathrm{Re}\,\omega = \pm k\sqrt{\frac{\eta}{\tau_\pi(\epsilon_{\rm eq} + P_{\rm eq})}}. \tag{4.55}$$

Therefore the characteristic speed of transverse mode v_η within the linear perturbation is give by

$$v_T^2 = \left(\frac{\partial\,\mathrm{Re}\,\omega}{\partial k}\right)^2 = \frac{\eta}{\tau_\pi(\epsilon_{\rm eq} + P_{\rm eq})}. \tag{4.56}$$

4.3.2 Sound mode

Next we see the sound mode. Let us consider the bulk current propagates in x direction i.e. $\delta u^1 = \delta u^1(t,x)$ and $\delta T^{11} = \delta T^{11}(t,x)$. In this case, Eq. (4.48) becomes

$$\delta T^{00} = \delta\epsilon, \qquad \delta T^{01} = (\epsilon_{\rm eq} + P_{\rm eq})\delta u^1, \qquad \delta T^{11} = c_s^2\delta\epsilon + \delta\pi^{11} + \delta\Pi. \tag{4.57}$$

Calculating as well as the transverse mode, the energy-momentum conservation law and the evolution equation Eq. (4.39) reduce to

$$\partial_t(\delta\epsilon) + (\epsilon_{\rm eq} + P_{\rm eq})\partial_x(\delta u^1) = 0, \tag{4.58}$$

$$(\epsilon_{\rm eq} + P_{\rm eq})\partial_t(\delta u^1) + c_s^2\partial_x(\delta\epsilon) + \partial_x(\delta\pi^{11}) + \partial_x(\delta\Pi) = 0, \tag{4.59}$$

$$\tau_\Pi\partial_t(\delta\Pi) + \delta\Pi + \zeta\partial_x(\delta u^1) = 0, \tag{4.60}$$

$$\tau_\pi\partial_t(\delta\pi^{11}) + \delta\pi^{11} + \frac{4}{3}\eta\partial_x(\delta u^1) = 0. \tag{4.61}$$

With these equations and the plane-wave solutions

$$\delta u^1 \sim \exp(-i\omega t + ikx), \qquad \delta\pi^{11} \sim \exp(-i\omega t + ikx), \qquad \delta\Pi \sim \exp(-i\omega t + ikx), \tag{4.62}$$

the dispersion relation is determined by

$$\omega^2 - \frac{ik^2}{\epsilon_{\rm eq} + P_{\rm eq}} \left(\frac{\zeta}{1 + i\omega\tau_\Pi} + \frac{4}{3} \frac{\eta}{1 + i\omega\tau_\pi} \right) \omega + k^2 c_s^2 = 0. \tag{4.63}$$

In the large k limit, Eq. (4.63) gives the characteristic speed of sound mode v_L as

$$v_L^2 = \left(\frac{\partial \, {\rm Re}\, \omega}{\partial k} \right)^2 = \frac{\zeta}{\tau_\Pi(\epsilon_{\rm eq} + P_{\rm eq})} + \frac{4}{3} \frac{\eta}{\tau_\pi(\epsilon_{\rm eq} + P_{\rm eq})} + c_s^2. \tag{4.64}$$

The characteristic speeds v_T and v_L have to be smaller than the speed of light for the causality. Thus the causality conditions are derived:

$$v_T^2 = \frac{\eta}{\tau_\pi(\epsilon_{\rm eq} + P_{\rm eq})} \leq 1, \tag{4.65}$$

$$v_L^2 = \frac{\zeta}{\tau_\Pi(\epsilon_{\rm eq} + P_{\rm eq})} + \frac{4}{3} \frac{\eta}{\tau_\pi(\epsilon_{\rm eq} + P_{\rm eq})} + c_s^2 \leq 1. \tag{4.66}$$

Both v_T and v_L are expressed by the transport coefficients and the thermodynamic quantities. As seen in Eq. (4.66), the causality condition of sound mode provides more strict constraint than that of transverse one.

summary

- We reviewed the relativistic ideal and dissipative hydrodynamics by a phenomenological derivation with the second law of thermodynamics.
- There are two choices of the local rest frame of fluid, i.e. Eckart (or particle) and Landau (or energy) frames.
- The first order theory (the relativistic Navier-Stokes theory) is known to violate causality due to the hyperbolic evolution equation of dissipative current.
- On the other hand, in the second order theory the hydrodynamic equation of each dissipation becomes parabolic and can be causal due to the relaxation times.
- We also introduced the characteristic speeds and the causality conditions of transverse and sound modes for pure gauge theory.

Chapter 5

Ratios of Transport Coefficients

Relativistic hydrodynamic simulations are useful tools to describe the space-time evolution of a hot quark-gluon matter created in relativistic heavy ion collisions. The simulations depend on several input parameters and boundary conditions such as an initial condition, equation of state, and transport coefficients. Since these input parameters are sources of ambiguity of hydrodynamic simulations, it is highly desirable to constrain them based on a microscopic theory or ab initio calculation that is QCD for heavy ion collisions. There are several studies which analyzed the first order transport coefficients from lattice QCD simulations [28, 29, 30, 31, 32]. These studies have used Kubo formula, which relates the transport coefficients to low energy behavior of corresponding spectral functions. In this method, one needs to extract the spectral functions from Euclidean correlators obtained on the lattice. This step, however, is non-trivial because of an ill-posed problem [33]. In this chapter, we focus on ratios between the first and second order transport coefficients. We attempt to derive relations between this ratio and canonical correlation of energy-momentum tensor in four-dimensional Euclidean space. According to the relations, the ratios can be directly obtained from Euclidean correlation functions without obtaining the spectral functions.

5.1 Linear response theory

Linear response theory describes a response of some physical quantity against small perturbations added onto a thermal equilibrium system. Let us first consider a system described by Hamiltonian [1]

$$H(t) = H_0 - AF(t), \tag{5.1}$$

where H_0 is Hamiltonian corresponding to equilibrium state. $F(t)$ is a time-dependent external force and A is a conjugate quantity of $F(t)$. We discuss how a physical quantity B varies under the perturbation $-AF(t)$. The thermal expectation value of B at time t is given by $\langle B\rangle_t = \mathrm{Tr}\,[\rho(t)B]$, where $\rho(t)$ is a density matrix at time t. What we calculate is a difference of $\langle B\rangle$ between at time t and initial time t_0,

$$\Delta\langle B\rangle_t \equiv \langle B\rangle_t - \langle B\rangle_{t_0} = \mathrm{Tr}\,[\rho(t)B] - \mathrm{Tr}\,[\rho(t_0)B]. \tag{5.2}$$

$\Delta\langle B\rangle_t$ is determined if $\rho(t)$ is obtained. In this and next sections, we write $\hbar$ explicitly.

[1] In this section, we discuss *mechanical perturbation*, which can be added to Hamiltonian as an external field such as the electric or the magnetic fields. On the other hand, *thermal perturbation* such as heat or concentration gradients is described as a boundary condition for a system. Although these perturbations must be discriminated from each other, they lead the same expression for the transport coefficients in a range of linear approximation.

The time evolution of $\rho(t)$ is given by

$$\rho(t) = U(t, t_0)\rho(t_0)U^\dagger(t, t_0). \tag{5.3}$$

$U(t, t_0)$ is a time evolution operator, which satisfies following equations,

$$i\hbar\frac{\partial}{\partial t}U(t, t_0) = H(t)U(t, t_0), \tag{5.4}$$

$$U(t_0, t_0) = 1, \tag{5.5}$$

$$U(t, t_0) = U^\dagger(t_0, t). \tag{5.6}$$

The solution of Eq. (5.4) with the initial condition Eq. (5.5) is

$$U(t, t_0) = \mathcal{T}\left(\exp\left[-\frac{i}{\hbar}\int_{t_0}^{t} H(s)ds\right]\right), \tag{5.7}$$

where $\mathcal{T}$ denotes time ordering. Dividing $U(t, t_0)$ into equilibrium and perturbative parts $U(t, t_0) = U_0(t, t_0)U'(t)$, $U'(t)$ also satisfies a similar equation as Eq. (5.4) and can be written as

$$U'(t) = \mathcal{T}\left(\exp\left[-\frac{i}{\hbar}\int_{t_0}^{t} H'(s)ds\right]\right), \tag{5.8}$$

$$H'(t) = U_0^\dagger(t, t_0)(-AF(t))U_0(t, t_0), \tag{5.9}$$

$$U_0(t, t_0) = \exp\left[-\frac{i}{\hbar}H_0(t - t_0)\right]. \tag{5.10}$$

Then the expectation value $\langle B\rangle_t$ under the small perturbation is calculated as follows,

$$\begin{aligned}
\langle B\rangle_t &= \mathrm{Tr}\,[\rho(t)B] \\
&= \mathrm{Tr}\,[U(t, t_0)\rho(t_0)U^\dagger(t, t_0)B] \\
&\simeq \mathrm{Tr}\left[\rho(t_0)\left(1 + \frac{i}{\hbar}\int_{t_0}^{t} H'(s)ds\right)U_0^\dagger(t, t_0)BU_0(t, t_0)\left(1 - \frac{i}{\hbar}\int_{t_0}^{t} H'(s)ds\right)\right] \\
&= \mathrm{Tr}\,[\rho(t_0)B(t, t_0)] + \frac{i}{\hbar}\int_{t_0}^{t}\mathrm{Tr}\,[\rho(t_0)[H'(s), B(t, t_0)]]\,ds \\
&= \mathrm{Tr}\,[\rho(t_0)B(t, t_0)] - \frac{i}{\hbar}\int_{t_0}^{t}\mathrm{Tr}\,[\rho(t_0)[A, B(t, s)]F(s)]\,ds.
\end{aligned} \tag{5.11}$$

Here we used a relation $O(t, t_0) = U_0^\dagger(t, t_0)\,O\,U_0(t, t_0)$ with $O = A$ and B. In the fifth line, we used a commutator $[\rho(t_0), U_0(t, t_0)] = 0$ and $U_0(t, t_0)U_0^\dagger(s, t_0) = U_0(t, t_0)U_0(t_0, s) = U_0(t, s)$.

Assuming that the initial state was in equilibrium at infinitely past, i.e. $\rho(t_0 \to -\infty) = \rho_{\mathrm{eq}}$ and $B(t, s) = B(t - s)$, the difference $\Delta\langle B\rangle_t$ reads

$$\Delta\langle B\rangle_t = \langle B\rangle_t - \langle B\rangle_{-\infty} = -\frac{i}{\hbar}\int_{-\infty}^{t}\langle[A, B(t - s)]\rangle_{\mathrm{eq}}F(s)ds, \tag{5.12}$$

where $\langle O\rangle_{\mathrm{eq}}$ denotes an equilibrium expectation value, $\langle O\rangle_{\mathrm{eq}} \equiv \mathrm{Tr}\,[\rho_{\mathrm{eq}}\,O]$. Let us introduce an oscillational force $F(s) = Fe^{i\omega s}$ and *complex admittance* $\chi(\omega)$ defined by

$$\chi(\omega) \equiv -\frac{i}{\hbar}\int_{-\infty}^{t}\langle[A, B(t - s)]\rangle_{\mathrm{eq}}\,e^{-i\omega(t-s)}ds. \tag{5.13}$$

Performing a transformation of integration variable $t - s \to t$, the complex admittance reduces to

$$\chi(\omega) = -\frac{i}{\hbar}\int_0^\infty \langle [A, B(t)] \rangle_{\rm eq}\, e^{-i\omega t} dt. \tag{5.14}$$

Fourier transformation of $\chi(\omega)$ is called *response function*,

$$\chi(t) = -\frac{i}{\hbar}\langle [A, B(t)] \rangle_{\rm eq} \quad (t > 0), \tag{5.15}$$

$$\chi(t) = 0 \quad (t < 0). \tag{5.16}$$

To rewrite the complex admittance, we use an identity for an arbitrary operator A [2]

$$[e^{-H_0/T}, A] = e^{-H_0/T}\int_0^{\hbar/T} d\lambda\, e^{\lambda H_0}[A, H_0]e^{-\lambda H_0}. \tag{5.17}$$

Using this identity and Heisenberg equation of motion one obtains

$$[\rho_{\rm eq}, A] = i\hbar\rho_{\rm eq}\int_0^{\hbar/T} d\lambda\, e^{\lambda H_0}\dot{A}e^{-\lambda H_0} = i\hbar\rho_{\rm eq}\int_0^{\hbar/T} d\lambda\, \dot{A}(-i\lambda), \tag{5.18}$$

$$\rho_{\rm eq} \equiv \frac{e^{-H_0/T}}{{\rm Tr}\, e^{-H_0/T}}. \tag{5.19}$$

Here $\dot{O}$ represents time derivative $\dot{O} = dO/dt$. With Eq. (5.18), one obtains the following equation

$$\begin{aligned}
\langle [A, B(t)] \rangle_{\rm eq} &= {\rm Tr}\,[\rho_{\rm eq}\,[A, B(t)]] \\
&= {\rm Tr}\,[[\rho_{\rm eq}, A]\, B(t)] \\
&= i\hbar{\rm Tr}\left[\rho_{\rm eq}\int_0^{\hbar/T} d\lambda\, \dot{A}(-i\lambda)B(t)\right] \\
&= i\hbar\int_0^{\hbar/T} d\lambda\, \langle \dot{A}(-i\lambda)B(t)\rangle_{\rm eq}.
\end{aligned} \tag{5.20}$$

Applying Eq. (5.20) to Eqs. (5.14) and (5.15), the complex admittance and the response function reduce to

$$\chi(\omega) = \int_0^\infty dt \int_0^{\hbar/T} d\lambda\, e^{-i\omega t}\langle \dot{A}(-i\lambda)B(t)\rangle_{\rm eq}, \tag{5.21}$$

$$\chi(t) = \int_0^{\hbar/T} d\lambda\, \langle \dot{A}(-i\lambda)B(t)\rangle_{\rm eq} \quad (t > 0). \tag{5.22}$$

If one adopts some current operator $J/\sqrt{V}$, where V is a volume of system, as $\dot{A}$ and B, the complex admittance and the response function are given by

$$\chi(\omega) = \frac{1}{V}\int_0^\infty dt \int_0^{\hbar/T} d\lambda\, \langle J(-i\lambda)J(t)\rangle_{\rm eq}\, e^{-i\omega t} \tag{5.23}$$

$$\chi(t) = \frac{1}{V}\int_0^{\hbar/T} d\lambda\, \langle J(-i\lambda)J(t)\rangle_{\rm eq} \quad (t > 0). \tag{5.24}$$

[2] To check this identity, one may multiply $e^{H_0/T}$ to each side from left and differentiate with respect to $1/T$,

$$({\rm LHS}) = \frac{d}{d(1/T)}e^{H_0/T}[e^{-H_0/T}, A] = e^{H_0/T}H_0[e^{-H_0/T}, A] - e^{H_0/T}[H_0e^{-H_0/T}, A] = e^{H_0/T}[A, H_0]e^{-H_0/T},$$

$$({\rm RHS}) = \frac{d}{d(1/T)}\int_0^{\hbar/T} d\lambda\, e^{\lambda H_0}[A, H_0]e^{-\lambda H_0} = e^{H_0/T}[A, H_0]e^{-H_0/T}.$$

Eqs. (5.23) and (5.24) are *Kubo formulas* [79] for quantum systems. Taking a classical limit $\hbar \to 0$ in Eqs. (5.23) and (5.24), Kubo formulas in this limit are obtained,

$$\chi(\omega) = \frac{1}{TV}\int_0^\infty dt\, \langle J(0)J(t)\rangle_{\rm eq}\, e^{-i\omega t}, \tag{5.25}$$

$$\chi(t) = \frac{1}{TV}\langle J(0)J(t)\rangle_{\rm eq} \quad (t > 0). \tag{5.26}$$

Thus responses of some quantity for small perturbations are expressed by the temporal correlator of currents in the linear response theory with the classical limit.

5.2 Formulation

In this section, we derive relations between viscosity to relaxation time ratio and corresponding canonical correlation of energy-momentum tensor for pure gauge theory. Since there is no charge flow in pure gauge theory, a local rest frame (LRF) of a fluid is naturally identified with the Landau (energy) one. In this frame, the energy and heat flows vanish, $W^\mu = 0$ and $q^\mu = 0$ (see subsection 4.1.2), and the first order transport coefficients are the bulk viscosity ζ and the shear one η. The second order transport coefficients are the relaxation times for the corresponding dissipative current, τ_Π and τ_π. In chapter 4, we introduced the entropy current as Eq. (4.36). Since there are no conserved currents, the entropy is given by

$$S = S_{\rm eq} - \frac{V}{2T}\left(\beta_\Pi \Pi^2 + \beta_\pi \pi_{ij}\pi_{ij}\right). \tag{5.27}$$

The viscosities and the relaxation times are related to each other as Eqs. (4.42),

$$\tau_\Pi = \beta_\Pi \zeta, \qquad \tau_\pi = 2\beta_\pi \eta. \tag{5.28}$$

5.2.1 Classical formulation

As an instructive example, we first derive formulas for the viscosity to relaxation time ratios for classical systems by two approaches. The two different approaches are based on the classical limit of Kubo formula Eq.(5.25) and *Einstein principle* [80, 81] with Eq. (5.27), respectively. They lead the same result and the ratios can be related with static fluctuations of dissipative current. These derivations were proposed by Refs. [34, 35].

Let us begin with the classical limit of Kubo formula Eq. (5.25) with $\omega = 0$. According to the linear response theory, the first order transport coefficients for classical systems are expressed by the temporal correlation of each dissipative current,

$$\zeta = \frac{V}{T}\int_0^\infty dt\, \langle \bar{\Pi}(0)\bar{\Pi}(t)\rangle, \tag{5.29}$$

$$\eta = \frac{V}{T}\int_0^\infty dt\, \langle \bar{\pi}_{12}(0)\bar{\pi}_{12}(t)\rangle, \tag{5.30}$$

where $\bar{A}$ denotes three-dimensional spatial average

$$\bar{A}(t) \equiv \frac{1}{V}\int d^3x\, A(\vec{x}, t), \tag{5.31}$$

and $\langle O \rangle$ is a statistical average in equilibrium

$$\langle O \rangle \equiv \frac{\mathrm{Tr}\, e^{-H/T} O}{\mathrm{Tr}\, e^{-H/T}}. \tag{5.32}$$

Following the IS equations Eqs. (4.39) and (4.41), the temporal correlation functions of dissipative current decay exponentially as in Eq. (4.44), i.e.

$$\langle \bar{A}(0)\bar{A}(t) \rangle = e^{-t/\tau_A} \langle \bar{A}(0)\bar{A}(0) \rangle. \tag{5.33}$$

Applying Eq. (5.33) to Eqs. (5.29) and (5.30) and performing t integral, one computes

$$\bar{A} = \frac{V}{T} \int_0^\infty dt\, \langle \bar{A}(t)\bar{A}(0) \rangle \tag{5.34}$$

$$= \frac{V}{T} \int_0^\infty dt\, e^{-t/\tau_A} \langle \bar{A}(0)\bar{A}(0) \rangle \tag{5.35}$$

$$= \frac{V}{T} \tau_A \langle \bar{A}^2(0) \rangle. \tag{5.36}$$

Thus following relations are obtained,

$$\frac{\zeta}{\tau_\Pi} = \frac{V}{T} \langle \bar{\Pi}^2(0) \rangle, \qquad \frac{\eta}{\tau_\pi} = \frac{V}{T} \langle \bar{\pi}_{12}^2(0) \rangle. \tag{5.37}$$

In this way, the viscosity to relaxation time ratios are related to the static fluctuations of dissipative current $\langle \Pi^2 \rangle$ and $\langle \pi_{12}^2 \rangle$. Note that Eqs. (5.37) are valid only for classical systems because above argument is based on the classical limit of Kubo formula Eqs.(5.29) and (5.30). We will expand the argument to quantum systems in the next subsection.

Let us derive Eqs. (5.37) with a different manner. According to the Einstein principle, a probability distribution $P(a)$ of some state variable a in equilibrium is given by $P(a) \sim e^{S(a)}$, where $S(a)$ is the entropy in a volume V. If one identifies the entropy with Eq. (5.27) to be that in the Einstein principle, a probability distribution of the state variable $\bar{A}$ is given by

$$P_A(\bar{A}) \propto \exp\left[-\frac{V}{T} \beta_A \bar{A}^2 \right]. \tag{5.38}$$

With this distribution function, the fluctuations (or the variances) of dissipative current are calculated to be

$$\langle \bar{\Pi}^2 \rangle = \frac{\int d\bar{\Pi}\, \bar{\Pi}^2\, P_\Pi(\bar{\Pi})}{\int d\bar{\Pi}\, P_\Pi(\bar{\Pi})} = \frac{T}{\beta_\Pi V} = \frac{\zeta T}{\tau_\Pi V}, \tag{5.39}$$

$$\langle \bar{\pi}_{ij}^2 \rangle = \frac{\int d\bar{\pi}\, \bar{\pi}_{12}^2\, P_\pi(\bar{\pi})}{\int d\bar{\pi}\, P_\pi(\bar{\pi})} = \frac{T}{2\beta_\pi V} = \frac{\eta T}{\tau_\pi V}, \tag{5.40}$$

where we used the fact that the statistical average of dissipative current in equilibrium vanishes i.e. $\langle \bar{A} \rangle = 0$ and hence $\langle (\delta \bar{A})^2 \rangle = \langle (\bar{A} - \langle \bar{A} \rangle)^2 \rangle = \langle \bar{A}^2 \rangle$. Eqs. (5.39) and (5.40) are identical to Eqs. (5.37).

It, however, should be remembered that state variables are assumed to be treated as classical variables in Einstein principle. In quantum mechanics, when a state variable a does not commute with Hamiltonian, a and the energy cannot be determined simultaneously because of the uncertainty principle. This means that the entropy cannot be defined as a function of non-conserving state variables in quantum systems [81]. The Einstein principle therefore is not applicable to such a situation.

5.2.2 Quantum formulation

In the subsection 5.2.1, we derived the ratios of the first and second order transport coefficients for classical systems. The ratios are described by the static fluctuations of each dissipative current, which are classical and macroscopic variables. However, what we are now interested in is the transport property of a hot quark-gluon matter where quantum effects would play significant roles. It is required to expand the classical relations Eqs. (5.37) to the ones in quantum field theory and to substitute field operators for the classical variables $\bar{A}$.

Let us apply the Kubo formula Eq. (5.23) to quantum field theory :

$$\chi(\omega) = \frac{1}{V}\int_0^\infty dt \int_0^{\hbar/T} d\lambda \, \langle J(-i\lambda)J(t)\rangle_{\rm eq} \, e^{-i\omega t}. \tag{5.41}$$

Although this formula seems to be the same as Eq. (5.23), J is now a quantum field operator. In order to extract physical quantity from Eq. (5.41), one must pay attention to a singularity specific to quantum field theory. In general, some correlation function of field operators has a singularity at identical space-time point, and the singularity brings about ultraviolet divergence of an integral of correlation function.

- An example : Two point correlation function of scalar field
  In quantum field theory, two point correlation function often diverges in short distance limit. Let us consider two point correlation function of a free scalar field $\phi(x)$, where $x = (t, \vec{x})$. The correlation function in momentum space is given by

$$\langle \mathcal{T}\phi(x)\phi(y)\rangle = \int \frac{d^4p}{(2\pi)^4}\frac{i}{p^2 - m^2}e^{-ip(x-y)}. \tag{5.42}$$

  Here m represents a mass of the scalar field. Eq. (5.42) diverges in the short distance limit $x \to y$, and one has to perform some appropriate regularization procedure to remove the ultraviolet divergence when the equal space-time correlator $\langle\phi(0)\phi(0)\rangle$ is explicitly concerned.

The bulk and shear viscosities are expressed by the correlation function of field operator corresponding to each dissipative current,

$$\zeta = \frac{V}{\hbar}\int_0^\infty dt \int_0^{\hbar/T} d\lambda \, \langle\bar{\Pi}(-i\lambda)\bar{\Pi}(t)\rangle, \tag{5.43}$$

$$\eta = \frac{V}{\hbar}\int_0^\infty dt \int_0^{\hbar/T} d\lambda \, \langle\bar{\pi}_{12}(-i\lambda)\bar{\pi}_{12}(t)\rangle. \tag{5.44}$$

Imposing Eq. (4.44) on $\bar{A} = \bar{\Pi}, \bar{\pi}$ in these equations as is the case in classical formulation, their temporal integrals may be computed as follows,

$$\int_0^\infty dt \int_0^{\hbar/T} d\lambda \, \langle\bar{A}(-i\lambda)\bar{A}(t)\rangle \to \int_0^\infty dt \int_0^{\hbar/T} d\lambda \, \langle\bar{A}(-i\lambda)\bar{A}(t)\rangle_{\rm reg} \tag{5.45}$$

$$\simeq \int_0^\infty dt \, e^{-t/\tau_A} \int_0^{\hbar/T} d\lambda \, \langle\bar{A}(-i\lambda)\bar{A}(0)\rangle_{\rm reg} \tag{5.46}$$

$$= \tau_A \int_0^{\hbar/T} d\lambda \, \langle\bar{A}(-i\lambda)\bar{A}(0)\rangle_{\rm reg}. \tag{5.47}$$

In the right-hand side of Eq. (5.45), we put a subscript "reg" to the correlation function. This means that $\langle\bar{A}(-i\lambda)\bar{A}(t)\rangle_{\rm reg}$ is a correlation function with some appropriate regularization. The Euclidean

correlation function $\langle \bar{A}(-i\lambda)\bar{A}(0)\rangle$ contains singularities at the origin and they should be excluded by regularization to obtain a physical viscosity. Eq. (5.45) represents the prescription of the regularization is carried out. We discuss the detail of this matter in a later section and use the regularized correlation function in the following.

We refer to the approximation Eq. (5.46) for Eq. (5.45) as relaxation time approximation, owing to an analogy to the standard approximation in non-equilibrium statistical mechanics, $\langle O(t)O(0)\rangle \simeq e^{-t/\tau}\langle O(0)O(0)\rangle$. Note, however, that Eq. (5.46) is slightly different from this approximation, because in Eq. (5.45) the correlator between field operators separated along complex time is concerned, while the standard relaxation time approximation assumes structure of correlators in real time. Despite this difference, the time scales appearing in exponential function in Eq. (5.46) would be equivalent to the relaxation times of dissipative current τ_A in Eqs. (4.39) and (4.41).

Substituting Eq. (5.47) in Eqs. (5.43) and (5.44), the relations between the transport coefficient ratio and the Euclidean correlation function of dissipative current are derived,

$$\frac{\zeta}{\tau_\Pi} = \frac{V}{\hbar}\int_0^{\hbar/T} d\lambda\, \langle \bar{\Pi}(-i\lambda)\bar{\Pi}(0)\rangle_{\rm reg}, \tag{5.48}$$

$$\frac{\eta}{\tau_\pi} = \frac{V}{\hbar}\int_0^{\hbar/T} d\lambda\, \langle \bar{\pi}_{12}(-i\lambda)\bar{\pi}_{12}(0)\rangle_{\rm reg}. \tag{5.49}$$

If one takes the limit $\hbar \to 0$ in Eqs. (5.48) and (5.49), the classical relations Eqs. (5.37) are reproduced. In the local rest frame of a fluid, one can replace the dissipative currents with the energy-momentum tensor $T_{\mu\nu}$. Then the relations Eqs. (5.48) and (5.49) are rewritten as

$$\frac{\zeta}{\tau_\Pi} = \frac{V}{9\hbar}\int_0^{\hbar/T} d\lambda\, \langle \delta\bar{T}_{ii}(-i\lambda)\delta\bar{T}_{jj}(0)\rangle_{\rm reg} = \frac{1}{9\hbar}\int_0^{\hbar/T} d^4x\, \langle \delta T_{ii}(x)\delta T_{jj}(0)\rangle_{\rm reg} \tag{5.50}$$

$$\frac{\eta}{\tau_\pi} = \frac{V}{\hbar}\int_0^{\hbar/T} d\lambda\, \langle \delta\bar{T}_{12}(-i\lambda)\delta\bar{T}_{12}(0)\rangle_{\rm reg} = \frac{1}{\hbar}\int_0^{\hbar/T} d^4x\, \langle \delta T_{12}(x)\delta T_{12}(0)\rangle_{\rm reg}, \tag{5.51}$$

where we used shorthand notations $x = (-i\lambda, \vec{x})$ and $\int_0^{\hbar/T} d^4x = \int d^3x \int_0^{\hbar/T} d\lambda$. Defining *Kubo's canonical correlation* as

$$\langle \delta\tilde{T}^2_{\mu\nu}\rangle \equiv \langle \left(\frac{T}{V}\int d^4x\, \delta T_{\mu\nu}(x)\right)^2 \rangle, \tag{5.52}$$

Eqs. (5.50) and (5.51) are expressed by

$$\frac{\zeta}{\tau_\Pi} = \frac{V}{9\hbar T}\langle \delta\tilde{T}^2_{ii}\rangle_{\rm reg}, \qquad \frac{\eta}{\tau_\pi} = \frac{V}{\hbar T}\langle \delta\tilde{T}^2_{12}\rangle_{\rm reg}. \tag{5.53}$$

As seen in Eqs. (5.53), the ratios of transport coefficients in quantum field theory are related to the canonical correlation of $T_{\mu\nu}$ in four-dimensional Euclidean space. We note that Eqs. (5.53) are also derived by the projection operator method [36].

Although the canonical correlation Eq. (5.52) can directly be measured by lattice QCD simulation, it is naively different from those in Eqs. (5.53) due to two reasons. First, $\langle \delta\tilde{T}^2_{\mu\nu}\rangle$ is an ultraviolet divergent quantity. A correlation function of field operator generally accompanies this issue and the divergence must be excluded by some renormalization process. Second, the contact terms, which do not affect Kubo formula, have a contribution to $\langle \delta\tilde{T}^2_{\mu\nu}\rangle$ in Euclidean space (see subsection 5.3.2 for the detailed argument). The contact terms give finite but temperature dependent contribution to $\langle \delta\tilde{T}^2_{\mu\nu}\rangle$ on the lattice and cannot be removed by the vacuum subtraction. Thus one must perform

an appropriate regularization for Eq. (5.52) to evaluate the ratios from lattice measurements of the canonical correlations of $T_{\mu\nu}$.

An advantage of the measurement of viscosity to relaxation time ratios with Eqs. (5.53) is that they can be observed directly in lattice QCD simulation. This is an important difference from the previous lattice studies of the first order transport coefficients. In order to get the transport coefficients, they observed the Euclidean (imaginary-time) correlation function on the lattice and extracted the spectral functions which have an information about each transport coefficient at low frequencies from the lattice results. This procedure, however, requires an ansatz for the spectral function because one must extract a continuous function from finite and small number of lattice data of the Euclidean correlation function. On the other hand, we take notice of the ratios of transport coefficients, and they can be directly measured on the lattice without any ansatz. Whereas the ratios are not the transport coefficients themselves, the ambiguity of hydrodynamic simulations is expected to be reduced by analyses of the ratios.

5.3 Regularization

5.3.1 Operator product expansion

We have derived the relations between the ratio of transport coefficients and the canonical correlation of $T_{\mu\nu}(x)$ for quantum field theory in the last section. As already mentioned there, one must treat the correlation function of field operator carefully since they contain singularity at identical space-time points. One of those is an ultraviolet divergence, which originates from short distance behavior of the Euclidean correlation function of $T_{\mu\nu}(x)$. Another is a temperature dependent contribution that is proportional to δ-function, i.e. the contact term.

Since both of these effects come from the short distance behavior of the Euclidean correlation function of $T_{\mu\nu}(x)$, we may employ the operator-product expansion (OPE) to investigate these effects. According to Ref. [82], the product of $T_{\mu\nu}(x)$ at short distance limit behaves as

$$T_{\mu\nu}(x)T_{\rho\sigma}(0) \sim C_{\mu\nu\rho\sigma}\frac{1}{|x|^8} + C_{\mu\nu\rho\sigma\alpha\beta}T_{\alpha\beta}(0)\delta^{(4)}(x) + \cdots \quad \text{for } x \sim 0, \tag{5.54}$$

where $C_{\mu\nu\rho\sigma}$ and $C_{\mu\nu\rho\sigma\alpha\beta}$ are c-number Wilson coefficients determined in perturbation theory. The first term on the right-hand side in Eq. (5.54) is proportional to $|x|^{-8}$ due to dimensional reason and leads to an ultraviolet divergence. This term neither has medium effects nor affects long distance behavior responsible for the hydrodynamics. Therefore it would be plausible that this divergence does not affect hydrodynamics and should be eliminated when one discusses transport coefficients. This contribution is completely removed by subtracting the correlation function in the vacuum ($T = 0$). The next terms on the right-hand side of Eq. (5.54) are proportional to dimension four operators. These terms contain the contact term, which is proportional to $\delta^{(4)}(x)$ as presented in Eq. (5.54). This contribution cannot be removed by the vacuum subtraction because the statistical average of the contact terms is proportional to $\langle T_{\mu\nu}\rangle$ and has temperature dependence. The higher order terms in Eq. (5.54) shown by dots neither yield divergence nor are singular.

When investigating the viscosity to relaxation time ratios based on Eqs. (5.50) and (5.51), one has to handle these extra contributions. To take this point carefully into account, we discuss regularization process for the physically meaningful ratios. From now we set $\hbar = 1$. First we show the vacuum subtraction to eliminate the contribution from first term in Eq. (5.54). One can write this subtraction procedure for Euclidean correlation function of $T_{\mu\nu}(x)$ as follows

$$\int_0^{1/T} d^4x\, \langle T_{\mu\nu}(x)T_{\rho\sigma}(0)\rangle_0 \equiv \int_0^{1/T} d^4x\, \langle T_{\mu\nu}(x)T_{\rho\sigma}(0)\rangle_T - \int_0^{1/T_0} d^4x\, \langle T_{\mu\nu}(x)T_{\rho\sigma}(0)\rangle_{T_0}. \tag{5.55}$$

Here we denoted the zero temperature by T_0 because one cannot take an infinite lattice size in actual lattice simulations. Due to this prescription, the first term in Eq. (5.54) is removed. Note that the range of temporal integration of vacuum term differs from the thermal one as in Eq. (5.55).

In addition to the vacuum subtraction, we should subtract the contribution from contact terms because they do not contribute to Kubo formula as discussed later,

$$\int_0^{1/T} d^4x \, \langle T_{\mu\nu}(x) T_{\rho\sigma}(0) \rangle_{\rm reg} \equiv \int_0^{1/T} d^4x \, \langle T_{\mu\nu}(x) T_{\rho\sigma}(0) \rangle_0 - C_{\mu\nu\rho\sigma\alpha\beta} \langle T_{\alpha\beta}(0) \rangle_0. \tag{5.56}$$

Unlike the vacuum subtraction for the canonical correlation of $T_{\mu\nu}(x)$ Eq. (5.55), $\langle T_{\alpha\beta}(0) \rangle_0$ represents a simple difference between $\langle T_{\alpha\beta}(0) \rangle_{T \neq 0}$ and $\langle T_{\alpha\beta}(0) \rangle_{T=0}$. $\langle T_{\mu\nu}(x) T_{\rho\sigma}(0) \rangle_{\rm reg}$ is the regularized correlation function which appears in Eq. (5.45).

As discussed above, we subtracted the contact terms from the Euclidean correlation functions in the regularization. In this argument, we assumed that Kubo formula, which is our starting point, does not contain a contribution from contact terms. We discuss this issue in the next subsection. We will conclude that the contact terms do not contribute to Kubo formula and one has to exclude the contribution from the Euclidean correlation function of $T_{\mu\nu}(x)$.

5.3.2 Contact terms in Kubo formula

We here investigate the contribution of contact terms to Kubo formula. From Eq. (5.54), the contact terms in Euclidean space are given by

$$g(-i\lambda, \vec{x}) \equiv C_{\mu\nu\rho\sigma\alpha\beta} \langle T_{\alpha\beta}(0) \rangle_0 \delta^{(4)}(x). \tag{5.57}$$

To evaluate the contribution of this terms to Kubo formula, which is dependent on the real-time t and the imaginary-time λ, we perform an analytic continuation $\lambda \to \lambda + it$ in Eq. (5.57). In order to obtain an analytic continuation of δ-function to complex argument, we utilize Poisson equation in four-dimensional space

$$\delta^{(4)}(x) = -\frac{1}{2\pi^2} \partial^2 \frac{1}{x^2}, \tag{5.58}$$

where $\partial^2 = \partial_0^2 + \partial_i^2$ and $x^2 = \lambda^2 + \vec{x}^2 = \lambda^2 + r^2$. The contact terms are then given by

$$g(-i\lambda, \vec{x}) = -\frac{1}{2\pi^2} C_{\mu\nu\rho\sigma\alpha\beta} \langle T_{\alpha\beta}(0) \rangle_0 \partial^2 \frac{1}{x^2 + \epsilon}. \tag{5.59}$$

where we added an infinitesimal quantity $\epsilon > 0$, which vanishes in the end of calculation, to the denominator of $1/x^2$ to suppress the singularity at $x^2 = 0$. Before the analytic continuation, let us carry out a differentiation and a spatial integration of $1/(x^2 + \epsilon)$,

$$\begin{aligned} \int d^3x \, \partial^2 \frac{1}{x^2 + \epsilon} &= -8\epsilon \int d^3x \, \frac{1}{(x^2 + \epsilon)^3} \\ &= -32\pi\epsilon \int_0^\infty dr \, \frac{r^2}{(r^2 + \lambda^2 + \epsilon)^3} \\ &= \frac{-2\pi\epsilon}{\lambda^2 + \epsilon} \int_{-\infty}^\infty dr \, \frac{1}{r^2 + \lambda^2 + \epsilon} \\ &= -\frac{2\pi^2\epsilon}{(\lambda^2 + \epsilon)^{3/2}}. \end{aligned} \tag{5.60}$$

In third equality, we used a following formula

$$\int dr\, \frac{r^2}{(r^2+c)^3} = -\frac{r}{4(r^2+c)^2} + \frac{r}{8c(r^2+c)} + \frac{1}{8c}\int \frac{dr}{r^2+c}. \tag{5.61}$$

Performing the analytic continuation $\lambda \to \lambda + it$ in Eq. (5.60), one obtains

$$g(t - i\lambda; \epsilon) = C_{\mu\nu\rho\sigma\alpha\beta}\langle T_{\alpha\beta}(0)\rangle_0 \frac{\epsilon}{\{(\lambda+it)^2+\epsilon\}^{3/2}}. \tag{5.62}$$

To evaluate the contribution of contact terms to Kubo formula, Eq. (5.41), we perform temporal integrals of $g(t - i\lambda; \epsilon)$,

$$\int_0^\infty dt \int_0^{1/T} d\lambda\, g(t - i\lambda; \epsilon) \tag{5.63}$$

$$= C_{\mu\nu\rho\sigma\alpha\beta}\langle T_{\alpha\beta}(0)\rangle_0 \int_0^\infty dt \int_0^{1/T} d\lambda \left[\frac{\epsilon}{\{(\lambda+it)^2+\epsilon\}^{3/2}} + \frac{\epsilon}{\{(\lambda-\frac{1}{T}+it)^2+\epsilon\}^{3/2}}\right] \tag{5.64}$$

$$= C_{\mu\nu\rho\sigma\alpha\beta}\langle T_{\alpha\beta}(0)\rangle_0 \int_0^\infty dt \int_{-1/T}^{1/T} d\lambda \frac{\epsilon}{\{(\lambda+it)^2+\epsilon\}^{3/2}} \tag{5.65}$$

$$\to C_{\mu\nu\rho\sigma\alpha\beta}\langle T_{\alpha\beta}(0)\rangle_0 \int_0^\infty dt \int_{-\infty}^{\infty} d\lambda \frac{\epsilon}{\{(\lambda+it)^2+\epsilon\}^{3/2}}, \tag{5.66}$$

where in the first equality we used the periodicity of λ integral. Note that the δ-functions in Eq. (5.57) locate at upper and lower limits of λ integral due to the periodicyty of λ direction. Therefore we must take into account the contributions from both δ-functions at $\lambda = 0$ and $\lambda = 1/T$ to Eq. (5.63). Moreover we expanded it to $\lambda \in [-\infty, \infty]$ in the forth line for later convenience. In the following, we show that the expanded intervals in Eq. (5.66) do not contribute to Eq. (5.64) in the limit of $\epsilon \to 0$.

We divide the λ integral of Eq. (5.66) into the original part and expanded ones,

$$\int_0^\infty dt \int_{-\infty}^{\infty} d\lambda \frac{\epsilon}{\{(\lambda+it)^2+\epsilon\}^{3/2}} = \int_0^\infty dt \left(\int_{-\infty}^{-1/T} + \int_{-1/T}^{1/T} + \int_{1/T}^{\infty}\right) d\lambda \frac{\epsilon}{\{(\lambda+it)^2+\epsilon\}^{3/2}}, \tag{5.67}$$

and then evaluate the third integral range, $\int_{1/T}^\infty d\lambda$, for fixed t. In the case of $t = 0$, the integral can be evaluated as follows,

$$\begin{aligned}\left|\int_{1/T}^\infty d\lambda \frac{\epsilon}{(\lambda^2+\epsilon)^{3/2}}\right| &\le \int_{1/T}^\infty d\lambda \left|\frac{\epsilon}{(\lambda^2+\epsilon)^{3/2}}\right| \\ &\le \int_{1/T}^\infty d\lambda \frac{\epsilon}{\lambda^3} \\ &= \left[-\frac{\epsilon}{2\lambda^2}\right]_{1/T}^\infty = \frac{\epsilon T^2}{2} \to 0 \quad (\epsilon \to 0).\end{aligned} \tag{5.68}$$

In the same way, we can show that the λ integral for fixed $t \neq 0$ vanishes,

$$\begin{aligned}\left|\int_{1/T}^{\infty} d\lambda \frac{\epsilon}{\{(\lambda+it)^2+\epsilon\}^{3/2}}\right| &\leq \int_{1/T}^{\infty} d\lambda \left|\frac{\epsilon}{(\lambda^2-t^2+\epsilon+2i\lambda t)^{3/2}}\right| \\ &= \int_{1/T}^{\infty} d\lambda \frac{\epsilon}{\{(\lambda^2-t^2+\epsilon)^2+(2\lambda t)^2)\}^{3/4}} \\ &\leq \int_{1/T}^{\infty} d\lambda \frac{\epsilon}{(2\lambda t)^{3/2}} \\ &= \frac{\epsilon}{(2t)^{3/2}}\left[-\frac{2}{\sqrt{\lambda}}\right]_{1/T}^{\infty} = \frac{\epsilon\sqrt{T}}{\sqrt{2}t^{3/2}} \to 0 \quad (\epsilon \to 0). \end{aligned} \tag{5.69}$$

Thus the third λ integral in Eq. (5.67) does not contribute to Eq. (5.64) in the limit of $\epsilon \to 0$. One can easily verify that the first one, $\int_{-\infty}^{-1/T} d\lambda$, also has no contribution to Eq. (5.67) and Eq. (5.66) is consistent with Eq. (5.64) for $\epsilon \to 0$.

Let us perform the integral of Eq. (5.66) by using another formula

$$\int \frac{dx}{(x^2+c)^{3/2}} = \frac{x}{c\sqrt{x^2+c}}. \tag{5.70}$$

With this formula, the λ integral is calculated as

$$\int_{-\infty}^{\infty} d\lambda \frac{\epsilon}{\{(\lambda+it)^2+\epsilon\}^{3/2}} = \int_{-\infty+it}^{\infty+it} dz \frac{\epsilon}{(z^2+\epsilon)^{3/2}} = \left[\frac{z}{\sqrt{z^2+\epsilon}}\right]_{z=-\infty+it}^{z=\infty+it}, \tag{5.71}$$

where we introduced a complex variable $z = \lambda + it$. $f(z) \equiv \sqrt{z^2+\epsilon}$ is a two-valued function and branch points locate at $z = \pm i\sqrt{\epsilon}$ (Fig. 5.1a).

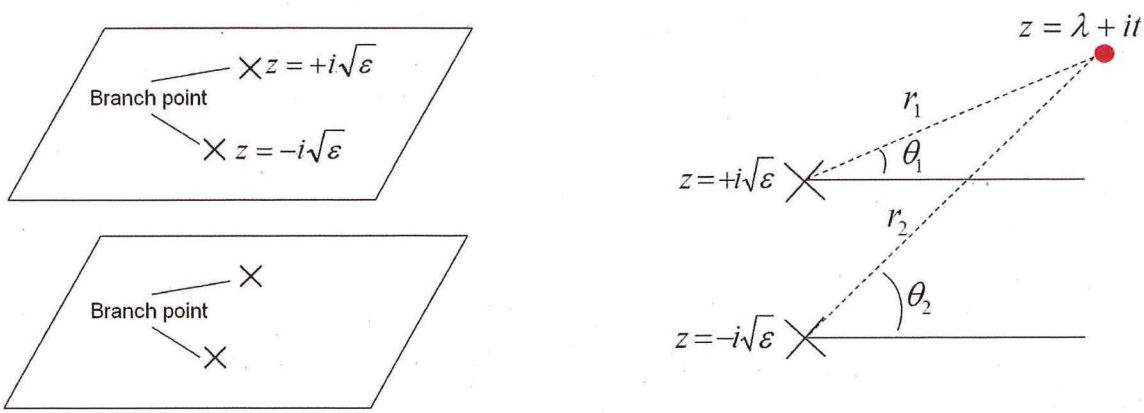

Figure 5.1: a): Riemann sheets for a two-valued function $f(z) = \sqrt{z^2+\epsilon}$. Two branch points locate at $z = \pm i\sqrt{\epsilon}$. b): Polar form.

In order to examine the right-hand side of Eq. (5.71), we introduce polar form (Fig. 5.1b),

$$z - i\sqrt{\epsilon} \equiv r_1 e^{i\theta_1}, \qquad z + i\sqrt{\epsilon} \equiv r_2 e^{i\theta_2}, \qquad -\pi < \theta_1, \theta_2 \leq \pi, \tag{5.72}$$

and rewrite $f(z)$ as follows

$$f(z) = (z - i\sqrt{\epsilon})^{1/2}(z + i\sqrt{\epsilon})^{1/2} = (r_1 e^{i\theta_1})^{1/2}(r_2 e^{i\theta_2})^{1/2}. \tag{5.73}$$

When the path of z integration passes through above the branch point $z = +i\sqrt{\epsilon}$, that is $t \in [\sqrt{\epsilon}, \infty]$, $z = +\infty + it$ and $z = -\infty + it$ correspond to $\theta_1 = \theta_2 = 0$ $(r_1, r_2 = \infty)$ and $\theta_1 = \theta_2 = \pi$ $(r_1, r_2 = \infty)$, respectively. In this case, $f(z)$ has opposite signs at $z = +\infty + it$ and $z = -\infty + it$,

$$f_{+\infty}(z) \equiv (r_1 e^0)^{1/2}(r_2 e^0)^{1/2} = \sqrt{r_1 r_2} \tag{5.74}$$

$$f_{-\infty}(z) \equiv (r_1 e^{i\pi})^{1/2}(r_2 e^{i\pi})^{1/2} = -\sqrt{r_1 r_2} = -f(z)_{+\infty}. \tag{5.75}$$

Then one may calculate the value of $f_{+\infty}(z)$ as follows

$$\left[\frac{z}{\sqrt{z^2+\epsilon}}\right]_{z=+\infty+it} = \lim_{a\to\infty} \frac{a+it}{\sqrt{(a+it)^2+\epsilon}} = \lim_{a\to\infty} \frac{1+i\frac{t}{a}}{\sqrt{1+i\frac{2t}{a}-\frac{t^2}{a^2}+\frac{\epsilon}{a^2}}} = \frac{1}{\sqrt{1}} = 1, \tag{5.76}$$

where we defined $f_{+\infty}(z) = \sqrt{1} \equiv 1$. Another limit is then given by

$$\left[\frac{z}{\sqrt{z^2+\epsilon}}\right]_{z=-\infty+it} = \lim_{a\to\infty} \frac{-a+it}{\sqrt{(-a+it)^2+\epsilon}} = \lim_{a\to\infty} \frac{-1+i\frac{t}{a}}{\sqrt{1+i\frac{2t}{a}-\frac{t^2}{a^2}+\frac{\epsilon}{a^2}}} = \frac{-1}{\sqrt{1}} = 1. \tag{5.77}$$

Here we used the relation Eq. (5.75) and $f_{-\infty}(z)$ is given by $f_{-\infty}(z) = \sqrt{1} = -f_{+\infty}(z) = -1$. Thus Eq. (5.71) for the case of $t \in [\sqrt{\epsilon}, \infty]$ becomes

$$\left[\frac{z}{\sqrt{z^2+\epsilon}}\right]_{z=-\infty+it}^{z=\infty+it} = 1 - 1 = 0. \tag{5.78}$$

On the other hand, when the integration path passes between the branch point $z = +i\sqrt{\epsilon}$ and the origin, i.e. $t \in [0, \sqrt{\epsilon}]$, the two limit of $z = \pm\infty + it$ correspond to $\theta_1 = \theta_2 = 0$ $(r_1, r_2 = \infty)$ and $\theta_1 = -\pi, \theta_2 = \pi$ $(r_1, r_2 = \infty)$, i.e.

$$f_{+\infty}(z) \equiv (r_1 e^0)^{1/2}(r_2 e^0)^{1/2} = \sqrt{r_1 r_2} \tag{5.79}$$

$$f_{-\infty}(z) \equiv (r_1 e^{-i\pi})^{1/2}(r_2 e^{i\pi})^{1/2} = \sqrt{r_1 r_2} = f_{+\infty}(z). \tag{5.80}$$

In this case, the values of $f(z)$ at two limits of $z = \pm\infty + it$ have the same signs. If one defines the value of $f_{+\infty}(z) \equiv 1$ as well as the previous argument, another side becomes

$$\left[\frac{z}{\sqrt{z^2+\epsilon}}\right]_{z=-\infty+it} = \lim_{a\to\infty} \frac{-a+it}{\sqrt{(-a+it)^2+\epsilon}} = \lim_{a\to\infty} \frac{-1+i\frac{t}{a}}{\sqrt{1+i\frac{2t}{a}-\frac{t^2}{a^2}+\frac{\epsilon}{a^2}}} = \frac{-1}{1} = -1, \tag{5.81}$$

where we used Eq. (5.80) in the third equality. Eq. (5.71) then reads

$$\left[\frac{z}{\sqrt{z^2+\epsilon}}\right]_{z=-\infty+it}^{z=\infty+it} = 1 - (-1) = 2. \tag{5.82}$$

From above discussion, Eq. (5.66) provides

$$\begin{aligned}\int_0^\infty dt \int_{-\infty}^\infty d\lambda \frac{\epsilon}{\{(\lambda+it)^2+\epsilon\}^{3/2}} &= \left(\int_0^{\sqrt{\epsilon}} + \int_{\sqrt{\epsilon}}^\infty\right) dt \int_{-\infty+it}^{\infty+it} dz \frac{\epsilon}{(z^2+\epsilon)^{3/2}} \\ &= \int_0^{\sqrt{\epsilon}} dt\, 2 + \int_{\sqrt{\epsilon}}^\infty dt\, 0 = 2\sqrt{\epsilon} \to 0 \quad (\epsilon \to 0).\end{aligned} \tag{5.83}$$

In this way, we could confirm that the contact terms Eq. (5.57) do not contribute to Kubo formulas. On the other hand, the Euclidean correlation function or the canonical correlation of $T_{\mu\nu}(x)$ which are observables on the lattice involve the contribution from contact terms. Therefore one has to subtract the contribution in lattice QCD simulation because the original Kubo formula Eq. (5.41) does not include it in the case of quantum field theory.

5.4 Viscosity to relaxation time ratio

In this section, we use the OPE results on the contact terms [83] and rewrite the viscosity to relaxation time ratios as expressions which are direct observables in lattice QCD simulation. For the following discussion, we introduce a Fourier transformation of the Euclidean correlation function of $T_{\mu\nu}(x)$,

$$G_{\mu\nu\rho\sigma}(q_4, \vec{q}) = \int d^4x \, G_{\mu\nu\rho\sigma}(x) \, e^{iqx} = \int d^4x \, \langle T_{\mu\nu}(x) T_{\rho\sigma}(0) \rangle \, e^{iqx}. \tag{5.84}$$

5.4.1 Shear channel

First we show the contact terms in the shear channel. In the leading order OPE calculation [83], the contact terms have most conveniently evaluated by taking the high frequency limit of the correlation function $G_{1212}(q_4, \vec{q})$ with zero spatial momentum,

$$\lim_{q_4 \to \infty} G_{1212}(q_4, \vec{0})_0 = C_{1212\alpha\beta} \langle T_{\alpha\beta}(0) \rangle_0 = \frac{2}{3} \langle T^{\text{t.l.}}_{44} \rangle_0 + \frac{1}{6} \langle F^2 \rangle_0, \tag{5.85}$$

where $T^{\text{t.l.}}_{\mu\nu}$ is defined to be traceless and $\langle F^2 \rangle = \langle F^a_{\mu\nu} F^a_{\mu\nu} \rangle$ is the gluon condensate. In the first equality of Eq. (5.85), the higher order terms in Eq. (5.54) vanish by Riemann-Lebesgue lemma.

- Riemann-Lebesgue lemma
  Let $f(q)$ be a Fourier transform of $f(x)$ that is an integrable function on $\mathbf{R}$,

$$\tilde{f}(q) = \int_{-\infty}^{+\infty} f(x) e^{-iqx} dx. \tag{5.86}$$

  Then $\tilde{f}(q)$ tends to 0 as $|q|$ tends to infinity,

$$\lim_{|q| \to \infty} \tilde{f}(q) = 0. \tag{5.87}$$

From Eqs. (5.55), (5.56), and (5.85), one obtains the physical ratio of shear viscosity to relaxation time of shear current in the leading order perturbation theory,

$$\begin{aligned}
\frac{\eta}{\tau_\pi} &= \frac{V}{T} \langle \delta \tilde{T}^2_{12} \rangle_{\text{reg}} \\
&= \int_0^{1/T} d^4x \, \langle \delta T_{12}(x) \delta T_{12}(0) \rangle_0 - C_{1212\alpha\beta} \langle T_{\alpha\beta}(0) \rangle_0 \\
&= \int_0^{1/T} d^4x \, \langle \delta T_{12}(x) \delta T_{12}(0) \rangle_T - \int_0^{1/T_0} d^4x \, \langle \delta T_{12}(x) \delta T_{12}(0) \rangle_{T_0} - \frac{2}{3} \left(\langle T^{\text{t.l.}}_{44} \rangle_0 + \frac{1}{4} \langle F^2 \rangle_0 \right) \\
&= \frac{V}{T} \langle \delta \tilde{T}^2_{12} \rangle_T - \frac{V}{T_0} \langle \delta \tilde{T}^2_{12} \rangle_{T_0} - \frac{2}{3} \left(\langle T^{\text{t.l.}}_{44} \rangle_0 + \frac{1}{4} \langle F^2 \rangle_0 \right).
\end{aligned} \tag{5.88}$$

Since the right-hand side of Eq. (5.88) includes only lattice observables, one can evaluate η/τ_π directly from lattice QCD simulations.

5.4.2 Bulk channel

The contact terms in the bulk channel have also derived by the OPE calculation [83] as well as in the shear channel,

$$\lim_{q_4\to\infty} G_{iijj}(q_4,\vec{0})_0 = (4\pi b_0 g^2)^2 \left(4\langle T_{44}^{\text{t.l.}}\rangle_0 + \langle F^2\rangle_0\right). \tag{5.89}$$

Here b_0 is given by Eq. (2.75), $b_0 = 11/(4\pi)^2$, for SU(3) gauge theory. The physical bulk viscosity to relaxation time ratio is given by

$$\begin{aligned}\frac{\zeta}{\tau_\Pi} &= \frac{V}{9T}\langle\delta\tilde{T}_{ii}^2\rangle_{\text{reg}} \\ &= \frac{1}{9}\left(\frac{V}{T}\langle\delta\tilde{T}_{ii}^2\rangle_T - \frac{V}{T_0}\langle\delta\tilde{T}_{ii}^2\rangle_{T_0}\right) - \frac{4}{9}(4\pi b_0 g^2)^2\left(\langle T_{44}^{\text{t.l.}}\rangle_0 + \frac{1}{4}\langle F^2\rangle_0\right).\end{aligned} \tag{5.90}$$

We end with account of a relation between the viscosity to relaxation time ratio and the thermodynamic quantities. $\langle F^2\rangle_0$ and $\langle T_{44}^{\text{t.l.}}\rangle_0$ in Eqs. (5.88) and (5.90) are related to the energy density ϵ and the pressure P as follows

$$\langle F^2\rangle_0 = \frac{2g}{\beta(g)}(\epsilon - 3P) = \frac{2g}{\beta(g)}\theta, \tag{5.91}$$

$$\langle T_{44}^{\text{t.l.}}\rangle_0 = -\epsilon^{t.l.} = -\frac{3}{4}(\epsilon^{t.l.} + P^{t.l.}) = -\frac{3}{4}\left\{\left(\epsilon^{t.l.} + \frac{1}{4}\theta\right) + \left(P^{t.l.} - \frac{1}{4}\theta\right)\right\} = -\frac{3}{4}(\epsilon + P), \tag{5.92}$$

where $\beta(g)$ denotes the beta function in Eq. (1.1), $\beta(g) = -b_0 g^3 + \cdots$. $\theta = \epsilon - 3P$ is generally called the trace anomaly. In the last equality of Eq. (5.92), we utilized the fact that the trace anomalies included in ϵ and P cancels out each other. Using these relations, the viscosity to relaxation time ratios read

$$\frac{\eta}{\tau_\pi} = \frac{V}{T}\langle\delta\tilde{T}_{12}^2\rangle_0 + \frac{\epsilon+P}{2} - \frac{2g}{\beta(g)}\frac{\epsilon-3P}{6}, \tag{5.93}$$

$$\frac{\zeta}{\tau_\Pi} = \frac{V}{9T}\langle\delta\tilde{T}_{ii}^2\rangle_0 + \frac{2}{3}(4\pi b_0 g^2)^2\left(\frac{\epsilon+P}{2} - \frac{2g}{\beta(g)}\frac{\epsilon-3P}{6}\right). \tag{5.94}$$

summary

- We have derived the relations of the viscosity to relaxation time ratio and the canonical correlation or the Euclidean correlator of $T_{\mu\nu}$ for quantum field theory.
- There exist two kinds of extra contributions which originate from the short distance behavior of the Euclidean correlator of $T_{\mu\nu}$, i.e. the ultraviolet divergence and the finite but temperature-dependent terms.
- To remove these contributions we have applied regularization procedures to the correlator, i.e. the vacuum subtraction and the removal of contact terms.
- We also confirmed that the contact terms have no contribution to Kubo formula but effect the canonical correlation of $T_{\mu\nu}$.

- The physical ratios can be expressed by only lattice observables, i.e. the canonical correlations of $T_{\mu\nu}$ and the thermodynamic quantities.
- Evaluating the ratios with lattice QCD simulation, we can constrain the free parameters in relativistic dissipative hydrodynamic models.

Chapter 6

Lattice Measurements

In the previous chapter, we derived the relations between the viscosity to relaxation time ratio and the canonical correlation of energy-momentum tensor for quantum field theory. The ratios are expressed by only lattice observables. In this chapter, we first introduce the energy-momentum tensor on the lattice. For lattice simulations, we adopt traceless part of energy-momentum tensor defined by field strength tensor constructed from clover type plaquette which respects parity of spatial coordinates. The relations Eqs. (5.93) and (5.94) require the sum of energy density and pressure, $\epsilon+P$, and the trace anomaly, $\theta = \epsilon - 3P$. The sum $\epsilon + P$ is directly obtained from measurements of energy-momentum tensor on the lattice. We compute the trace anomaly by a conventional approach with standard Wilson gauge action. Using these observables, we determine the viscosity to relaxation time ratios within SU(3) gauge theory. The lattice simulations are performed for temperature range relevant to ultra-relativistic heavy ion collisions at the RHIC and LHC. We also analyze the characteristic speeds of transverse and sound modes in a gluon medium. We find that the characteristic speeds obtained from our lattice measurements are larger than any other theoretical predictions.

6.1 Formulation

6.1.1 Energy-momentum tensor on the lattice

Let us introduce energy-momentum tensor on the lattice. The traceless part of energy-momentum tensor is generally described as

$$T^{\rm t.l.}_{\mu\nu} = 2{\rm Tr}\left[F_{\mu\rho}F_{\nu\rho} - \frac{1}{4}\delta_{\mu\nu}F_{\rho\sigma}F_{\rho\sigma}\right]. \tag{6.1}$$

Here the metric is given by $\delta_{\mu\nu} = {\rm diag}(+,+,+,+)$, because we now consider Euclidean space. We adopt clover type plaquette $U^{\rm cl}_{\mu\nu}$ (Fig. 6.1) for the field strength $F_{\mu\nu}$ on the lattice,

$$\begin{aligned} a^2 g F_{\mu\nu} &\equiv -\frac{i}{2}\left\{U^{\rm cl}_{\mu\nu} - (U^{\rm cl}_{\mu\nu})^\dagger\right\}_{\rm traceless\ part} \\ &= -\frac{i}{2}\left\{U^{\rm cl}_{\mu\nu} - (U^{\rm cl}_{\mu\nu})^\dagger - \frac{1}{3}{\rm Tr}\left[U^{\rm cl}_{\mu\nu} - (U^{\rm cl}_{\mu\nu})^\dagger\right]\right\} \equiv \hat{U}^{\rm cl}_{\mu\nu}, \end{aligned} \tag{6.2}$$

$$U^{\rm cl}_{\mu\nu} \equiv \frac{1}{4}(U^{(1)}_{\mu\nu} + U^{(2)}_{\mu\nu} + U^{(3)}_{\mu\nu} + U^{(4)}_{\mu\nu}), \tag{6.3}$$

where $U_{\mu\nu}^{(i)}$ are given by

$$
\begin{aligned}
U_{\mu\nu}^{(1)} &= U_\mu(n)U_\nu(n+\hat{\mu})U_\mu^\dagger(n+\hat{\nu})U_\nu^\dagger(n), \\
U_{\mu\nu}^{(2)} &= U_\nu(n)U_\nu^\dagger(n-\hat{\mu}+\hat{\nu})U_\mu^\dagger(n-\hat{\mu})U_\mu(n-\hat{\mu}), \\
U_{\mu\nu}^{(3)} &= U_\mu^\dagger(n-\hat{\mu})U_\nu^\dagger(n-\hat{\mu}-\hat{\nu})U_\mu(n-\hat{\mu}-\hat{\nu})U_\nu(n-\hat{\nu}), \\
U_{\mu\nu}^{(4)} &= U_\nu^\dagger(n-\hat{\nu})U_\mu(n-\hat{\nu})U_\nu(n+\hat{\mu}-\hat{\nu})U_\mu^\dagger(n+\hat{\mu}).
\end{aligned}
$$

Here the link variables $U_\mu(n)$ are defined by Eq. (2.23). If one defines $F_{\mu\nu}$ with standard plaquette Eq. (2.22), $T_{\mu\nu}$ breaks the invariant under the parity of spatial coordinates and its off-diagonal components have finite expectation value $\langle T_{12}\rangle \neq 0$, which must vanish in equilibrium. With Eq. (6.2), diagonal and off-diagonal components of $T_{\mu\nu}^{\mathrm{t.l.}}$ on the lattice are rewritten as

$$
T_{\mu\mu}^{\mathrm{t.l.}} = \mathrm{Tr}\left[\sum_{\sigma\neq\mu}\frac{\hat{U}_{\mu\sigma}^{\mathrm{cl}}}{a^2g}\frac{\hat{U}_{\mu\sigma}^{\mathrm{cl}}}{a^2g} - \sum_{\rho,\sigma\neq\mu,\rho>\sigma}\frac{\hat{U}_{\rho\sigma}^{\mathrm{cl}}}{a^2g}\frac{\hat{U}_{\rho\sigma}^{\mathrm{cl}}}{a^2g}\right] = \frac{1}{a^4g^2}\mathrm{Tr}\left[\sum_{\sigma\neq\mu}(\hat{U}_{\mu\sigma}^{\mathrm{cl}})^2 - \sum_{\rho,\sigma\neq\mu,\rho>\sigma}(\hat{U}_{\rho\sigma}^{\mathrm{cl}})^2\right], \tag{6.4}
$$

$$
T_{\mu\nu} = 2\mathrm{Tr}\left[\frac{\hat{U}_{\mu\sigma}^{\mathrm{cl}}}{a^2g}\frac{\hat{U}_{\nu\sigma}^{\mathrm{cl}}}{a^2g}\right] = \frac{2}{a^4g^2}\mathrm{Tr}[\hat{U}_{\mu\sigma}^{\mathrm{cl}}\hat{U}_{\nu\sigma}^{\mathrm{cl}}] \quad (\mu\neq\nu). \tag{6.5}
$$

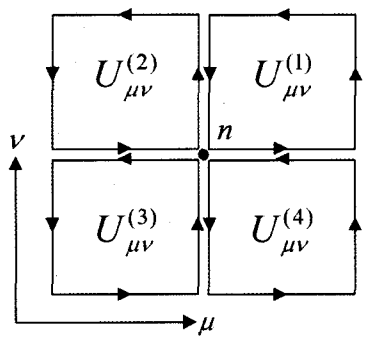

Figure 6.1: Cover type plaquette.

We remark on a relation between $T_{\mu\nu}$ in the continuum theory and on the lattice. In the continuum theory, $T_{\mu\nu}$ is obtained as the Noether current for the translation symmetry. On the other hand, $T_{\mu\nu}$ on the lattice is no longer a conserved current due to the discretized translation symmetry. This means that a renormalization factor $Z(g)$ depending on the bare coupling g is required to connect them, $T_{\mu\nu}^{\mathrm{cont}} = Z(g)T_{\mu\nu}^{\mathrm{lat}}$. From non-perturbative analyses of anisotropy coefficients [1], $Z(g)$ in SU(3) gauge theory is estimated as [31]

$$
Z(g) = \frac{1 - 1.0225g^2 + 0.1305g^4}{1 - 0.8557g^2}, \quad \left(\frac{6}{g^2} \geq 5.7\right). \tag{6.6}
$$

We use this factor on analyses in the following arguments.

[1] In lattice gauge theory, the spatial and temporal lattice spacings can be different, i.e. $a_\tau \neq a_\sigma$. The anisotropy coefficient ξ is defined by a ratio $\xi \equiv a_\tau/a_\sigma$. In this study, we use an isotropic lattice spacing $a = a_\tau = a_\sigma$.

6.1.2 Vacuum subtraction on the lattice

In this subsection, we discuss the vacuum subtraction for the ratios η/τ_π and ζ/τ_Π on the lattice. Before proceeding with this subject, we clarify how to relate lattice observables to physical quantities. While lattice observables are dimensionless, the lattice spacing a is only dimensional quantity on the lattice. Physical quantities and lattice observables are connected by the lattice spacing.

Let us consider the energy density ϵ as an instructive example. The energy density in the continuum theory $\epsilon^{\rm cont}$ is defined by the difference between the ones at $T \neq 0$ and at $T = 0$ (vacuum), because it diverges at the vacuum. $\epsilon^{\rm cont}$ can be related to the energy density on the lattice $\epsilon^{\rm lat}$ as follows,

$$\frac{\epsilon^{\rm cont}}{T^4} \equiv \frac{\epsilon^{\rm cont}_T - \epsilon^{\rm cont}_{T=0}}{T^4} = \frac{1}{a^4}\frac{\epsilon^{\rm lat}_T - \epsilon^{\rm lat}_{T=0}}{T^4} = N_\tau^4(\epsilon^{\rm lat}_T - \epsilon^{\rm lat}_{T=0}), \tag{6.7}$$

where we used the relation $1/T = aN_\tau$ in the last equality. In this way, one may naively subtract $\epsilon^{\rm lat}_{T=0}$ from $\epsilon^{\rm lat}_T$ in lattice measurements.

In the case of the viscosity to relaxation time ratios, the vacuum subtraction procedure on the lattice gets a little complicated. One has to be careful of the subtraction for the canonical correlation of $T_{\mu\nu}$. First we see the shear channel ratio η/τ_π. The vacuum subtraction for η/τ_π is performed as follows,

$$\begin{aligned}
\frac{1}{T^4}\frac{\eta}{\tau_\pi} &\equiv \frac{1}{T^4}\left[\left(\frac{V}{T}\langle\tilde{T}^2_{12}\rangle\right)_0 - (\text{contact terms})\right] \\
&= \frac{1}{T^4}\left[\left(\frac{V}{T}\langle\tilde{T}^2_{12}\rangle\right)_T - \left(\frac{V}{T_0}\langle\tilde{T}^2_{12}\rangle\right)_{T_0}\right] - \frac{1}{T^4}(\text{contact terms}) \\
&= \frac{1}{T^4}\left[\left(\frac{1}{a^8}\frac{V}{T}Z^2(g)\langle\tilde{T}^2_{12}\rangle^{\rm lat}\right)_T - \left(\frac{1}{a^8}\frac{V}{T_0}Z^2(g)\langle\tilde{T}^2_{12}\rangle^{\rm lat}\right)_{T_0}\right] - \frac{1}{T^4}(\text{contact terms}) \\
&= Z^2(g)N_\sigma^3 N_\tau^4\left[\left(N_\tau\langle\tilde{T}^2_{12}\rangle^{\rm lat}\right)_T - \left(N_{\tau 0}\langle\tilde{T}^2_{12}\rangle^{\rm lat}\right)_{T_0}\right] - \frac{1}{T^4}(\text{contact terms}).
\end{aligned} \tag{6.8}$$

We used the relation $V = (aN_\sigma)^3$ in the fourth line. We regard an enough low temperature T_0 as zero temperature $T = 0$. T_0 denotes the corresponding $N_{\tau 0}$ represents the number of temporal lattice sites which corresponds to the vacuum. As discussed in section 5.4, the contact terms can be expressed by only the thermodynamic quantities which are lattice observables.

For the bulk channel, the vacuum subtraction with Eq. (6.1) becomes more complicated because the spatial diagonal components of $T_{\mu\nu}$ include the trace anomaly $\theta = \epsilon - 3P$, i.e. $T_{ii} = T^{\rm t.l.}_{ii} - \frac{3}{4}\theta$. The bulk viscosity to relaxation time ratio is then related with $\langle\delta\tilde{T}^2_{ii}\rangle$ on the lattice as follows,

$$\begin{aligned}
\frac{1}{T^4}\frac{\zeta}{\tau_\Pi} &\equiv \frac{1}{T^4}\left[\left(\frac{V}{9T}\langle\delta\tilde{T}^2_{ii}\rangle\right)_0 - (\text{contact terms})\right] \\
&= \frac{1}{T^4}\left(\frac{V}{9T}\langle(\delta\tilde{T}^{\rm t.l.}_{ii} - \frac{3}{4}\delta\theta)^2\rangle\right)_0 - \frac{1}{T^4}(\text{contact terms}) \\
&= \frac{1}{T^4}\left(\frac{V}{9T}\left\{\langle(\delta\tilde{T}^{\rm t.l.}_{ii})^2\rangle - \frac{3}{2}\langle\delta\tilde{T}^{\rm t.l.}_{ii}\delta\theta\rangle + \frac{9}{16}\langle\delta\theta^2\rangle\right\}\right)_0 - \frac{1}{T^4}(\text{contact terms}) \\
&= \frac{1}{9}N_\sigma^3 N_\tau^4\left(N_\tau\left\{Z^2(g)\langle(\delta\tilde{T}^{\rm t.l.}_{ii})^2\rangle^{\rm lat} + \frac{9}{2}B(g)Z(g)\langle\delta\tilde{T}^{\rm t.l.}_{ii}\delta S\rangle^{\rm lat} + \frac{81}{16}B^2(g)\langle\delta S^2\rangle^{\rm lat}\right\}\right)_0 \\
&\qquad - \frac{1}{T^4}(\text{contact terms}),
\end{aligned} \tag{6.9}$$

where S denotes the action and $B(g)$ the beta function (see subsection 2.4.3). We used Eq. (2.71) in the last line. In this way, one must not take difference between $\langle \delta\tilde{T}^2_{\mu\nu} \rangle^{\rm lat}$ at finite temperature and at the vacuum simply in data analyses. One needs to multiply each number of temporal lattice sites N_τ to $\langle \delta\tilde{T}^2_{\mu\nu} \rangle^{\rm lat}$ before the vacuum subtraction.

6.2 Set up

In table 6.1, we list lattice simulation parameters used in this study. We have performed SU(3) lattice gauge simulations with a standard Wilson gauge action defined in Eq. (2.21). In order to investigate the lattice spacing and spatial volume dependences, simulations have been carried out on four isotropic lattices. The lattice spacing a for each inverse coupling β is determined by the string tension $\sqrt{\sigma} = 460$ MeV and the parametrization of $a\sqrt{\sigma}$ in Eq. (2.72) [71]. We use $T_c/\sqrt{\sigma} = 0.63$ [84] and normalize T by T_c. The temporal length $aN_\tau = 1/T$ of each lattice corresponds to a range of temperature $0.5 \lesssim T/T_c \lesssim 4$, which covers those realized in heavy ion collisions at RHIC and LHC. Gauge configurations are updated by heat bath and overrelaxation algorithms discussed in section 3.1. We also list the renormalization factors $Z(g)$ and $B(g)$ in table 6.1.

Table 6.1: Lattice simulation parameters. N_σ and N_τ are the numbers of lattice sites in spatial and temporal directions, respectively. a and L_σ denote the lattice spacing and spatial lattice size. Renormalization factors $Z(g)$ and $B(g)$ are also listed.

$\beta = 6/g^2$	N_σ	N_τ	a[fm]	L_σ[fm]	$Z(g)$	$B(g)/6$
6.499	32	4, 6, 8, 32	0.046	1.5	0.796366	0.125501
6.205	32	4, 6, 8, 32	0.068	2.2	0.772442	0.112127
6.000	32	4, 6, 8, 16	0.094	3.0	0.748441	0.098172
6.000	16	4, 6, 8, 16	0.094	1.5	0.748441	0.098172

We have generated $40,000 - 2,100,000$ configurations at every 50 sweeps in Monte Carlo time for each parameter. Statistical errors were estimated by the jackknife method with bin sizes in a range of $50 - 1250$ (see subsection 3.2.2). To perform the vacuum subtraction, we regarded a lattice with the largest N_τ for each β as the vacuum one. In fact, our numerical result with the largest N_τ for each β corresponds to temperature well below T_c, where medium effects on expectation values are well suppressed as seen in the following subsections.

6.3 Numerical results

6.3.1 Jackknife error

Fig. 6.2 shows the bin size dependence of the jackknife error for $\langle \tilde{T}^2_{12} \rangle$ on the lattices with different temporal size $N_\tau = 4, 6, 8, 32$ and $\beta = 6.499$. In this analysis, we did not perform the vacuum subtraction. We can see that the statistical error does not depend on bin size. This means that the autocorrelation of gauge configurations are well suppressed even in smallest bin size $n = 50$.

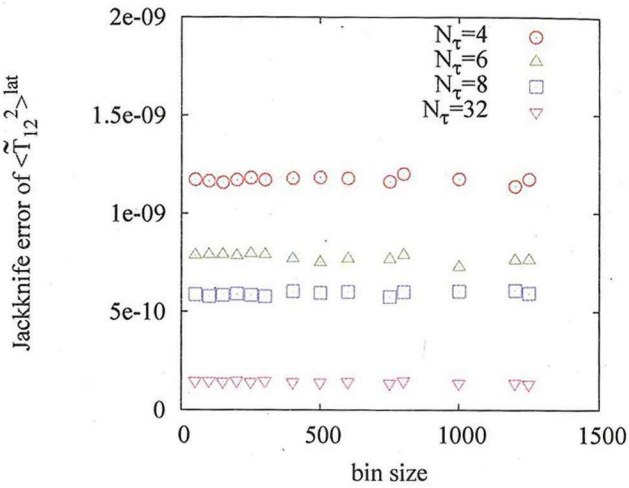

Figure 6.2: Bin size dependence of jackknife error of $\langle \tilde{T}_{12}^2 \rangle^{\text{lat}}$. We set the inverse coupling $\beta = 6.499$ and prepared four lattices with different number of temporal sites N_τ. In this figure, the vacuum and the contact term subtractions are not carried out. The bin size dependence of jackknife error cannot be seen for all results we analyzed.

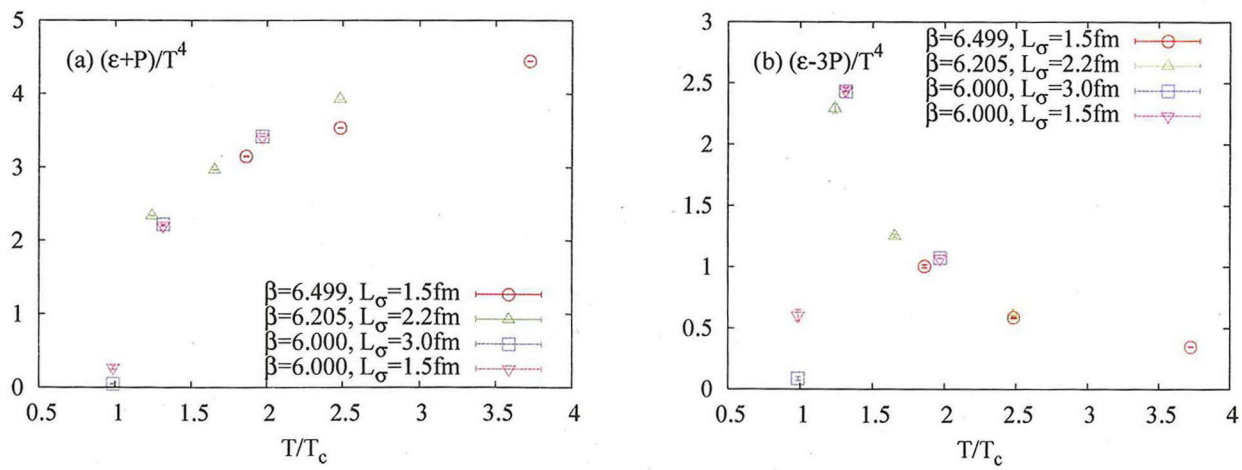

Figure 6.3: Temperature dependences of thermodynamic quantities. a): Sum of the energy density and the pressure or the entropy density, $\epsilon + P = Ts$. We acquired the sum from direct observation of $-\frac{4}{3}Z(g)\langle T_{44}^{\text{t.l.}} \rangle$ on the lattice. b): The trace anomaly, $\theta = \epsilon - 3P$, measured on the lattice with a standard procedure and Wilson gauge action. As discussed in section 2.3.2, SU(3) gauge theory shows a first order phase transition at some critical temperature T_c. Both figures show a characteristic behavior above T_c with a small statistical error. We can confirm that the lattice spacing and spatial volume dependences of these observables are well suppressed. These results are consistent with past lattice studies.

6.3.2 Thermodynamic quantities

In Fig. 6.3, we show the temperature dependence of thermodynamic quantities $\epsilon + P$ and $\theta = \epsilon - 3P$ [2]. $\epsilon + P$ is responsible for the causality conditions Eqs. (4.65) and (4.66), and the contact terms Eqs. (5.93) and (5.94). The trace anomaly θ is also included in the contact terms.

In the lattice simulations, we used the traceless part of energy-momentum tensor defined by Eq. (6.1) for measurements of $\epsilon + P$. The expectation value of $\epsilon + P$ was simply taken from $-\frac{4}{3}Z(g)\langle T_{44}^{\text{t.l.}}\rangle_0^{\text{lat}}$ because a contribution of the trace anomaly is canceled out in this observable, i.e.

$$\epsilon + P = \left(\epsilon^{\text{t.l.}} + \frac{1}{4}\theta\right) + \left(P^{\text{t.l.}} - \frac{1}{4}\theta\right) = \epsilon^{\text{t.l.}} + P^{\text{t.l.}} = \frac{4}{3}\epsilon^{\text{t.l.}} = -\frac{4}{3}Z(g)\langle T_{44}^{\text{t.l.}}\rangle_0^{\text{lat}}. \tag{6.10}$$

We used $\epsilon^{\text{t.l.}} = 3P^{\text{t.l.}}$ in the third equality. Hence the definition of Eq. (6.1) is enough for this measurement. While the definition of $\epsilon + P$ is different from that used in the conventional analyses of lattice thermodynamics discussed in subsection 2.4.3, the difference should be of higher order in lattice spacing and converge in the continuum limit. Fig. 6.3a shows a rapid increase at the critical temperature T_c. This indicates a phase transition as discussed in subsection 2.3.2 and Appendix A. SU(3) gauge theory makes the deconfinement phase transition and degrees of freedom of a system increase immediately above T_c.

We also measured the trace anomaly with the Wilson gauge action Eq. (2.20) using Eqs. (2.69)-(2.71). The Wilson gauge action on the lattice is constructed from the standard plaquette (see Eq. (2.68)). The numerical results in Fig. 6.3b are consistent with well known behavior measured by previous studies on the lattice. (see, for instance, Ref. [85]).

Thermodynamic quantities presented in Fig. 6.3 are obtained with a reasonable statistics for all temperature range. We can evaluate lattice spacing dependence of the thermodynamic quantities by comparing the results with different inverse couplings. The numerical results show that the lattice spacing dependence is well suppressed. The spatial volume dependence of observables can be estimated by comparing results on two lattices with $\beta = 6.000$. The spatial volume of lattice with $L_\sigma = 3.0\,\text{fm}$ is eight times larger than that of smaller lattice with $L_\sigma = 1.5\,\text{fm}$. Fig. 6.3 show that the spatial volume dependence of the thermodynamic quantities is also suppressed in the lattice simulations.

6.3.3 Viscosity to relaxation time ratio : shear channel

Fig. 6.4a shows that the temperature dependence of canonical correlation of T_{12} with the vacuum subtraction $(V\langle\tilde{T}_{12}^2\rangle/T)_0$. The numerical results take negative values for $\beta = 6.000$ at $T < 2T_c$. On the finer lattices with $\beta = 6.499$ and 6.205, the negative values are also observed for $N_\tau = 4$ whereas the results with $N_\tau \geq 6$ are consistent with zero within statistical error. The results indicate that $(V\langle\tilde{T}_{12}^2\rangle/T)_0$ is not the ratio η/τ_π, because the latter must be positive from definitions of transport coefficients. Thus the existence of temperature dependent contributions, i.e. the contact terms, is suggested in the canonical correlations. To obtain the physical ratio, one must remove the contact terms by an additional regularization (see section 5.3 for this issue) [3].

In Fig. 6.4b, we show the temperature dependence of η/τ_π given by Eq. (5.93). The figure shows that the numerical results with all sets of configurations are consistent within the statistical error for the range of temperature $1 \lesssim T/T_c \lesssim 4$. We found that the lattice spacing dependence of the present results is well suppressed. Comparing the results on the two different spatial volumes with $\beta = 6.000$,

[2] In this chapter, we omit the subscript "eq" which means equilibrium state because what one directly obtains from lattice measurements is always an equilibrium value of some physical quantity.

[3] If one misses the contact terms, η/τ_π can be negative. This means that either η or τ_π takes negative value. However these transport coefficients must be non-negative by definition.

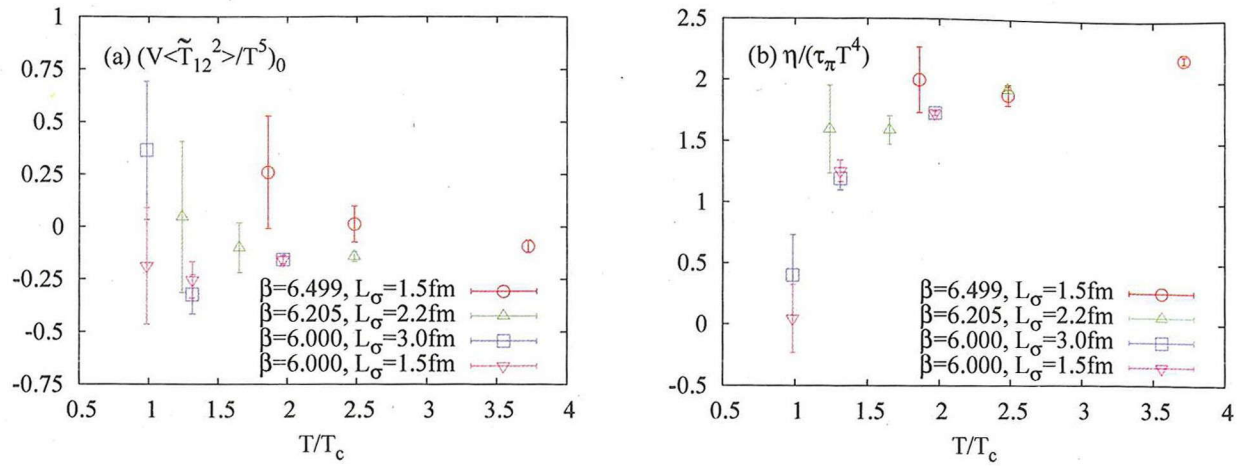

Figure 6.4: a): Temperature dependence of canonical correlation of T_{12} with vacuum subtraction $(V\langle\tilde{T}_{12}^2\rangle/T)_0$. This observable seems to be dependent on the lattice spacing and to converge at high temperature region. The spatial volume dependence cannot be seen within the margin of error. b): Temperature dependence of the shear viscosity to relaxation time ratio η/τ_π in which the regularization prescriptions, i.e. the vacuum subtraction and the removal of contact terms, have been performed. η/τ_π behaves like the thermodynamic quantities shown in Fig. 6.3. This behavior mainly originates from $(\epsilon + P)/2$ in Eq. (5.93).

we can see that the spatial volume dependence of the ratio is also suppressed. η/τ_π rapidly increases above T_c as well as the thermodynamic quantities in Fig. 6.3. This behavior mainly originates from the second term in Eq. (5.93), $(\epsilon + P)/2$, for $1.5 \lesssim T/T_c$. In the vicinity of T_c the trace anomaly also has a significant contribution to η/τ_π (see Fig. 6.3).

6.3.4 Viscosity to relaxation time ratio : bulk channel

In Fig. 6.5a we show that the canonical correlation of $\delta T_{ii}^{\text{t.l.}}$ with the vacuum subtraction $(V\langle\delta\tilde{T}_{ii}^2\rangle/9T)_0$ as a function of T. Unlike the shear channel, for each lattice parameter, the bulk channel takes non-negative value within statistical error for $1 \lesssim T/T_c \lesssim 4$. However the extra temperature dependent terms are included in the canonical correlation as is the case of the shear channel. Since the extra terms do not contribute to Kubo formula as discussed in section 5.3.2, the contribution must be removed in lattice measurements.

In Fig. 6.5b, we show the temperature dependence of the ratio ζ/τ_Π given by Eq. (5.94) or (6.9). The figure shows that the results are consistent within the statistical error as well as the shear channel except below T_c. The lattice spacing dependence is suppressed for $1.5 \lesssim T/T_c \lesssim 4$. However it is hard to say about the lattice spacing dependence of the present results below $1.5\,T_c$ due to the large statistical errors. Comparing the two results with $\beta = 6.000$, we found that the spatial volume dependence is suppressed above T_c.

As well as η/τ_π, ζ/τ_Π has a tendency to increase in the vicinity of T_c. However the origin of this behavior of ζ/τ_Π is different from that of η/τ_π. The behavior of η/τ_π around T_c is governed by the contact terms whereas the canonical correlation of T_{12} equals to zero or negative within a statistical error. On the other hand, the canonical correlation of δT_{ii} has a dominant contribution to ζ/τ_Π. This contribution, for instance, reaches about one third of ζ/τ_Π for the finest lattice with $\beta = 6.499$.

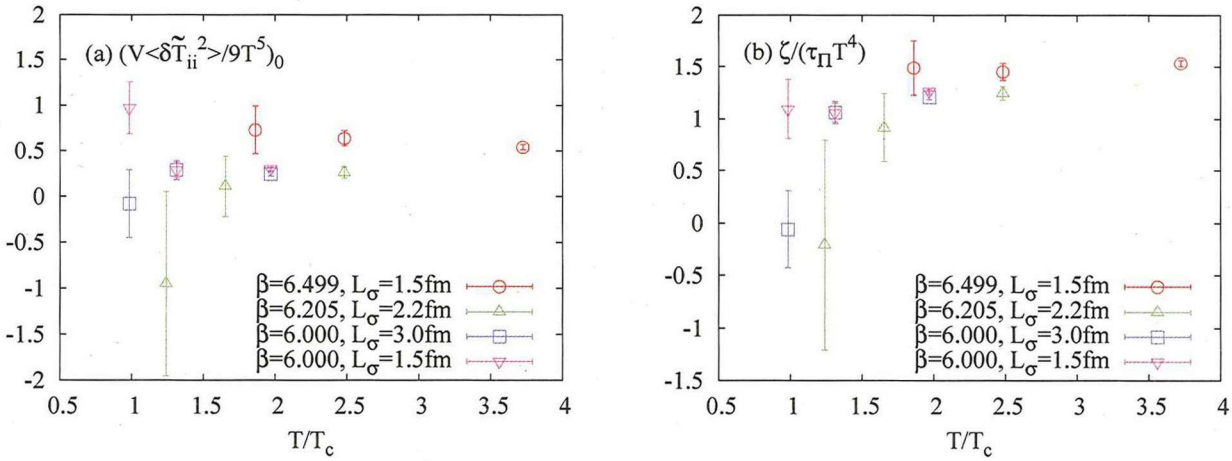

Figure 6.5: a): Temperature dependence of canonical correlation of δT_{ii} with vacuum subtraction $(V\langle\delta\tilde{T}_{ii}^2\rangle/9T^5)_0$. Within the statistics, the results take non-negative values in the whole temperature range we explored. In high temperature region, the ratio seems to converge a finite value. b): The bulk viscosity to relaxation time ratio ζ/τ_Π as a function of temperature. The contributions from the vacuum and contact terms are both removed in this figure. Although the lattice spacing and spatial dependences are suppressed above T_c, more higher statistics near T_c is desirable.

6.3.5 Characteristic speeds

In a pure gluonic system with the entropy Eq. (5.27), the ratios η/τ_π and ζ/τ_Π are related to the characteristic speeds v_T and v_L, respectively. The maximum value of each characteristic speed squared is given by

$$v_T^2 = \frac{\eta}{\tau_\pi(\epsilon + P)}, \tag{6.11}$$

$$v_L^2 = \frac{\zeta}{\tau_\Pi(\epsilon + P)} + \frac{4}{3}\frac{\eta}{\tau_\pi(\epsilon + P)} + c_s^2, \tag{6.12}$$

where c_s is the speed of sound (see section 4.3). v_T and v_L have to be smaller than the speed of light to keep the causality conditions.

Fig. 6.6a shows v_T^2 as a function of T obtained from our lattice simulations. Although the errorbar grows as T is lowered, the numerical results are consistent for $1 \lesssim T/T_c \lesssim 4$. The spatial volume dependence is suppressed above T_c. We found that v_T^2 take values from 0.5 to 0.6 within a statistical error for the T range analyzed. This means that the propagation of transverse mode in the gluonic media satisfies the causality condition. v_T^2 demonstrates an increasing tendency close to T_c. The statistical error, however, increases as the temperature is lowered. We need to collect more data to give a definite conclusion on the behavior of v_T^2 near T_c.

The temperature dependence of $v_L^2 - c_s^2$ is shown in Fig. 6.6b. As well as v_T^2, we found an increasing behavior of $v_L^2 - c_s^2$ in low temperature. The results on the finest lattice with $\beta = 6.499$ are not really consistent with the ones on coarser lattices with $\beta = 6.205, 6.000$. The spatial volume dependence cannot be seen within a statistical error in the figure. The numerical results take values from 1.0 to 1.2 for $1 \lesssim T/T_c \lesssim 4$. Since the speed of sound is positive $c_s^2 > 0$, the sound mode obviously violates

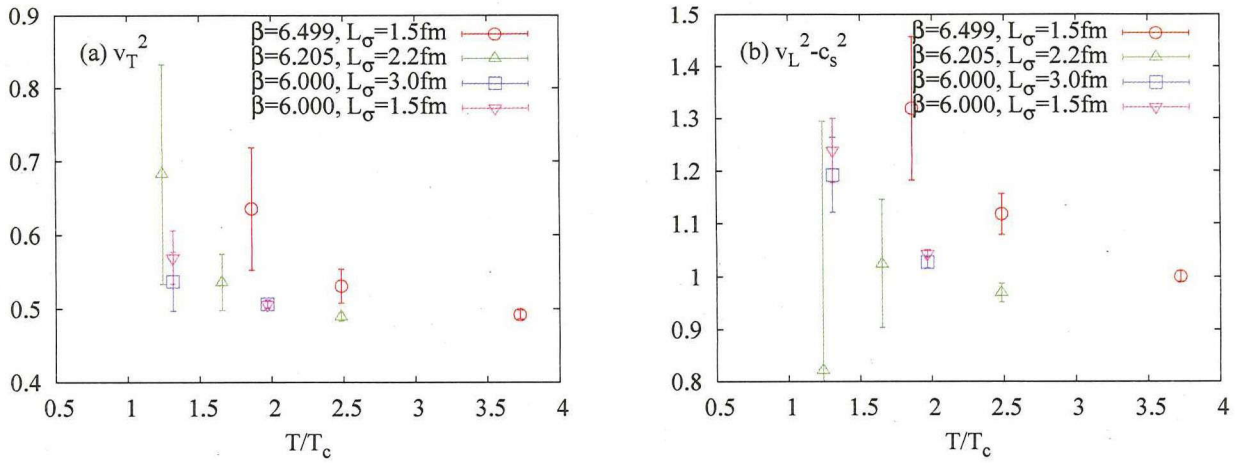

Figure 6.6: Characteristic speed of a): transverse and b): sound modes. v_T and v_L denote the propagation speed of transverse and longitudinal plane wave in gluon media, respectively. Both of them are dependent on the lattice spacing slightly. The spatial volume dependence cannot be seen above T_c. While v_T^2 preserves the causality condition above T_c, v_L^2 becomes superluminal regardless of the values of square of sound speed c_s^2.

the causality condition [4]. This indicates that second order hydrodynamics with bulk viscous effect is an acausal theory. However its behavior should be argued in careful manner, due to a large statistical error of $v_L^2 - c_s^2$ near T_c.

6.4 Discussion

It is of interest to compare v_T^2 and v_L^2 obtained from our lattice simulations with other theoretical predictions. First, a kinetic theory based on the Boltzmann equation with Grad 14 moment approximation [27] predicts $\eta/\tau_\pi \simeq 2P/3$ in the high energy limit. With the relation $\epsilon = 3P$ for ultra-relativistic particles, Eqs. (6.11) and (6.12) reduce to

$$v_T^2|_{\rm kt} = \frac{\eta}{4P\tau_\pi} = \frac{1}{6} \simeq 0.17 \tag{6.13}$$

$$v_L^2|_{\rm kt} = \frac{\eta}{3P\tau_\pi} + \frac{1}{3} = \frac{5}{9} \simeq 0.56. \tag{6.14}$$

In Eq. (6.14), the fact that the bulk viscosity ζ of ultra-relativistic particles vanishes is used.

Second approach is based on a field theory with the projection operator method [36, 37]. In the leading order (non-interaction) calculation, this method predicts

$$v_T^2|_{\rm ft} = \frac{P}{\epsilon + P}, \tag{6.15}$$

$$v_L^2|_{\rm ft} = \frac{1}{3} - \frac{2}{9}\frac{\epsilon - 3P}{\epsilon + P} + \frac{4}{3}\frac{P}{\epsilon + P}, \tag{6.16}$$

[4] If one sets $\epsilon = 3P$, which is the case of Stefan-Boltzmann (SB) limit, and the sound speed $c_s^2 = 1/3$, $v_L^2 - c_s^2$ must be smaller than 2/3 from the causality condition of sound mode.

for a relativistic bosonic fluid. If one assumes the ultra-relativistic limit, Eqs. (6.15) and (6.16) become $v_T^2|_{\rm ft} \simeq 0.25$ and $v_L^2|_{\rm ft} \simeq 0.67$.

Third prediction is given by a string theory with gauge/gravity correspondence. This theory provides

$$v_T^2|_{\rm st} = \frac{1}{4 - 2\ln 2}, \tag{6.17}$$

$$v_L^2|_{\rm st} = \frac{2\eta}{\tau_\pi(\epsilon + P)}(1 - c_s^2) + c_s^2. \tag{6.18}$$

Here Eq. (6.17) is derived in conformal hydrodynamic equations and takes a constant value $v_T^2|_{\rm st} \simeq 0.36$ [78, 86]. On the other hand, Eq. (6.18) is derived by non-conformal theory [87] where relations $\zeta/\eta = 2(1/3 - c_s^2)$ and $\tau_\Pi = \tau_\pi$ are used. If one sets $c_s^2 = 1/3$, Eq. (6.18) is coincident to conformal situation and leads to $v_L^2|_{\rm st} \simeq 0.85$.

The lattice QCD simulations without quarks constrain the characteristic speeds as

$$0.5 \lesssim v_T^2|_{\rm lat} \lesssim 0.6, \tag{6.19}$$

$$1.0 \lesssim v_L^2|_{\rm lat} - c_s^2 \lesssim 1.2 \tag{6.20}$$

for the range of temperature $1.5 \lesssim T/T_c \lesssim 4$. Both of $v_T^2|_{\rm lat}$ and $v_L^2|_{\rm lat}$ are larger than the above theoretical predictions. Our numerical results indicate that the propagation of sound mode in second order viscous hydrodynamics exceeds the speed of light. Thus the second order hydrodynamic models with bulk viscous effect must need some correction to preserve the causality.

It should be noted that these predictions for the characteristic speeds assume different situations, respectively. The kinetic results with Grad 14 moment approximation is obtained by *classical* Boltzmann equation in which quantum effects are not included. It is confirmed that quantum effects make a qualitative difference to the behavior of ζ/τ_Π at low T [37]. Quantum effects should be taken into account in the above arguments. The field theoretical predictions are obtained by an application of the chiral perturbation theory to *non-interacting* relativistic bosonic fluids in the hadron phase. However, we now focus on the strongly interacting or coupled QCD system. The interaction between particles can change the behavior of each characteristic speed. The conformal or non-conformal gauge/gravity correspondence are powerful tools for investigations of the strongly coupled gauge theory. However, it is not QCD itself but rather an effective model because of its conformal invariance and/or the supersymmetry. One must attend to these differences when comparing the predictions each other or employing them on hydrodynamic simulations.

Finally, we estimate the relaxation times τ_π and τ_Π with our lattice results. From Eqs. (6.11) and (6.12) with the thermodynamic relation $\epsilon + P = Ts$, the relaxation times are described as

$$\tau_\pi = \frac{1}{v_T^2 T}\frac{\eta}{s}, \qquad \tau_\Pi = \frac{1}{\left(v_L^2 - \frac{4}{3}v_T^2 - c_s^2\right)T}\frac{\zeta}{s}. \tag{6.21}$$

The specific shear viscosity η/s is frequently presented in discussions of perfect fluidity of the hot QCD matter created by ultra-relativistic heavy ion collisions. The value $\eta/s = 1/(4\pi)$ is conjectured as a lower bound by gauge/gravity correspondence [88]. On the other hand, comparisons of relativistic viscous hydrodynamic results with experimental data [5] constrain an upper limit $\eta/s \leq 2 - 2.5 \times 1/(4\pi)$ [19, 21, 89]. From these limits of η/s, $\eta/\{\tau_\pi(\epsilon + P)\}$ on the lattice, and Eq. (6.21), τ_π is roughly estimated as $\tau_\pi = O(10^{-1})$-$O(10^{-2})$ fm. In a similar way, τ_Π can be evaluated with a relation

[5] The *elliptic flow* is often used as the experimental data due to its strong sensitivity to the shear viscosity (see, for instance, Ref. [18]). In general, particle production in a transverse plane with respect to a reaction plane Ψ_n as a function

$\zeta/s = 2\eta/s(1/3 - c_s^2)$ obtained from string theory, $\tau_\Pi = O(10^{-1}) - O(10^{-2})$ fm. We, however, note that the propagation of sound mode violates the causality condition in our lattice measurements.

Although the above estimates are rough arguments, the viscous effects for the hot QCD matter may relax with a short time compared to a typical time scale of heavy ion collisions at the RHIC and LHC $\sim O(10^1)$ fm. These short relaxation times supports the validity of ideal hydrodynamic models for ultra-relativistic heavy ion collisions. Moreover, in the hadron phase for a temperature range $140 \leq T \leq 200$ MeV, τ_π is predicted as $\tau_\pi \simeq 2 - 4$ fm in Ref [34]. This large difference of τ_π's above and below T_c may be considered as a consequence of the deconfinement phase transition. We note that our estimates of the relaxation times are based on the assumption of QGP with low specific shear viscosity. While this assumption is supported by the first principle calculations [30, 31], there is not enough understanding of it. New developments are desirable for this subject.

summary

- We measured the thermodynamic quantities, the canonical correlation of energy momentum tensor, the viscosity to relaxation time ratios, and the characteristic speeds with SU(3) lattice gauge simulation.
- To obtain the viscosity to relaxation time ratios, we have performed two regularization prescriptions, i.e. the subtractions of the vacuum contribution and the contact terms.
- While the behavior of η/τ_π is mostly dominated by not the canonical correlation of δT_{ij} but the contact terms, the correlation of δT_{ii} gives a significant contribution to ζ/τ_Π.
- We found the constraints of characteristic speeds $0.5 \lesssim v_T^2|_{\rm lat} \lesssim 0.6$ and $1.0 \lesssim v_L^2|_{\rm lat} - c_s^2 \lesssim 1.2$ from SU(3) lattice measurements and they are larger than any other theoretical predictions.
- The lattice results indicate that v_T preserves but v_L violates the causality condition in the second order viscous hydrodynamics, so that some correction may be required to bulk channel.
- The relaxation times of hot gluonic matter are expected to be so short, $O(10^{-1})$-$O(10^{-2})$, compared to a time scale of heavy ion collisions, which supports the success of ideal hydrodynamic description of the evolution of QGP.

---

of an azimuthal angle ϕ can be described as

$$E\frac{d^3N}{d^3p} = \frac{1}{2\pi}\frac{d^2N}{p_T dp_T dy}\left(1 + 2\sum_{n=1}^{\infty} v_n \cos[n(\phi - \Psi_n)]\right), \tag{6.22}$$

where v_2 is the elliptic flow. It denotes an azimuthal anisotropy of the particle production. The RHIC and LHC observed large v_2 that supports collective behavior of the hot QCD matter.

Chapter 7

Conclusions and Outlook

In this thesis, we measured the viscosity to relaxation time ratios for the range of temperature $0.5 \lesssim T/T_c \lesssim 4$ with SU(3) lattice gauge simulation. We first formulated the relations between the ratio and the canonical correlation of $T_{\mu\nu}$ for quantum field theory (subsection 5.2.2). The relations were obtained from an application of the relaxation time approximation to Kubo formulas. To obtain the physical ratios from the relations, we performed two regularization prescriptions for the canonical correlations on the lattice. One is the vacuum subtraction and another is the removal of contact terms (section 5.3).

The canonical correlations include a temperature independent divergence. We took differences between the canonical correlations at $T \neq 0$ and $T = 0$ to remove the divergence (subsection 5.3.1). In addition to this regularization procedure, we also removed the contact terms which depend on temperature. The contact terms do not contribute to Kubo formulas due to the real-time integral (subsection 5.3.2). On the other hand, they give a finite contribution to the canonical correlations. Therefore the contact terms must be removed in lattice measurements of the canonical correlations. We used the leading order OPE results for the estimates of contact terms (section 5.4). They are expressed by the thermodynamic quantities, $\epsilon + P$ and θ, which are lattice observables.

We obtained the sum of $\epsilon + P$ from measurements of $T^{\mathrm{t.l.}}_{\mu\nu}$ directly and the trace anomaly θ by a conventional approach with Wilson gauge action (subsection 6.3.2). By the first principle calculation, we determined the temperature dependence of the ratio in shear and bulk channels, η/τ_π and ζ/τ_Π (subsections 6.3.3 and 6.3.4). We found that both channels show rapid increasing behavior above T_c but its origin is different for each ratio. The ratio η/τ_π is mainly governed by not the canonical correlation but the contact terms. In the bulk channel, the canonical correlation contributes ζ/τ_Π as well as the contact terms. We constrained the free parameters of relativistic dissipative hydrodynamic models by these analyses.

Then we analyzed the characteristic speeds of transverse and sound modes, v_T^2 and v_L^2, for the same temperature range (subsection 6.3.5). They relate to the ratios η/τ_π, ζ/τ_Π, and the thermodynamic quantities (section 4.3). We found that v_T^2 in the hot gluon medium takes $0.5 \lesssim v_T^2 \lesssim 0.6$ for $1.5 \lesssim T/T_c \lesssim 4$. This indicates that the propagation of this mode preserves the causality in the second order hydrodynamics. On the other hand, from our lattice measurements, we evaluated v_L^2 as $1.0 \lesssim v_L^2 - c_s^2 \lesssim 1.2$ for $1.5 \lesssim T/T_c \lesssim 4$. This means that the propagation of sound mode excesses the speed of light. For the sake of causality, some prescription should be required to the gluonic fluid with bulk viscous effect.

We compared our first principle results of the characteristic speeds with other theoretical predictions (section 6.4); kinetic theory with moment approximation, field theory with projection operator method, and string theory with gauge/gravity correspondence. We found that both of our lattice re-

sults of v_T^2 and v_L^2 are larger than any other theoretical predictions. We should note that each analysis assumes a different situation.

We estimated the relaxation times of shear and bulk currents for the hot gluonic matter under an assumption of the low specific shear viscosity η/s (section 6.4). Both relaxation times take the value of $O(10^{-1})$-$O(10^{-2})$ fm. The time scale is shorter than that of heavy ion collisions at the RHIC and LHC. These are rough estimates but consistent with the ideal hydrodynamical description of hot QCD matter created by the relativistic heavy ion collisions. Moreover our result of τ_π is shorter than that of hadronic matter $\tau_\pi \sim O(1)$ fm. This may suggest the deconfinement phase transition.

We refer to several remarks on the present study and future directions:

- Relaxation of correlation function
  In the present study, we considered that each correlation function of $T_{\mu\nu}$ decays exponentially with single relaxation time. However several relaxation times may exist for each dissipative current. Also the relaxation times may decay not exponentially but power law. In these cases, the relaxation time approximation does not apply to the correlation functions simply.

- Newtonian or Non-Newtonian fluid
  We identified the relaxation times in Eq. (5.46) with the ones in Eq. (4.44), which are derived from a linearity between dissipative currents and thermodynamic forces. This means that the hot gluonic matter is Newtonian fluid, but it is non-trivial. If the linearity does not hold, i.e. Non-Newtonian fluid case, our formulation of the ratios may be modified.

- Improvement of statistical precision
  The analyses of the ratios of transport coefficients need large amounts of data $\simeq O(10^7)$. Especially, the statistical errors are large in $T/T_c \lesssim 1.5$. We cannot make definitive conclusions for the observables there. To raise the statistical precision in the vicinity of T_c, one needs additional enormous quantity of data and computer time. However it may not be a practical approach. Some prescription to reduce the statistical error is desired.

- Dynamical quarks
  Our lattice simulations are in the quenched approximation, i.e. with no dynamical quarks. Since the gluons are dominant in the relativistic heavy ion collisions, the qualitative behavior of our results may not change. However the contribution from quarks is required for more quantitative and accurate comparison with experiments.

- Ratios of other transport coefficients
  Our formulation of the viscosity to relaxation time ratios are applicable to ratios of other transport coefficients. The heat conductivity and the diffusion constant to corresponding relaxation time ratios, κ/τ_q and D/τ_D, are such examples. The former (latter) relates to the canonical correlation of T_{i4} (δN_μ), and we need to take into account dynamical quarks in lattice measurements.

- Specific heat
  The specific heat c_V relates to a canonical correlation of δT_{44}. The correlation does not need the subtraction of vacuum and contact terms because of temporal translation symmetry of T_{44} (see appendix C). If one obtains c_V from lattice measurements, the speed of sound can be evaluated by a relation $c_s^2 = s/c_V$. We have the entropy density s from lattice simulations, so that the temperature dependence of v_L^2 can be determined with Eq. (4.64).

From creation to exploration of matter in extreme states ; the hot/dence QCD matter physics embarks on new era.

Acknowledgments

The author would like to thank my adviser professor Masayuki Asakawa very much for discussions, valuable advice, and encouragements. The author is thankful to assistant professor Masakiyo Kitazawa for teaching me various things and continuous encouragements. The author is also grateful to associate professors Toru Sato, Masashi Wakamatsu, and all colleagues of nuclear theory group of Osaka University for many stimulating discussions and encouragements. Finally the author is very grateful to my friends and family. I would like to devote this dissertation to my grandmother.

Appendix A

QCD Thermodynamics

A.1 Simple model for QCD thermodynamics

Here we argue that the deconfinement phase transition occurs at zero baryon density with a simple model. The main purpose is a derivation of the thermodynamic quantities in the hadron (confined) and QGP (deconfined) phases. The energy density ϵ, the pressure P, and the entropy density s are written by using the partition function Z as

$$\epsilon = \frac{T^2}{V}\frac{\partial \ln Z}{\partial T}, \quad P = T\frac{\partial \ln Z}{\partial V}, \quad s = \frac{\epsilon + P}{T}. \tag{A.1}$$

Let us consider free pion gas as a hadron phase. Its partition function is given by

$$\ln Z_\pi = -d_\pi V \int \frac{d^3k}{(2\pi)^3} \ln(1 - e^{-E(k)/T}), \quad E(k) = \sqrt{k^2 + m_\pi^2}, \tag{A.2}$$

where d_π denotes the isospin degrees of freedom for pions, $d_\pi = 3$. Setting $m_\pi = 0$ for simplicity (without loss of generality), Eq. (A.2) becomes

$$\ln Z_\pi = -d_\pi \frac{VT^3}{2\pi^2} \int_0^\infty dx\, x^2 \ln(1 - e^{-x}) \tag{A.3}$$

$$= d_\pi \frac{VT^3}{6\pi^2}\Gamma(4)\zeta(4) = d_\pi \frac{V}{90}\pi^2 T^3, . \tag{A.4}$$

In the first line we used $x \equiv k/T$. In the second equality, we performed the integration by part . $\zeta(s)$ is Riemanns's zeta function defined by

$$\zeta(s) = \sum_{n=1}^{\infty} \frac{1}{n^s}, \tag{A.5}$$

and $\zeta(4) = \pi^4/90$. Thus the energy density and the pressure for the pion gas are given by

$$\epsilon_\pi = \frac{T^2}{V}\frac{\partial \ln Z_\pi}{\partial T} = d_\pi \frac{3}{90}\pi^2 T^4, \tag{A.6}$$

$$P_\pi = T\frac{\partial \ln Z_\pi}{\partial V} = d_\pi \frac{1}{90}\pi^2 T^4, \tag{A.7}$$

$$s_\pi = d_\pi \frac{4}{90}\pi^2 T^3. \tag{A.8}$$

Next, let us consider the QGP phase. We assume here that the QGP phase is composed of free massless quarks and gluons. Eq. (A.2) is applied to the gluon gas with the degrees of freedom of gluons is $d_g = (\text{spin}) \times (\text{color}) = 2 \times (N_c^2 - 1)$. Thus the gluon partition function reads

$$\ln Z_g = d_g \frac{V}{90} \pi^2 T^3. \tag{A.9}$$

On the other hand, the partition function of quarks is given by

$$\ln Z_q = d_q V \frac{7}{8} \int \frac{d^3k}{(2\pi)^3} \ln(1 + e^{-E(k)/T}), \tag{A.10}$$

where the baryon chemical potential equals to zero. The partition function for quark gas becomes

$$\ln Z_q = d_q \frac{7}{8} \frac{V}{90} \pi^2 T^3, \tag{A.11}$$

where the degrees of freedom of a quark is given by $d_q = (\text{spin}) \times (\text{q and } \bar{\text{q}}) \times (\text{color}) \times (\text{flavor}) = 2 \times 2 \times N_c \times N_f$. The factor 7/8 in Eq. (A.11) comes from the Fermi statistics of quarks (see Appendix. A.2.2).

From Eqs. (A.9) and (A.11), we obtain the partition function and the thermodynamics quantities in the QGP phase :

$$\ln Z_p = d_p \frac{V}{90} \pi^2 T^3, \quad d_p = d_g + \frac{7}{8} d_q, \tag{A.12}$$

$$\epsilon_p = d_p \frac{3}{90} \pi^2 T^4 + B, \tag{A.13}$$

$$P_p = d_p \frac{1}{90} \pi^2 T^4 - B, \tag{A.14}$$

$$s_p = d_p \frac{4}{90} \pi^2 T^3. \tag{A.15}$$

Here B is *the bag constant*, which is introduced to incorporate the effect that the vacuum energy density in the quark-gluon gas is higher than that in the hadron one.

We show the temperature dependence of the energy density, the pressure, and the entropy density schematically in Fig. A.1-A.3. The pressures P_π and P_p become the same value at some critical temperature T_c,

$$P_\pi(T_c) = P_p(T_c). \tag{A.16}$$

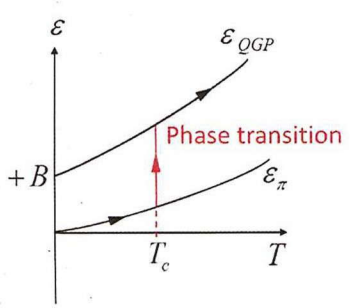

Figure A.1: ϵ vs T.

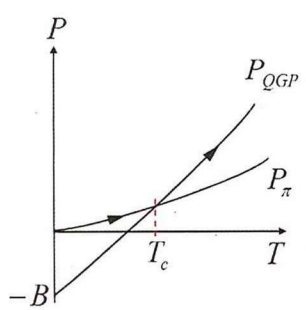

Figure A.2: P vs T.

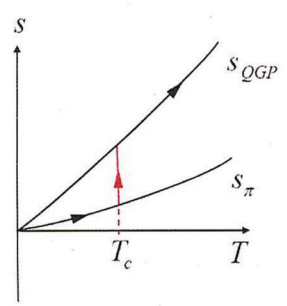

Figure A.3: s vs T.

Since the higher pressure phase is more stable, a phase transition occurs at T_c. From Eqs. (A.7), (A.14), and (A.16), the critical temperature is written as

$$T_c^4 = \frac{90B}{\pi^2(d_p - d_\pi)}. \tag{A.17}$$

In the case of $N_c = 3$ and $N_f = 2$, each degree of freedom is given by $d_g = 16$, $d_q = 24$, and $d_p = 37$, respectively. If one sets the bag constant $B^{1/4} \simeq 220$ MeV, the critical temperature becomes $T_c \simeq 160$ MeV.

A.2 Derivation of partition functions

A.2.1 Free pion gas

First we derivate the partition function of free pion gas. In the following, we assume the vanishing chemical potential case. The thermodynamic potential Ω_π is given by

$$\Omega_\pi = d_\pi VT \int \frac{d^3k}{(2\pi^3)} \ln(1 - e^{\frac{E(k)}{T}}), \quad E(k) = \sqrt{k^2 + m^2}. \tag{A.18}$$

Expanding the log term, Eq. (A.18) becomes

$$\begin{aligned} \Omega_\pi &= -d_\pi VT \int_0^\infty \frac{dk}{2\pi^2} k^2 \sum_{n=1}^\infty \frac{1}{n} e^{-\frac{nE(k)}{T}} \\ &= -d_\pi \frac{m^2VT^2}{2\pi^2} \sum_{n=1}^\infty \frac{1}{n^2} K_2\left(\frac{nm}{T}\right), \end{aligned} \tag{A.19}$$

where we introduced modified Bessel function $K_2(x)$ in the second equality,

$$\int_0^\infty dk\, k^2 e^{-\frac{E(k)}{T}} = m^2 T K_2\left(\frac{m}{T}\right). \tag{A.20}$$

Using the expansion of $K_2(x) = 2/x^2 + \mathcal{O}(x^0)$, Eq. (A.19) is calculated as

$$\begin{aligned} \Omega_\pi &= -d_\pi \frac{m^2VT^2}{2\pi^2} \left[\frac{1}{1^2} K_2(\frac{m}{T}) + \frac{1}{2^2} K_2(\frac{2m}{T}) + \frac{1}{3^2} K_2(\frac{3m}{T}) + \cdots\right] \\ &= -d_\pi \frac{m^2VT^2}{2\pi^2} \left[\left(\frac{1}{1^2} \frac{2}{\left(\frac{m}{T}\right)^2} + \cdots\right) + \left(\frac{1}{2^2} \frac{2}{\left(\frac{2m}{T}\right)^2} + \cdots\right) + \left(\frac{1}{3^2} \frac{2}{\left(\frac{3m}{T}\right)^2} + \cdots\right) + \cdots\right] \\ &\simeq -d_\pi \frac{VT^4}{\pi^2} \sum_{n=1}^\infty \frac{1}{n^4} = -d_\pi \frac{VT^4}{\pi^2} \zeta(4). \end{aligned} \tag{A.21}$$

Here we took the massless limit in the third line. Thus the partition function of free pion gas Eq. (A.4) is derived from Eq. (A.21),

$$\ln Z_\pi = -\frac{\Omega_\pi}{T} = d_\pi \frac{V}{90} \pi^2 T^3. \tag{A.22}$$

A.2.2 Free quark-gluon gas

Since the same derivation for the free pion gas is applied to free gluon gas, the partition function of gluons is given by

$$\ln Z_g = -\frac{\Omega_\pi}{T} = d_g \frac{V}{90}\pi^2 T^3. \tag{A.23}$$

While pions and gluons are governed by the Bose statistics, quarks follow Fermi statistics. Thus the thermodynamic potential for free quark gas is calculated to be

$$\begin{aligned}
\Omega_q &= d_q \frac{V}{T}\int \frac{d^3k}{(2\pi)^3}\ln(1+e^{-\frac{E(k)}{T}}) \\
&= -d_q \frac{m^2VT^2}{2\pi^2}\sum_{n=1}^{\infty}\frac{(-1)^{n+1}}{n^2}K_2\left(\frac{nm}{T}\right) \\
&= -d_q \frac{m^2VT^2}{2\pi^2}\left[\frac{1}{1^2}\frac{2}{(\frac{m}{T})^2} - \frac{1}{2^2}\frac{2}{(\frac{2m}{T})^2} + \frac{1}{3^2}\frac{2}{(\frac{3m}{T})^2} - \cdots\right] \\
&= -d_q \frac{VT^4}{\pi^2}\sum_{n=1}^{\infty}\frac{(-1)^{n+1}}{n^4} \\
&= -d_q(1-\frac{1}{2^3})\frac{VT^4}{\pi^2}\zeta(4).
\end{aligned} \tag{A.24}$$

In the last equality, we used the formula

$$\sum_{n=1}^{\infty}\frac{(-1)^{n+1}}{n^s} = (1-2^{1-s})\zeta(s). \tag{A.25}$$

We thus obtain the partition function of quark gas Eq. (A.11)

$$\ln Z_q = -\frac{\Omega_q}{T} = d_q \frac{7}{8}\frac{V}{90}\pi^2 T^3. \tag{A.26}$$

Since a total partition function is given by a product of partition functions for each degree of freedom, the partition function of quark-gluon gas is written as

$$\ln Z_p = \ln Z_q + \ln Z_g = d_p \frac{V}{90}\pi^2 T^3, \quad d_p \equiv d_g + \frac{7}{8}d_q. \tag{A.27}$$

Appendix B

Coefficient of Contact Terms

In this appendix, we evaluate the coefficient of contact terms by a perturbative calculation of Euclidean correlator

$$G_{\mu\nu\rho\sigma}(x,y) = \langle T_{\mu\nu}(x) T_{\rho\sigma}(y)\rangle, \tag{B.1}$$

for free SU(N_c) gauge theory at finite temperature T (see also appendix in Ref. [90]). We have

$$\begin{aligned} G_{\mu\nu\rho\sigma}(x,y) =& \langle (\partial_\mu A^a_\alpha(x) - \partial_\alpha A^a_\mu(x))(\partial_\nu A^a_\alpha(x) - \partial_\alpha A^a_\nu(x))(\partial_\rho A^b_\beta(y) - \partial_\beta A^b_\rho(y))(\partial_\sigma A^b_\beta(y) - \partial_\beta A^b_\sigma(y))\rangle \\ =& \sum\!\!\!\!\!\!\int_{PQRS} e^{i(P+Q)x} e^{i(R+S)y} \langle (P_\mu A^a_\alpha(P) - P_\alpha A^a_\mu(P))(Q_\nu A^a_\alpha(Q) - Q_\alpha A^a_\nu(Q)) \\ & \times (R_\rho A^b_\beta(R) - R_\beta A^b_\rho(R))(S_\sigma A^b_\beta(S) - S_\beta A^b_\sigma(S))\rangle, \end{aligned} \tag{B.2}$$

where $\sum\!\!\!\!\!\!\int_P \equiv T\sum_n \int \frac{d^3p}{(2\pi)^3}$. The Fourier transformation of $G_{\mu\nu\rho\sigma}(x,0)$ becomes

$$G_{\mu\nu\rho\sigma}(T) = \int_0^\beta d\tau \int d^3x e^{-iTx} G_{\mu\nu\rho\sigma}(x,0) \tag{B.3}$$

$$\begin{aligned} =& \int_0^\beta d\tau \int d^3x e^{-iTx} \sum\!\!\!\!\!\!\int_{PQRS} e^{i(P+Q)x} \\ & \times \langle (P_\mu A^a_\alpha(P) - P_\alpha A^a_\mu(P))(Q_\nu A^a_\alpha(Q) - Q_\alpha A^a_\nu(Q))(R_\rho A^b_\beta(R) - R_\beta A^b_\rho(R))(S_\sigma A^b_\beta(S) - S_\beta A^b_\sigma(S))\rangle. \end{aligned} \tag{B.4}$$

Each term composing the correlator is calculated as follows

$$\begin{aligned} & \sum\!\!\!\!\!\!\int_{PQRS} e^{i(P+Q)x} P_\mu Q_\nu R_\rho S_\sigma \langle A^a_\alpha(P) A^a_\alpha(Q) A^b_\beta(R) A^b_\beta(S)\rangle \\ &= \sum\!\!\!\!\!\!\int_{PQRS} e^{i(P+Q)x} P_\mu Q_\nu R_\rho S_\sigma (\langle A^a_\alpha(P) A^b_\beta(R)\rangle \langle A^a_\alpha(Q) A^b_\beta(S)\rangle + \langle A^a_\alpha(P) A^b_\beta(S)\rangle \langle A^a_\alpha(Q) A^b_\beta(R)\rangle) \\ &= \sum\!\!\!\!\!\!\int_{PQ} e^{i(P+Q)x} \frac{1}{P^2Q^2} (P_\mu Q_\nu P_\rho Q_\sigma \delta_{\alpha\beta}\delta_{\alpha\beta} + P_\mu Q_\nu P_\sigma Q_\rho \delta_{\alpha\beta}\delta_{\alpha\beta}) \delta^{ab}\delta^{ab} \\ &= (N_c^2 - 1) \sum\!\!\!\!\!\!\int_{PQ} e^{i(P+Q)x} \frac{4}{P^2Q^2} P_\mu Q_\nu (P_\rho Q\sigma + P_\sigma Q_\rho), \end{aligned} \tag{B.5}$$

where we used Feynman gauge

$$\langle A^a_\alpha(P) A^b_\beta(R)\rangle = \frac{1}{T}\delta_{n_P+n_R,0}(2\pi)^3 \delta(\vec{p}+\vec{r})\delta_{\alpha\beta}\delta^{ab}\frac{1}{P^2}. \tag{B.6}$$

Calculating other terms as well, Eq. (B.4) reduces to

$$
\begin{aligned}
G_{\mu\nu\rho\sigma}(T) =&(N_c^2-1)\int_0^\beta d\tau\int d^3x\sum\int_{PQ} e^{-i(T-P-Q)x}\\
&\times\frac{1}{P^2Q^2}[2(P_\mu P_\nu Q_\rho Q_\sigma+P_\rho P_\sigma Q_\mu Q_\nu)+P^2(Q_\nu Q_\rho\delta_{\mu\sigma}+Q_\nu Q_\sigma\delta_{\mu\rho})+Q^2(P_\mu P_\rho\delta_{\nu\sigma}+P_\mu P_\sigma\delta_{\nu\rho})\\
&+PQ\{2P_\mu Q_\nu\delta_{\rho\sigma}+(P_\rho Q_\sigma+P_\sigma Q_\rho)\delta_{\mu\nu}-(P_\mu Q_\rho+P_\rho Q_\mu)\delta_{\nu\sigma}-(P_\nu Q_\sigma+P_\sigma Q_\nu)\delta_{\mu\rho}\\
&-(P_\mu Q_\sigma+P_\sigma Q_\mu)\delta_{\nu\rho}-(P_\nu Q_\rho+P_\rho Q_\nu)\delta_{\mu\sigma}\}+(PQ)^2(\delta_{\mu\rho}\delta_{\nu\sigma}+\delta_{\mu\sigma}\delta_{\nu\rho})].
\end{aligned}
\tag{B.7}
$$

Let us consider $\mu=\rho=1$ and $\nu=\sigma=2$,

$$
\begin{aligned}
G_{1212}(T) =&(N_c^2-1)\int_0^\beta d\tau\int d^3x\sum\int_{PQ} e^{-i(T-P-Q)x}\\
&\times\frac{1}{P^2Q^2}[4p_1p_2q_1q_2+P^2q_2^2+Q^2p_1^2-2PQ(p_1q_2+p_2q_1)+(PQ)^2].
\end{aligned}
\tag{B.8}
$$

Substituting $T\to Q$ and $Q\to -K$ after P integration, one obtains

$$
\begin{aligned}
G_{1212}(Q) =&(N_c^2-1)T\sum_n\int\frac{d^3k}{(2\pi)^3}\\
&\times\frac{1}{(Q+K)^2K^2}[4(q_1+k_1)(q_2+k_2)k_1k_2+(Q+K)^2k_2^2+K^2(q_1+k_1)^2\\
&-2(Q+K)K\{(q_1+k_1)k_1+(q_2+k_2)k_2\}+((Q+K)K)^2].
\end{aligned}
\tag{B.9}
$$

In case of $Q=(q_4,\vec{0})$, the correlator reads

$$
\begin{aligned}
G_{1212}(q_4) =&(N_c^2-1)T\sum_n\int\frac{d^3k}{(2\pi)^3}\\
&\times\frac{1}{(Q+K)^2K^2}[4k_1^2k_2^2+(Q+K)^2k_2^2+K^2k_1^2-2(Q+K)K(k_1^2+k_2^2)+((Q+K)K)^2].
\end{aligned}
\tag{B.10}
$$

Let us calculate Matsubara sum.

$$
\begin{aligned}
T\sum_n\frac{1}{K^2}&=T\sum_n\frac{1}{k_4^2+k^2}=T\sum_n\frac{-1}{(ik_4)^2-k^2}=-T\sum_n\left(\frac{1}{ik_4-k}-\frac{1}{ik_4+k}\right)\frac{1}{2k}\\
&=-T\sum_n\sum_{s=\pm1}\frac{1}{ik_4-sk}\frac{s}{2k}=-\sum_{s=\pm1}\int\frac{dz}{2\pi i}\frac{1}{e^{\beta z}-1}\frac{1}{z-sk}\frac{s}{2k}\\
&=\sum_{s=\pm1}\frac{1}{e^{\beta sk}-1}\frac{s}{2k}=\frac{n(k)-n(-k)}{2k}=\frac{1+2n(k)}{2k},
\end{aligned}
\tag{B.11}
$$

where $n(k)$ denotes the Bose distribution function. Calculating other terms as well, one obtains

$$T\sum_n \frac{1}{(Q+K)^2} = \frac{1+2n(k)}{2k}, \tag{B.12}$$

$$T\sum_n \frac{1}{(Q+K)^2K^2} = \frac{1+2n(k)}{2k}\left[\frac{1}{q_4^2+2ikq_4} + \frac{1}{q_4^2-2ikq_4}\right], \tag{B.13}$$

$$T\sum_n \frac{(Q+K)K}{(Q+K)^2K^2} = \frac{1+2n(k)}{2k}\left[\frac{ikq_4}{q_4^2+2ikq_4} - \frac{ikq_4}{q_4^2-2ikq_4}\right], \tag{B.14}$$

$$T\sum_n \frac{((Q+K)K)^2}{(Q+K)^2K^2} = -\frac{1+2n(k)}{2k}\left[\frac{k^2q_4^2}{q_4^2+2ikq_4} + \frac{k^2q_4^2}{q_4^2-2ikq_4}\right] \tag{B.15}$$

Taking the limit $q_4 \to \infty$, the correlator becomes

$$\begin{aligned}
\lim_{q_4\to\infty} G_{1212}(q_4) &= (N_c^2-1)\int \frac{d^3k}{(2\pi)^3}\frac{1+2n(k)}{2k}\left[(k_1^2+k_2^2)-2k^2\right] \\
&= -\frac{2}{3}(N_c^2-1)\int \frac{d^3k}{(2\pi)^3}k(1+2n(k)) \\
&= -\frac{2}{3}(N_c^2-1)\int \frac{dk}{2\pi^2}k^3(1+2n(k)) \\
&= \infty - 2\frac{2}{90}(N_c^2-1)\pi^2T^4.
\end{aligned} \tag{B.16}$$

In the second equality we used a relation $3k_i^2 = k^2$ $(i = 1, 2, 3)$ and the polar coordinate in the third equality. In the last equality, we calculated as

$$\begin{aligned}
\int dkk^3n(k) &= \int dkk^3\frac{1}{e^{\beta k}-1} = \int dkk^3\frac{e^{-\beta k}}{1-e^{-\beta k}} \\
&= \int dkk^3\sum_{n=1}^{\infty}e^{-n\beta k} = \sum_{n=1}^{\infty}\int dkk^3e^{-n\beta k} \\
&= \frac{6}{\beta^4}\sum_{n=1}^{\infty}\frac{1}{n^4} = 6T^4\zeta(4) = \frac{6\pi^4}{90}T^4.
\end{aligned} \tag{B.17}$$

The divergence in Eq. (B.16) is removed by zero-temperature subtraction of $G^\eta(q_4)$. Recalling the pressure Eq. (A.7) and the degrees of freedom of $\mathrm{SU}(N_c)$ gauge field (see also Appendix. A), the coefficient of contact terms in the shear channel for the free gauge theory is given by

$$\lim_{q_4\to\infty} G_{1212}(q_4)_{T-0} = C_{1212\alpha\beta}\langle T_{\alpha\beta}\rangle_{T-0} = -2\frac{2}{90}(N_c^2-1)\pi^2T^4 = -2P = -\frac{\epsilon+P}{2}. \tag{B.18}$$

Here we used a relation $\epsilon = 3P$ for the free gauge theory. Thus the first term in Eq. (5.85) can be confirmed and the second does not appear because of $\epsilon - 3P$ vanishes in the free gauge theory.

Appendix C

Specific Heat

The specific heat c_V is related to a fluctuation of energy density $\delta\epsilon^2$,

$$c_V = \frac{V}{T^2}\langle\delta\epsilon^2\rangle. \tag{C.1}$$

Rewriting ϵ with a component of the energy-momentum tensor T_{44}, one obtains

$$\begin{aligned}
\langle\delta\epsilon^2\rangle &= \langle\delta\tilde{T}_{44}^2\rangle \\
&= \langle\left(T\int_0^{1/T} d\lambda\,\delta\bar{T}_{44}(\lambda)\right)^2\rangle \\
&= T\langle\int_0^{1/T} d\lambda\,\delta\bar{T}_{44}(\lambda)\delta\bar{T}_{44}(0)\rangle \qquad \text{(C.2)} \\
&\to \langle\delta\bar{T}_{44}(\frac{1}{2T})\delta\bar{T}_{44}(0)\rangle. \qquad \text{(C.3)}
\end{aligned}$$

In the forth line, we used a translation symmetry of T_{44} with respect to time, $T_{44}(\lambda) = T_{44}(\frac{1}{2T})$. Since Eq. (C.3) does not include an identical space-time point, the divergence and contact terms in Eq. (C.2) have no contribution to it. Thus the measurements of specific heat does not required the regularization prescriptions. The specific heat is given by

$$\begin{aligned}
\frac{c_V}{T^3} &= \frac{V}{T^5}\langle\delta\tilde{T}_{44}^2\rangle \\
&\to \frac{V}{T^5}\langle\delta\bar{T}_{44}(\frac{1}{2T})\delta\bar{T}_{44}(0)\rangle \\
&= N_\sigma^3 N_\tau^5\langle\delta\bar{T}_{44}(\frac{N_\tau}{2})\delta\bar{T}_{44}(0)\rangle^{\text{lat}}. \qquad \text{(C.4)}
\end{aligned}$$

Furthermore, the speed of sound c_s relates to the entropy density s and c_V as follows,

$$c_s^2 = \frac{\partial P}{\partial\epsilon} = \frac{(\partial P/\partial T)_V}{(\partial\epsilon/\partial T)_V} = \frac{s/T^3}{c_V/T^3}. \tag{C.5}$$

Using this relation with Eq. (4.64), the characteristic speed of sound mode v_L can be determined by lattice measurements.

Appendix D

Tables of Numerical Results

β	N_σ^3	N_τ	$\langle T_{44}^{\text{t.l.}}\rangle^{\text{lat}} \times 10^8$	$\langle T_{44}^{\text{t.l.}}\rangle_0^{\text{lat}} \times 10^8$	$\epsilon^{t.l.}/T^4$	N_{conf}
6.499	32^3	4	$-1636069(310)$	$-1636028(314)$	4.1882(8)	300,000
		6	$-257173(129)$	$-257132(139)$	3.3324(18)	1,000,000
		8	$-72503(109)$	$-72462(121)$	2.9680(50)	1,000,000
		32	$-41(53)$	$0(-)$	$0(-)$	1,000,000
6.205	32^3	4	$-1488702(290)$	$-1488654(306)$	3.8110(8)	300,000
		6	$-221949(231)$	$-221901(251)$	2.8758(33)	300,000
		8	$-55451(194)$	$-55403(217)$	2.2693(89)	300,000
		32	$-48(97)$	$0(-)$	$0(-)$	300,000
6.000	32^3	4	$-1338696(301)$	$-1338602(330)$	3.4268(8)	300,000
		6	$-171995(234)$	$-171901(271)$	2.2278(35)	300,000
		8	$-1317(191)$	$-1223(234)$	0.0501(96)	300,000
		16	$-94(136)$	$0(-)$	$0(-)$	300,000
6.000	16^3	4	$-1338351(657)$	$-1338345(723)$	3.4262(19)	500,000
		6	$-170683(528)$	$-170677(608)$	2.2120(79)	500,000
		8	$-6679(439)$	$-6673(533)$	0.2733(218)	500,000
		16	$-6(302)$	$0(-)$	$0(-)$	500,000

Table D.1: $\langle T_{44}^{\text{t.l.}}\rangle^{\text{lat}}$ and the energy density $\epsilon^{\text{t.l.}}$.

β	N_σ^3	N_τ	$\langle F^2\rangle^{\rm lat}$	$\langle F^2\rangle_0^{\rm lat}$	$(\epsilon-3P)/T^4$	$N_{\rm conf}$
6.499	32^3	4	$-1.2771263(16)$	$-0.0005556(17)$	0.3213(10)	300,000
		6	$-1.2767567(14)$	$-0.0001860(15)$	0.5445(44)	300,000
		8	$-1.2766712(12)$	$-0.0001005(13)$	0.9299(120)	300,000
		32	$-1.2765707(6)$	0(−)	0(−)	300,000
6.205	32^3	4	$-1.2293091(53)$	$-0.0011310(57)$	0.5844(29)	40,000
		6	$-1.2286418(46)$	$-0.0004637(50)$	1.2129(131)	40,000
		8	$-1.2284464(39)$	$-0.0002683(44)$	2.2180(364)	40,000
		32	$-1.2281781(20)$	0(−)	0(−)	40,000
6.000	32^3	4	$-1.1897434(23)$	$-0.0023742(26)$	1.0740(12)	300,000
		6	$-1.1884324(20)$	$-0.0010632(24)$	2.4349(55)	300,000
		8	$-1.1873814(19)$	$-0.0000122(23)$	0.0880(164)	300,000
		16	$-1.1873692(13)$	0(−)	0(−)	300,000
6.000	16^3	4	$-1.1897426(64)$	$-0.0023737(74)$	1.0738(33)	300,000
		6	$-1.1884371(56)$	$-0.0010682(67)$	2.4464(153)	300,000
		8	$-1.1874523(55)$	$-0.0000834(66)$	0.6039(486)	300,000
		16	$-1.1873689(37)$	0(−)	0(−)	300,000

Table D.2: Trace anomaly $\theta = \epsilon - 3P = -\beta(g)\langle F^2\rangle_0/2g$. Field strength tensor $F_{\mu\nu}$ is defined by standard plaquette.

β	N_σ^3	N_τ	$\langle N_\tau \tilde{T}_{12}^2\rangle^{\rm lat}\times 10^{11}$	$\langle N_\tau \tilde{T}_{12}^2\rangle_0^{\rm lat}\times 10^{11}$	$(V\langle \tilde{T}_{12}^2\rangle/T^5)_0$	$N_{\rm conf}$
6.499	32^3	4	183142(470)	−1695(537)	−0.090175(28569)	300,000
		6	184891(183)	54(317)	0.014543(85376)	2,000,000
		8	185144(179)	307(315)	0.261320(268130)	2,100,000
		32	184837(259)	0(−)	0(−)	1,000,000
6.205	32^3	4	180885(316)	−2808(484)	−0.140546(24225)	650,000
		6	183299(284)	−394(464)	−0.167321(99835)	830,000
		8	183751(259)	58(449)	0.046448(359574)	1,000,000
		32	183693(367)	0(−)	0(−)	510,000
6.000	32^3	4	180194(363)	−3310(455)	−0.155537(21380)	500,000
		6	182151(279)	−1353(391)	−0.321861(93014)	850,000
		8	183989(342)	485(438)	0.364642(329306)	580,000
		16	183504(274)	0(−)	0(−)	890,000
β	N_σ^3	N_τ	$\langle N_\tau \tilde{T}_{12}^2\rangle^{\rm lat}\times 10^{10}$	$\langle N_\tau \tilde{T}_{12}^2\rangle_0^{\rm lat}\times 10^{10}$	$(V\langle \tilde{T}_{12}^2\rangle/T^5)_0$	$N_{\rm conf}$
6.000	16^3	4	144325(214)	−2650(2988)	−0.155654(17550)	900,000
		6	146128(206)	−847(293)	−0.251981(87126)	1,000,000
		8	146777(208)	−198(295)	−0.186080(277147)	1,000,000
		16	146975(209)	0(−)	0(−)	1,000,000

Table D.3: Canonical correlation of shear channel with vacuum subtraction.

β	N_σ^3	N_τ	$\langle N_\tau(\delta\tilde{T}_{ii}^{\text{t.l.}})^2\rangle^{\text{lat}} \times 10^{10}$	$\langle N_\tau(\delta\tilde{T}_{ii}^{\text{t.l.}})^2\rangle_0^{\text{lat}} \times 10^{10}$	N_{conf}
6.499	32^3	4	96267(252)	8782(281)	300,000
		6	89064(89)	1579(153)	1,990,000
		8	88028(86)	543(152)	2,100,000
		32	87485(125)	0(−)	1,000,000
6.205	32^3	4	94471(165)	7615(238)	650,000
		6	88178(137)	1322(219)	830,000
		8	87257(124)	401(211)	1,000,000
		32	86856(171)	0(−)	510,000
6.000	32^3	4	93224(187)	6497(277)	500,000
		6	88014(136)	1287(261)	850,000
		8	87003(161)	276(275)	580,000
		16	86727(131)	0(−)	890,000
β	N_σ^3	N_τ	$\langle N_\tau(\tilde{T}_{ii}^{\text{t.l.}})^2\rangle^{\text{lat}} \times 10^{9}$	$\langle N_\tau(\tilde{T}_{ii}^{\text{t.l.}})^2\rangle_0^{\text{lat}} \times 10^{9}$	N_{conf}
6.000	16^3	4	75056(112)	5446(149)	900,000
		6	70180(98)	570(139)	1,000,000
		8	69645(99)	35(139)	1,000,000
		16	69610(98)	0(−)	1,000,000

Table D.4: Canonical correlation of $\delta T_{ii}^{\text{t.l.}}$ with vacuum subtraction.

β	N_σ^3	N_τ	$\langle N_\tau\delta\tilde{T}_{ii}^{\text{t.l.}}\delta S\rangle^{\text{lat}} \times 10^{11}$	$\langle N_\tau\delta\tilde{T}_{ii}^{\text{t.l.}}\delta S\rangle_0^{\text{lat}} \times 10^{11}$	N_{conf}
6.499	32^3	4	2387(715)	2818(804)	300,000
		6	800(265)	1231(453)	1,990,000
		8	285(255)	716(448)	2,100,000
		32	−431(368)	0(−)	1,000,000
6.205	32^3	4	−1034(968)	−605(2243)	190,000
		6	680(1045)	1109(2277)	150,000
		8	−605(860)	−176(2198)	220,000
		32	−429(2023)	0(−)	40,000
6.000	32^3	4	6366(644)	5399(797)	500,000
		6	3760(490)	2793(679)	850,000
		8	651(580)	−316(747)	580,000
		16	967(470)	0(−)	890,000
β	N_σ^3	N_τ	$\langle N_\tau\delta\tilde{T}_{ii}^{\text{t.l.}}\delta S\rangle^{\text{lat}} \times 10^{10}$	$\langle N_\tau\delta\tilde{T}_{ii}^{\text{t.l.}}\delta S\rangle_0^{\text{lat}} \times 10^{10}$	N_{conf}
6.000	16^3	4	5039(391)	5014(527)	900,000
		6	2952(358)	2927(503)	1,000,000
		8	1019(360)	994(505)	1,000,000
		16	25(354)	0(−)	1,000,000

Table D.5: Product of $\delta\tilde{T}_{ii}^{\text{t.l.}}$ and the SU(3) gauge action δS with vacuum subtraction.

β	N_σ^3	N_τ	$\langle N_\tau \delta S^2 \rangle^{\rm lat} \times 10^{10}$	$\langle N_\tau \delta S^2 \rangle_0^{\rm lat} \times 10^{10}$	$N_{\rm conf}$
6.499	32^3	4	15079(45)	−192(51)	300,000
		6	15277(18)	6(31)	1,990,000
		8	15254(17)	−17(30)	2,100,000
		32	15271(25)	0(−)	1,000,000
6.205	32^3	4	18031(69)	−716(181)	190,000
		6	18390(81)	−357(186)	150,000
		8	18397(67)	−350(180)	220,000
		32	18747(167)	0(−)	40,000
6.000	32^3	4	21288(53)	−1212(69)	500,000
		6	22116(44)	−384(62)	850,000
		8	22416(54)	−84(70)	580,000
		16	22500(44)	0(−)	890,000
β	N_σ^3	N_τ	$\langle N_\tau \delta S^2 \rangle^{\rm lat} \times 10^{9}$	$\langle N_\tau \delta S^2 \rangle_0^{\rm lat} \times 10^{9}$	$N_{\rm conf}$
6.000	16^3	4	17117(32)	−851(46)	900,000
		6	17732(32)	−236(46)	1,000,000
		8	18141(34)	173(47)	1,000,000
		16	17968(33)	0(−)	1,000,000

Table D.6: Canonical correlation of the trace anomaly with vacuum subtraction.

β	N_σ^3	N_τ	$\eta/\{\tau_\pi(\epsilon+P)\}$	$\zeta/\{\tau_\Pi(\epsilon+P)\}$
6.499	32^3	4	0.49277(611)	0.34450(642)
		6	0.53190(2337)	0.40994(2337)
		8	0.63621(8256)	0.47220(8187)
6.205	32^3	4	0.48985(587)	0.31665(1604)
		6	0.53687(3834)	0.30919(10985)
		8	0.68345(14919)	−0.08925(42872)
6.000	32^3	4	0.50686(595)	0.35252(667)
		6	0.53776(4044)	0.47612(4687)
		8	8.0868(6.5294)	−1.2540(7.3648)
6.000	16^3	4	0.50682(442)	0.36907(480)
		6	0.57055(3615)	0.47948(3730)
		8	0.18675(101436)	4.0027(9697)

Table D.7: The viscosity to relaxation time ratios.

Bibliography

[1] D. J. Gross and F. Wilczek, "ULTRAVIOLET BEHAVIOR OF NON-ABELIAN GAUGE THEORIES," Phys. Rev. Lett. **30**, 1343 (1973).

[2] H. D. Politzer, "RELIABLE PERTURBATIVE RESULTS FOR STRONG INTERACTIONS?," Phys. Rev. Lett. **30**, 1346 (1973).

[3] S. Bethke, "World Summary of α_s (2012)," arXiv:1210.0325 [hep-ex].

[4] M. G. Alford, K. Rajagopal and F. Wilczek, "QCD at finite baryon density: Nucleon droplets and color superconductivity," Phys. Lett. B **422**, 247 (1998) [arXiv:hep-ph/9711395].

[5] M. G. Alford, K. Rajagopal and F. Wilczek, "Color-flavor locking and chiral symmetry breaking in high density QCD," Nucl. Phys. B **537**, 443 (1999) [arXiv:hep-ph/9804403].

[6] M. Asakawa and K. Yazaki, "CHIRAL RESTORATION AT FINITE DENSITY AND TEMPERATURE," Nucl. Phys. A **504**, 668 (1989).

[7] T. Hatsuda, M. Tachibana, N. Yamamoto and G. Baym, "New critical point induced by the axial anomaly in dense QCD," Phys. Rev. Lett. **97**, 122001 (2006) [hep-ph/0605018].

[8] C. DeTar, "QCD Thermodynamics on the Lattice: Recent Results," arXiv:1101.0208 [hep-lat].

[9] J. D. Bjorken, "Highly Relativistic Nucleus-Nucleus Collisions: The Central Rapidity Region," Phys. Rev. D **27**, 140 (1983).

[10] E. Iancu, "QCD in heavy ion collisions," arXiv:1205.0579 [hep-ph].

[11] E. V. Shuryak, "What RHIC experiments and theory tell us about properties of quark-gluon plasma?," Nucl. Phys. A **750**, 64 (2005) [hep-ph/0405066].

[12] P. F. Kolb, P. Huovinen, U. W. Heinz and H. Heiselberg, "Elliptic flow at SPS and RHIC: From kinetic transport to hydrodynamics," Phys. Lett. B **500**, 232 (2001) [arXiv:hep-ph/0012137].

[13] P. Huovinen, P. F. Kolb, U. W. Heinz, P. V. Ruuskanen and S. A. Voloshin, "Radial and elliptic flow at RHIC: Further predictions," Phys. Lett. B **503**, 58 (2001) [arXiv:hep-ph/0101136].

[14] T. Hirano, U. W. Heinz, D. Kharzeev, R. Lacey and Y. Nara, "Hadronic dissipative effects on elliptic flow in ultrarelativistic heavy-ion collisions," Phys. Lett. B **636**, 299 (2006) [arXiv:nucl-th/0511046].

[15] C. Nonaka and S. A. Bass, "Space-time evolution of bulk QCD matter," Phys. Rev. C **75**, 014902 (2007) [arXiv:nucl-th/0607018].

[16] K. Aamodt *et al.* [The ALICE Collaboration], "Elliptic flow of charged particles in Pb-Pb collisions at 2.76 TeV," Phys. Rev. Lett. **105**, 252302 (2010). [arXiv:1011.3914 [nucl-ex]].

[17] B. Muller, J. Schukraft and B. Wyslouch, "First Results from Pb+Pb collisions at the LHC," arXiv:1202.3233 [hep-ex].

[18] P. Romatschke and U. Romatschke, "Viscosity Information from Relativistic Nuclear Collisions: How Perfect is the Fluid Observed at RHIC?," Phys. Rev. Lett. **99**, 172301 (2007) [arXiv:0706.1522 [nucl-th]].

[19] H. Song and U. W. Heinz, "Extracting the QGP viscosity from RHIC data - A Status report from viscous hydrodynamics," J. Phys. G **36**, 064033 (2009) [arXiv:0812.4274 [nucl-th]].

[20] B. Schenke, S. Jeon and C. Gale, "Elliptic and triangular flow in event-by-event (3+1)D viscous hydrodynamics," Phys. Rev. Lett. **106**, 042301 (2011) [arXiv:1009.3244 [hep-ph]].

[21] H. Song, S. A. Bass, U. Heinz, T. Hirano and C. Shen, "200 A GeV Au+Au collisions serve a nearly perfect quark-gluon liquid," Phys. Rev. Lett. **106**, 192301 (2011) [Erratum-ibid. **109**, 139904 (2012)] [arXiv:1011.2783 [nucl-th]].

[22] C. Eckart, "The Thermodynamics of irreversible processes. 3.. Relativistic theory of the simple fluid," Phys. Rev. **58**, 919 (1940).

[23] L.D. Landau and E.M. Lifshitz, *Fluid mechanics* (Pergamon, New York, 1959).

[24] W. A. Hiscock and L. Lindblom, "Stability and causality in dissipative relativistic fluids," Annals Phys. **151**, 466 (1983).

[25] W. A. Hiscock and L. Lindblom, "Generic instabilities in first-order dissipative relativistic fluid theories," Phys. Rev. D **31** (1985) 725.

[26] W. Israel, "Nonstationary irreversible thermodynamics: A Causal relativistic theory," Annals Phys. **100**, 310 (1976).

[27] W. Israel and J. M. Stewart, "Transient relativistic thermodynamics and kinetic theory," Annals Phys. **118**, 341 (1979).

[28] F. Karsch and H. W. Wyld, "THERMAL GREEN'S FUNCTIONS AND TRANSPORT COEFFICIENTS ON THE LATTICE," Phys. Rev. D **35**, 2518 (1987).

[29] G. Aarts and J. M. Martinez Resco, "Transport coefficients, spectral functions and the lattice," JHEP **0204**, 053 (2002) [arXiv:hep-ph/0203177].

[30] A. Nakamura and S. Sakai, "Transport coefficients of gluon plasma," Phys. Rev. Lett. **94**, 072305 (2005) [arXiv:hep-lat/0406009].

[31] H. B. Meyer, "A Calculation of the shear viscosity in SU(3) gluodynamics," Phys. Rev. D **76**, 101701 (2007) [arXiv:0704.1801 [hep-lat]].

[32] D. Kharzeev and K. Tuchin, "Bulk viscosity of QCD matter near the critical temperature," JHEP **0809**, 093 (2008) [arXiv:0705.4280 [hep-ph]].

[33] M. Asakawa, T. Hatsuda and Y. Nakahara, "Maximum entropy analysis of the spectral functions in lattice QCD," Prog. Part. Nucl. Phys. **46**, 459 (2001) [arXiv:hep-lat/0011040].

[34] A. Muronga, "Generalized entropy and transport coefficients of hadronic matter," Eur. Phys. J. ST **155**, 107 (2008) [arXiv:0710.3280 [nucl-th]].

[35] S. Pratt, "Formulating viscous hydrodynamics for large velocity gradients," Phys. Rev. C **77**, 024910 (2008) [arXiv:0711.3911 [nucl-th]].

[36] T. Koide, E. Nakano and T. Kodama, "Shear viscosity coefficient and relaxation time of causal dissipative hydrodynamics in QCD," Phys. Rev. Lett. **103**, 052301 (2009) [arXiv:0901.3707 [hep-th]].

[37] X. -G. Huang, T. Kodama, T. Koide and D. H. Rischke, "Bulk Viscosity and Relaxation Time of Causal Dissipative Relativistic Fluid Dynamics," Phys. Rev. C **83**, 024906 (2011) [arXiv:1010.4359 [nucl-th]].

[38] K. G. Wilson, "CONFINEMENT OF QUARKS," Phys. Rev. D **10**, 2445 (1974).

[39] M. Creutz, "Confinement And The Critical Dimensionality Of Space-Time," Phys. Rev. Lett. **43**, 553 (1979) [Erratum-ibid. **43**, 890 (1979)].

[40] M. Creutz, "Monte Carlo Study Of Quantized SU(2) Gauge Theory," Phys. Rev. D **21**, 2308 (1980).

[41] M. Creutz, "Asymptotic Freedom Scales," Phys. Rev. Lett. **45**, 313 (1980).

[42] M. Creutz and K. J. M. Moriarty, "Numerical Studies Of Wilson Loops In SU(3) Gauge Theory In Four-Dimensions," Phys. Rev. D **26**, 2166 (1982).

[43] H. Hamber and G. Parisi, "Numerical Estimates Of Hadronic Masses In A Pure SU(3) Gauge Theory," Phys. Rev. Lett. **47**, 1792 (1981).

[44] J. D. Stack, "The Heavy Quark Potential In SU(3) Lattice Gauge Theory," Phys. Rev. D **29**, 1213 (1984).

[45] D. Barkai, K. J. M. Moriarty and C. Rebbi, "The Force Between Static Quarks," Phys. Rev. D **30**, 1293 (1984).

[46] S. W. Otto and J. D. Stack, "The SU(3) Heavy Quark Potential With High Statistics," Phys. Rev. Lett. **52**, 2328 (1984).

[47] S. A. Gottlieb, J. Kuti, D. Toussaint, A. D. Kennedy, S. Meyer, B. J. Pendleton and R. L. Sugar, "The Deconfining Phase Transition And The Continuum Limit Of Lattice Quantum Chromodynamics," Phys. Rev. Lett. **55**, 1958 (1985).

[48] D. Barkai, K. J. M. Moriarty and C. Rebbi, "Hadron Masses In Quenched Quantum Chromodynamics," Phys. Lett. B **156**, 385 (1985).

[49] F. R. Brown, N. H. Christ, Y. F. Deng, M. S. Gao and T. J. Woch, "Nature of the Deconfining Phase Transition in SU(3) Lattice Gauge Theory," Phys. Rev. Lett. **61**, 2058 (1988).

[50] K. D. Born, E. Laermann, N. Pirch, T. F. Walsh and P. M. Zerwas, "HADRON PROPERTIES IN LATTICE QCD WITH DYNAMICAL FERMIONS," Phys. Rev. D **40**, 1653 (1989).

[51] J. E. Drut and T. A. Lahde, "Lattice field theory simulations of graphene," arXiv:0901.0584 [cond-mat.str-el].

[52] Y. Araki and T. Hatsuda, "Chiral Gap and Collective Excitations in Monolayer Graphene from Strong Coupling Expansion of Lattice Gauge Theory," Phys. Rev. B **82**, 121403 (2010) [arXiv:1003.1769 [cond-mat.str-el]].

[53] D. B. Kaplan, E. Katz and M. Unsal, "Supersymmetry on a spatial lattice," JHEP **0305**, 037 (2003) [hep-lat/0206019].

[54] F. Sugino, "Various super Yang-Mills theories with exact supersymmetry on the lattice," JHEP **0501**, 016 (2005) [hep-lat/0410035].

[55] H. B. Nielsen and M. Ninomiya, "No Go Theorem For Regularizing Chiral Fermions," Phys. Lett. B **105**, 219 (1981).

[56] L. H. Karsten and J. Smit, "Lattice Fermions: Species Doubling, Chiral Invariance, And The Triangle Anomaly," Nucl. Phys. B **183**, 103 (1981).

[57] L. Susskind, "Lattice Fermions," Phys. Rev. D **16**, 3031 (1977).

[58] L. H. Karsten, "Lattice Fermions In Euclidean Space-Time," Phys. Lett. B **104**, 315 (1981).

[59] H. S. Sharatchandra, H. J. Thun and P. Weisz, "Susskind Fermions On A Euclidean Lattice," Nucl. Phys. B **192**, 205 (1981).

[60] Y. Shamir, "Chiral fermions from lattice boundaries," Nucl. Phys. B **406**, 90 (1993) [arXiv:hep-lat/9303005].

[61] V. Furman and Y. Shamir, "Axial Symmetries In Lattice QCD With Kaplan Fermions," Nucl. Phys. B **439**, 54 (1995) [arXiv:hep-lat/9405004].

[62] H. Neuberger, "Exactly massless quarks on the lattice," Phys. Lett. B **417**, 141 (1998) [arXiv:hep-lat/9707022].

[63] H. Neuberger, "More about exactly massless quarks on the lattice," Phys. Lett. B **427**, 353 (1998) [arXiv:hep-lat/9801031].

[64] G. 't Hooft, "On The Phase Transition Towards Permanent Quark Confinement," Nucl. Phys. B **138**, 1 (1978).

[65] L. D. McLerran and B. Svetitsky, "A Monte Carlo Study Of SU(2) Yang-Mills Theory At Finite Temperature," Phys. Lett. B **98**, 195 (1981).

[66] J. Kuti, J. Polonyi and K. Szlachanyi, "Monte Carlo Study Of SU(2) Gauge Theory At Finite Temperature," Phys. Lett. B **98**, 199 (1981).

[67] L. D. McLerran and B. Svetitsky, "Quark Liberation At High Temperature: A Monte Carlo Study Of SU(2) Gauge Theory," Phys. Rev. D **24**, 450 (1981).

[68] B. Svetitsky and L. G. Yaffe, "Critical Behavior At Finite Temperature Confinement Transitions," Nucl. Phys. B **210**, 423 (1982).

[69] L. G. Yaffe and B. Svetitsky, "First Order Phase Transition In The SU(3) Gauge Theory At Finite Temperature," Phys. Rev. D **26**, 963 (1982).

[70] T. Celik, J. Engels and H. Satz, "The Order Of The Deconfinement Transition In SU(3) Yang-Mills Theory," Phys. Lett. B **125**, 411 (1983).

[71] R. G. Edwards, U. M. Heller and T. R. Klassen, "Accurate scale determinations for the Wilson gauge action," Nucl. Phys. B **517**, 377 (1998) [arXiv:hep-lat/9711003].

[72] N. Cabibbo and E. Marinari, "A New Method for Updating SU(N) Matrices in Computer Simulations of Gauge Theories," Phys. Lett. B **119**, 387 (1982).

[73] S. L. Adler, "An Overrelaxation Method For The Monte Carlo Evaluation Of The Partition Function For Multiquadratic Actions," Phys. Rev. D **23**, 2901 (1981).

[74] C. Whitmer, "Overrelaxation Methods For Monte Carlo Simulations Of Quadratic And Multiquadratic Actions," Phys. Rev. D **29**, 306 (1984).

[75] F. R. Brown and T. J. Woch, "Overrelaxed Heat Bath and Metropolis Algorithms for Accelerating Pure Gauge Monte Carlo Calculations," Phys. Rev. Lett. **58**, 2394 (1987).

[76] A. Muronga, "Causal theories of dissipative relativistic fluid dynamics for nuclear collisions," Phys. Rev. C **69**, 034903 (2004) [arXiv:nucl-th/0309055].

[77] U. W. Heinz, H. Song and A. K. Chaudhuri, "Dissipative hydrodynamics for viscous relativistic fluids," Phys. Rev. C **73**, 034904 (2006) [arXiv:nucl-th/0510014].

[78] R. Baier, P. Romatschke, D. T. Son, A. O. Starinets and M. A. Stephanov, "Relativistic viscous hydrodynamics, conformal invariance, and holography," JHEP **0804**, 100 (2008) [arXiv:0712.2451 [hep-th]].

[79] R. Kubo, "Statistical Mechanical Theory Of Irreversible Processes. 1. General Theory And Simple Applications In Magnetic And Conduction Problems," J. Phys. Soc. Jap. **12**, 570 (1957).

[80] A. Einstein, Annals Phys. **33** (1910) 1277.

[81] L.D. Landau and E.M. Lifshitz, *Statistical physics:pt. 2* (Pergamon, New York, 1980).

[82] H. Osborn and A. C. Petkou, "Implications of conformal invariance in field theories for general dimensions," Annals Phys. **231**, 311 (1994) [arXiv:hep-th/9307010].

[83] S. Caron-Huot, "Asymptotics of thermal spectral functions," Phys. Rev. **D79**, 125009 (2009). [arXiv:0903.3958 [hep-ph]].

[84] B. Beinlich, F. Karsch, E. Laermann and A. Peikert, "String tension and thermodynamics with tree level and tadpole improved actions," Eur. Phys. J. C **6**, 133 (1999) [arXiv:hep-lat/9707023].

[85] G. Boyd, J. Engels, F. Karsch, E. Laermann, C. Legeland, M. Lutgemeier and B. Petersson, "Thermodynamics of SU(3) lattice gauge theory," Nucl. Phys. B **469**, 419 (1996) [arXiv:hep-lat/9602007].

[86] M. Natsuume and T. Okamura, "Causal hydrodynamics of gauge theory plasmas from AdS/CFT duality," Phys. Rev. D **77**, 066014 (2008) [Erratum-ibid. D **78**, 089902 (2008)] [arXiv:0712.2916 [hep-th]].

[87] I. Kanitscheider and K. Skenderis, "Universal hydrodynamics of non-conformal branes," JHEP **0904**, 062 (2009) [arXiv:0901.1487 [hep-th]].

[88] P. Kovtun, D. T. Son and A. O. Starinets, "Viscosity in strongly interacting quantum field theories from black hole physics," Phys. Rev. Lett. **94**, 111601 (2005) [arXiv:hep-th/0405231].

[89] U. Heinz, C. Shen and H. -C. Song, "The viscosity of quark-gluon plasma at RHIC and the LHC," AIP Conf. Proc. **1441**, 766 (2012) [arXiv:1108.5323 [nucl-th]].

[90] P. Romatschke and D. T. Son, "Spectral sum rules for the quark-gluon plasma," Phys. Rev. D **80**, 065021 (2009) [arXiv:0903.3946 [hep-ph]].